Discovering new targets for glucocorticoids

Dissertation

der Mathematisch-Naturwissenschaftlichen Fakultät

der Eberhard Karls Universität Tübingen

zur Erlangung des Grades eines

Doktors der Naturwissenschaften

(Dr. rer. nat.)

vorgelegt von

Yvonne Etzel

aus Darmstadt

Tübingen

2012

Tag der mündlichen Qualifikation:	12. November 2012
Dekan:	Prof. Dr. Wolfgang Rosenstiel
1. Berichterstatter:	Prof. Dr. Gabriele Dodt
2. Berichterstatter:	Prof. Dr. Oliver Werz

J'ai decidé d'être horeux,

parce que c'est bon pour la santé

Voltaire

Table of Content

Abbreviations

AAA ATPases	ATPases associated with diverse cellular activities
ABPP	activity-based protein profiling
ACTH	adrenocorticotropic hormone
AF	activation function
AktP	phosphorylated Akt (protein kinase B)
ANT	adenine nucleotide translocator
AP-1	activator protein 1
Arg	arginine
ATP	adenosine triphosphate
CBP	cAMP-responsive element-binding protein (CREB)-binding protein
cGR	cytosolic glucocorticoid receptor
CMO	*O*-(carboxymethyl)oxime
CRH	corticotropin-releasing hormone
CTD	C-terminal domain
Cys	cysteine
DARTS	drug affinity responsive target stability
DBD	DNA-binding domain
Dex	dexamethasone
DIC	*N,N'*-diisopropylcarbodiimide
DMEM	Dulbecco's modified eagle medium
DMSO	dimethyl sulfoxide
EDTA	ethylendiamintetraacetic acid
ELISA	enzyme-linked immunosorbent assay
FKBP51/52	FK506 binding protein 51/52
FYN	p59fyn, tyrosine kinase
GC	glucocorticoid
GFP	green fluorescent protein
GR	glucocorticoid receptor
GRE	glucocorticoid receptor response element
HAT	histone acetyltransferase
HDAC	histone deacetylase
hGR	human glucocorticoid receptor
HPA	hypothalamic-pituitary-adrenocortical
HR	hinge region
Hsp	heat shock protein
ICAT	isotope-coded affinity tag
IEX	ion exchange chromatography
IGF1	insulin-like growth factor 1
IKK	IκB kinase
iTRAQ	isobaric tags for relative and absolute quantification
LBD	ligand-binding domain
Lck	lymphocyte-specific protein tyrosine kinase p56lck
Lys	lysine
MAPK	mitogen activated protein kinase
mGR	membrane-bound glucocorticoid receptor
MS	mass spectrometry
mTOR	mammalian target of rapamycin
NADPH	β-nicotinamide adenine dinucleotide 2′-phosphate
neg	negative control – incubation in absence of H_2O_2

neg H_2O_2	negative control – incubation in presence of H_2O_2
NF-κB	nuclear factor κB
nGRE	negative GRE
NL	nuclear localization
NLS	nuclear localization sequence
NPC	nuclear pore complex
NTD	N-terminal domain
P-TEFb	transcriptional elongation factor
p/CAF	p300/CBP associated factor
PBMC	peripheral blood mononuclear cell
PBS	phosphate buffered saline
PGRMC1/2	progesterone receptor membrane component 1/2
PI3K	phosphatidylinositol 3-kinase
PIP_2	phosphatidylinositol 4,5-bisphosphate
PIP_3	phosphatidylinositol (3,4,5)-trisphosphate
PKA	protein kinase A
PKB	protein kinase B / Akt
PP2A/PPP2	serine/threonine-protein phosphatase 2A
PP2B/PPP3	calcineurin
PPP	phosphoprotein phosphatase family of Ser/Thr phosphatases
Prdx1	peroxiredoxin 1
PTEN	phosphatase and tensin homolog
PTS1	peroxisomal targeting sequence 1
PVDF	polyvinylidene fluorid
PVN	paraventricular nucleus
raptor	regulatory associated protein of mTOR
RING	really interesting new gene
ROS	reactive oxygen species
SDS	sodium dodecyl sulfate
SDS-PAGE	sodium dodecyl sulfate polyacrylamide gel electrophoresis
SEGRA	selective glucocorticoid receptor agonists
Ser	serine
SH	sex hormones
SILAC	stable isotope labeling of amino acids in cell culture
SPROX	stability of proteins from rates of oxidation
Src	sarcoma family of nonreceptor tyrosine kinases
SRC	steroid receptor coactivator
TBS	tris buffered saline
TCR	T-cell receptor
TF	transcription factor
TFRE	transcription factor response element
Thr	threonine
Tm	tropomyosin
TNFα	tumor necrosis factor α
TPM	tropomyosine gene
VitC	ascorbic acid
X-ALD	X-linked adrenoleukodystrophy
yHisTrx1	N-terminal His_6-tagged thioredoxin 1, yeast
yTrxR	thioredoxin reductase, yeast
β-ME	β-mercaptoethanol

1. Introduction

1.1. Glucocorticoids

1.1.1. Introduction

In the last fifty years, glucocorticoids (GC) are counted among the most effective and widely used drugs in the anti-inflammatory and immunosuppressive treatment of diseases such as rheumatoid arthritis, asthma, multiple sclerosis and bowel disease[1-3].

In the human body, the release of cortisol is controlled by the hypothalamic-pituitary-adrenocortical (HPA) axis (Figure 1-1). Different stimuli like emotional (amygdala) or physiological (prefrontal cortex, hippocampus) aspects can stimulate the paraventricular nucleus (PVN). Corticotropin-releasing hormone (CRH) is activated inside the PVN liberating adrenocorticotropic hormone (ACTH) in the pituitary gland. ACTH activates the release of cortisol from the adrenal glands[4]. Cortisol can act in the regulation of the energy pathway, in cell differentiation and proliferation, especially in the bone and connective tissues[1, 5].

Treatment with glucococorticoids exerts a diverse range of side effects such as degradation of skeletal muscles, skin atrophy and fat redistribution. These symptoms originate from a hyperfunction of the adrenal cortex and are referred to as the Cushing's syndrome[1]. Furthermore, an excess of glucocorticoids can lead to osteoporosis, growth retardation in children, insulin resistance and hypertension[6-10].

Most glucocorticoid actions are mediated through the glucocorticoid receptor and lead to a genomic change of appropriate genes. Nevertheless, some rapid effects cannot be explained with this pathway. They occur within seconds to minutes and hence, cannot be caused by the genomic mode of action as the regulation of gene expression takes at least 30 min[5, 11]. Therefore, a nongenomic mode of action is discussed. The exact molecular targets of most of these interactions remain to be elucidated and are the aim of this thesis.

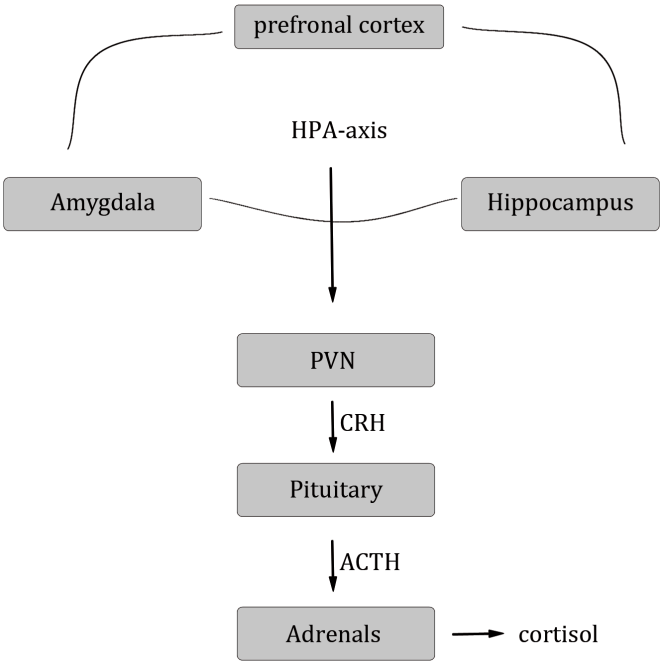

Figure 1-1 Cortisol release mechanism: The hyptothalamic-pituaitary-adrenocortical (HPA)-axis leads to stimulation of the paraventricular nucleus (PVN), which releases corticotropin-releasing hormone (CRH). CRH stimulates the pituitary to set adrenocorticotropic hormone (ACTH) free. ACTH leads to liberation of cortisol from the adrenals. Image modified from Groeneweg[4].

1.1.2. Genomic pathway

The genomic mode of action is the most studied glucocorticoid pathway. It involves binding of the GC to the glucocorticoid receptor (GR), nuclear translocation of the receptor complex, its DNA binding that leads to an impact on gene regulation. Between 10 and 100 genes per cell are regulated directly by the GR[12].

1.1.2.1.Domain structure of the glucocorticoid receptor

The human GR belongs to the nuclear receptor superfamily that consists of over 60 receptor molecules[13]. The GR regulates the expression of glucocorticoid responsive genes as a ligand-dependent transcription factor[14-16]. In humans, GR mRNA is mostly expressed in lung, spleen, brain and liver[8].

Three different splice variants of the human GR (hGR) are known: GRα, GRβ and GR-P. GRα and GRβ are identical in their first 727 amino acids. GRα is located in the cytoplasm and displays the active form of hGR. GRβ exhibits 0.2-1 % of total GR expression. It is not able to bind to GCs and inhibits GRα function. GR-P is thought to be a GRα activator[14, 17-19].

The human GR comprises of an N-terminal domain (NTD), a DNA-binding domain (DBD), a hinge region (HR) and a ligand-binding domain (LBD) (Figure 1-2). This composition is consistent with most members of the nuclear receptor superfamily[14, 18, 20]. The NTD

contains a ligand-independent activation function (AF-1) that interacts with e.g. coactivators for the initiation of transcription. The DBD consists of two zinc finger motifs that can bind to glucocorticoid receptor response elements (GRE). It also contains dimerization and nuclear localization (NL) sites. The hinge region is involved in dimerization of the GR and the structural flexibility as a dimer[14]. Dimerization occurs when monomeric GR interacts with GRE that acts as an allosteric activator. A scaffold that facilitates the correct position for dimerization of GR is provided by GRE[8]. The LBD contains AF-2 that implies ligand-dependent GR dimerization, nuclear translocation and interaction with coactivators after binding to heat shock proteins (Hsps)[14].

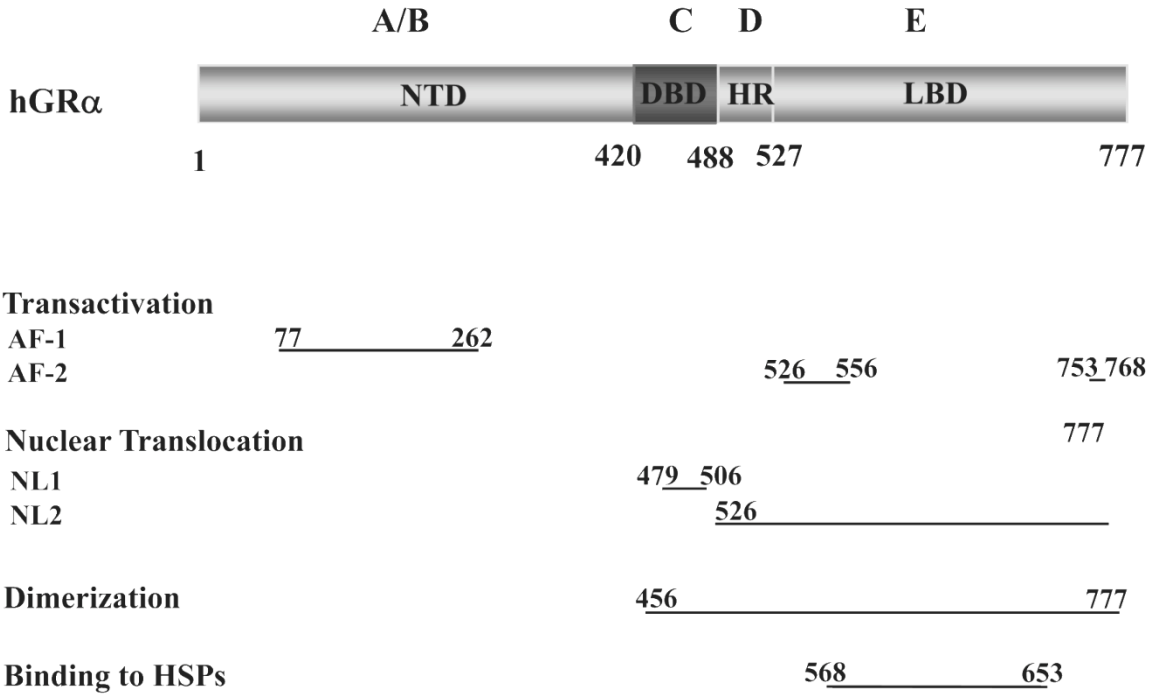

Figure 1-2 Schematic domain structure of human GRα: The hGRα consists of a NTD, DBD, HR and LBD. For transactivation two activation factors exist within the NTD and the LBD, respectively. The nuclear translocation sequences can be found in the DBD/HR as well as HR/LBD domains. Dimerization requires DBD, HR and LBD. The binding to Hsps needs the LBD. NTD (A/B), N-terminal domain; DBD (C), DNA-binding domain; HR (D), hinge region; LBD (E), ligand-binding domain; AF, activation function; NL, nuclear localization; Hsps, heat shock proteins. The indicated numbers refer to the position of amino acids in GR. Image taken from Nicolaides[14].

The glucocorticoid receptor is mainly located in the cytoplasm. For correct folding, the GR exists as a multimeric protein complex. Hsp70 binds to LBD of GR as a first step in GR folding. This binding is accelerated by Hsp70 co-chaperone Hsp40 that joins the ATP-bound form of Hsp70. In a further step, a dimer of Hsp90 is attached to the Hsp70-Hsp40-GR complex. This multimeric chaperone complex is called the foldosome. Maturation of hGR is a complex process and is reviewed extensively by Vandevyver[20]. The mature hGR receptor consists of Hsp90, p23 and immunophillin FKBP51 (FK506

binding protein 51). After ligand binding inhibitory FKBP51 is exchanged to FKBP52, which is postulated to favor GR activity (Figure 1-3)[14, 20]. p23 is a co-chaperone for Hsp90 that maximizes receptor hormone-binding ability and stabilizes Hsp90 conformation[21].

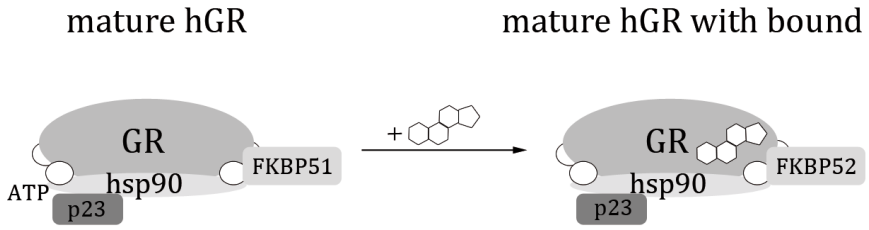

Figure 1-3 hGR complex in bound / unbound conformation: The multimeric chaperone complex of mature hGR (left) and after binding to GC (right) is shown. FKBP51/52, FK506 binding protein 51/52. Image modified from Vandevyver[20].

1.1.2.2.Mode of action of the glucocorticoid receptor – nuclear translocation, transactivation and transrepression

Nuclear translocation

GCs can influence gene expression via the GR after translocation of the GR into the nucleus. After binding of a GC, the GR undergoes a conformational change and exposes the nuclear localization sequences NL1 and NL2. The GR is rapidly imported into the nucleus with NL1 ($t_{1/2}$ = 4-6 min) whereas NL2 mediates slower and incomplete nuclear import ($t_{1/2}$ = 45-60 min)[14, 20]. Recently, it was proposed that Hsp90 is important for translocation into the nucleus, therefore Echeverría et al. suggested a dissociation from Hsp90 of the GR not until inside the nucleus[22]. Other studies reported, that components of the GR complex are involved in GR trafficking. In the absence of Hsp90, nuclear translocation is still possible, but delayed. A diffusion-like process of the nuclear import is discussed when Hsp90 is absent[20].

The nuclear import machinery for the GR is depicted in Figure 1-4. Mature GR consists of an Hsp90 dimer, p23 and immunophillin FKBP51. Upon binding of freely diffusing GC to the GR, FKBP51 is exchanged to FKBP52, which binds to dynamitin, a subunit of the microtubule-dependent motor complex. This complex is called transportosome. After binding of dynamitin, the GR multimeric protein complex moves along the cytoskeleton towards the nuclear pore complex (NPC). If the cytoskeleton is disrupted and Hsp90 is absent, it will not delay nuclear import. Hence, the cytoskeleton and Hsp90 are not required for localization of the multimeric protein complex to the NPC. When Hsp90 is not present, GR moves towards the NPC by diffusion[20]. Importins recognize NLS through their C-terminal cargo-binding domain. Importins are large proteins (90-130 kDa) that

bind to cargo-NLS and translocate it into the nucleus. They contain an N-terminal RanGTP-binding domain that binds to RanGTP in the nucleus and releases the cargo. Importin 7, 8 and α/β mediate GR translocation. It is described that importin β and Nup62 (nuclear pore glycoprotein) interact with GR and parts of the multimeric protein complex, like Hsp90, p23 and FKBP52. This emphasizes the postulated dependence of the multimeric chaperone complex of the GR in nuclear translocation[20].

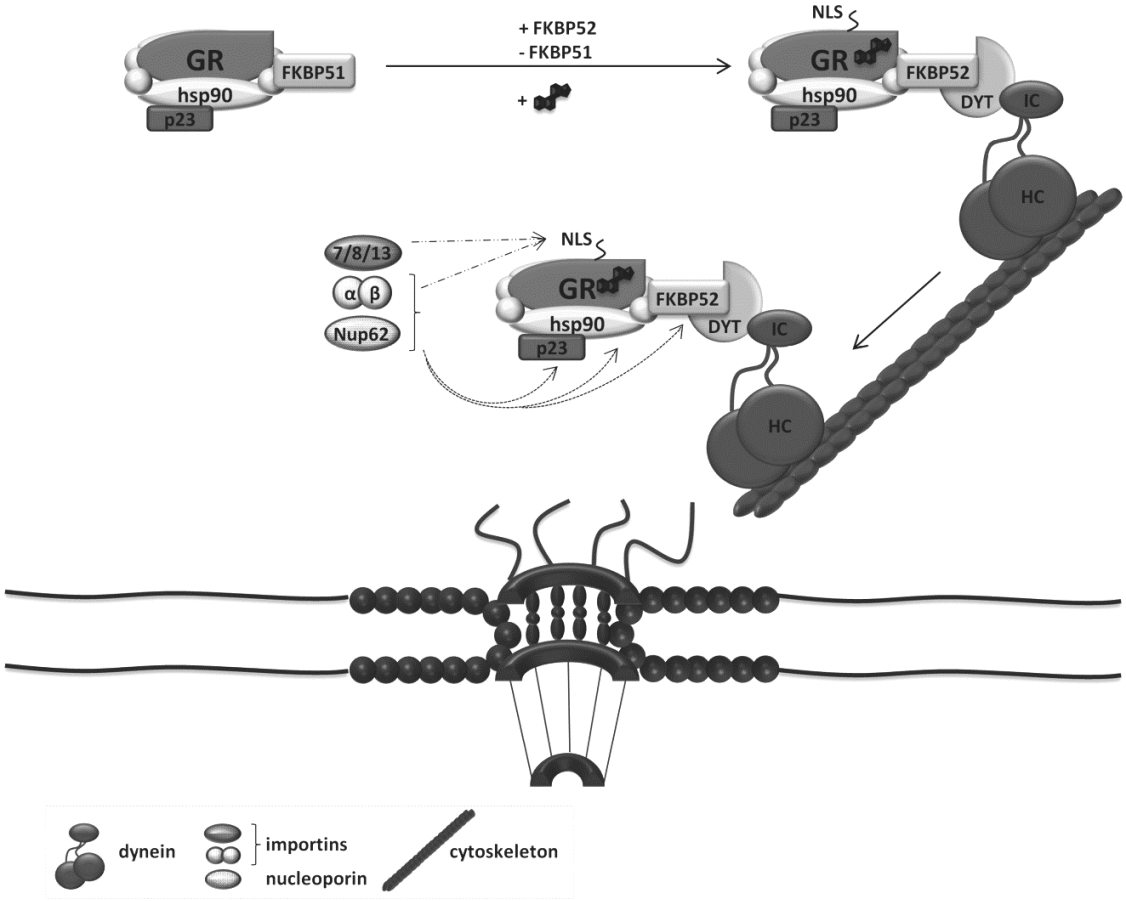

Figure 1-4 Nuclear import of GR: The activated GR multimeric complex binds to dynamitin that transports the complex to the nuclear pore. Nuclear pore complex components recognize NLS from GR and are able to translocate the multimeric complex into the nucleus. NLS, nuclear localization signal; DYT, dynamitin; IC, interchain, HC, heavy chain of dynein. Image taken from Vandevyver[20].

Transactivation

After GR translocation into the nucleus, the receptor can dimerize and bind to glucocorticoid receptor response elements (GRE). GRE are hexameric palindromic base pairs that are separated by three base pairs. The attachment of the GR to the GRE will transactivate corresponding genes. Most genes regulated by transactivation are involved in metabolic processes[17, 23].

The AF-1 and AF-2 domains of the GR interact with coactivators that bridge the DNA-bound GR to the transcription initiation complex. The transmission signal can than be processed to the RNA polymerase II. The coactivators are p300 and CBP (cAMP-

responsive element-binding protein (CREB)-binding protein), p300/CBP associated factor (p/CAF) and the p160 family of coactivators like steroid receptor coactivator-1 (SRC-1). The p160 family binds to AF-1 and AF-2 domains of the GR and directs p300 and CBP as well as p/CAF to the promoter region. The p160 family exhibits an intrinsic histone acteyltransferase (HAT) activity that can decondensate chromatin. RNA-polymerase II can therefore initiate transcription. Besides the mentioned coactivators, GR interacts with other chromatin modulators to initiate transcription (for review see Nicolaides et al.[14]). A scheme of the GR transactivation is depicted in Figure 1-5 left.

Another possibility of gene activation is the protein-protein interaction of GR with other transcription factors (TF). If the gene contains promoters for GR and other TFs, it is called a composite promoter and can activate gene transcription as well (Figure 1-5 left lower panel).

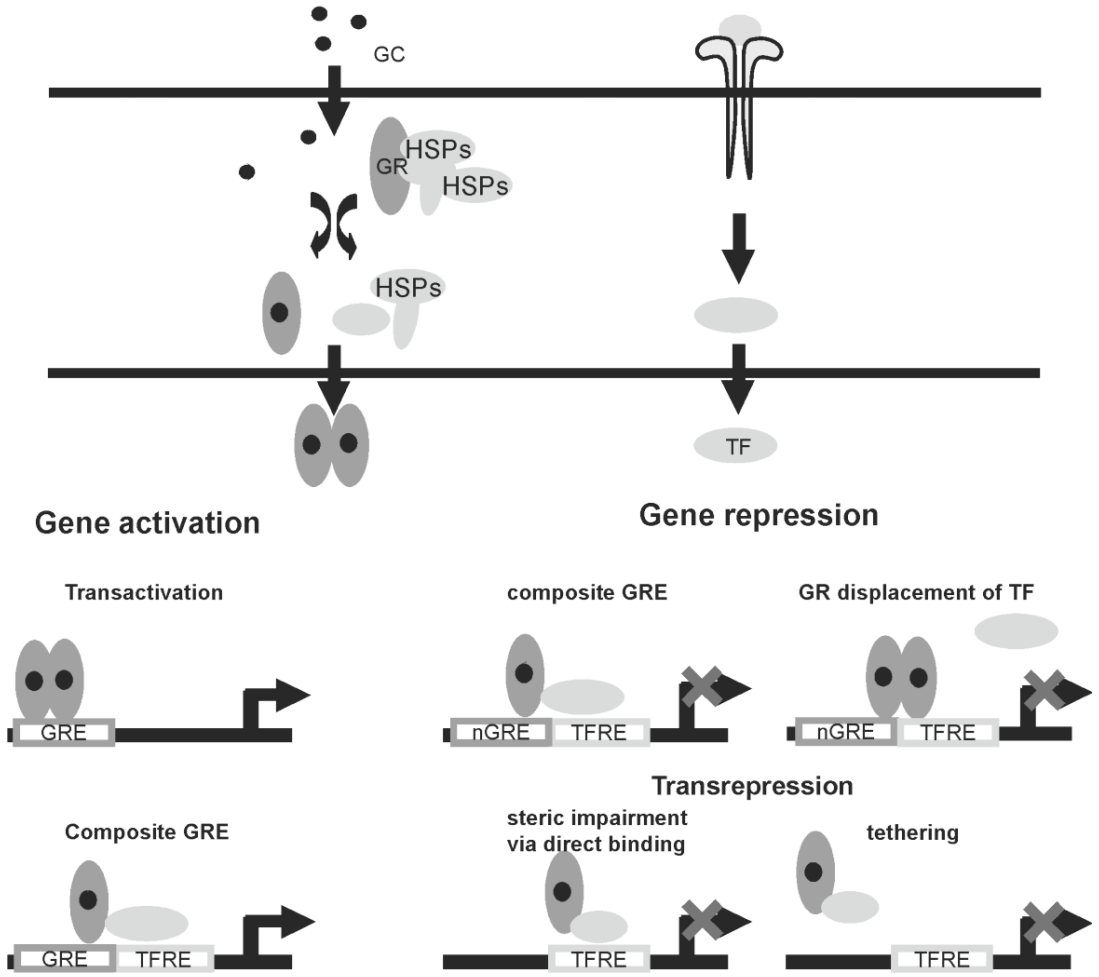

Figure 1-5 Transactivation and transrepression of the GR: Transactivation (left): The dimerized GR binds to GRE and initiates transactivation, or monomeric GR attaches to TF and the resulting complex binds to GRE and TFRE to start transcription. Transrepression (right): The dimerized GR binds to nGRE and TFRE, whereas monomeric GR binds to TF and the resulting complex binds to nGRE and TFRE. The GR can also bind to TF leading to steric impairment or the GR binds to TF hampering the binding to TFRE resulting in transrepression. nGRE, negative glucocorticoid receptor response element; TFRE, transcription factor response element. Image taken from Labeur[17].

Transrepression

Glucocorticoids repress inflammation stimuli mostly through transrepression. There are two different modes of transrepression, protein-protein interaction of the GR with the TF on the TFRE (steric impairment) or inhibition of the TF without DNA-binding (tethering) (Figure 1-5 right lower panel). Other gene repression modes are through composite GRE at negative GRE (nGRE) or GR displacement of TF and binding of GR to nGRE[14, 17]. nGRE correspond only poorly to GRE, therefore the tethering mechanism is more likely[2]. A prominent example of different GR gene transcription mode of actions can be depicted in the inhibition of NF-κB (nuclear factor kappa light chain enhancer of activated B cells) and AP-1 (activator protein 1)[24, 25]. For a more detailed understanding, the repression of NF-κB signaling through the GR is discussed (Figure 1-6).

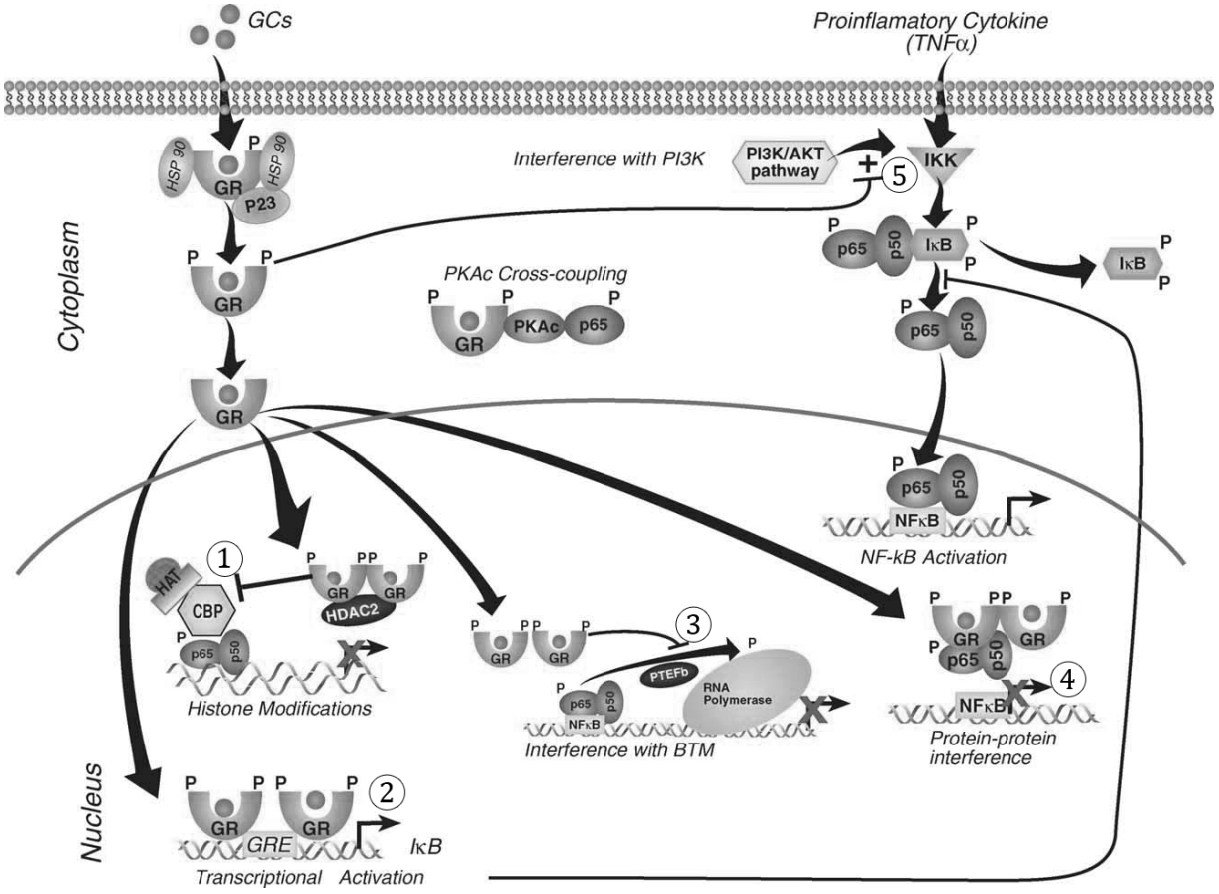

Figure 1-6 Repression of NF-κB signaling by GR: GCs can inhibit NF-κB expression through various pathways: 1) The binding of the GR to HDACs inhibits NF-κB promotor activity. 2) An increase of IκB expression is possible in certain cell types. 3) Dimerized GR can bind to PTEFb to inhibit phosphorylation of RNA-polymerase II and therefore gene transcription. 4) Dimerized GR can inhibit TF p65/p50 of NF-κB leading to gene repression. 5) The GR can interfere with the PI3K pathway resulting in an increase in IKK expression and therefore a transrepression of NF-κB. P-TEFb, transcriptional elongation factor that phosphorylates C-terminal domain (CTF) of RNA polymerase. Image taken from Smoak[24].

NF-κB is a transcription factor that plays an important role in the inflammatory response and associated disorders. It consists predominantly of a heterodimer, p50 and p65. When proinflammatory cytokines like TNFα (tumor necrosis factor α) are exposed

to cells, NF-κB will be activated. Therefore, inhibitory NF-κB opponent IκB (inhibitor of NF-κB) is phosphorylated by IKK (IκB kinase) and degraded by the proteasome, releasing the nuclear localization signal of NF-κB resulting in the translocation of the latter into the nucleus. Inside the nucleus, the heterodimer will bind NF-κB specific response elements leading to gene expression of inflammatory genes such as TNFα, IL-1β (interleukin 1β) and COX-2 (cyclooxygenase)[2, 24].

GCs will influence NF-κB gene expression through various pathways. In certain cell types, GC can transactivate IκB expression (Figure 1-6 2), which refrains NF-κB in the cytosol by masking its NLS and reducing NF-κB target gene transactivation[2, 26-29]. Tethering of the GR to NF-κB p65 subunit is another repression process, which is independent of NF-κB DNA-binding, IκB expression and NF-κB site occupancy (Figure 1-6 4)[2, 24, 27]. Furthermore, NF-κB gene expression is prevented via recruiting histone deacetylase (HDAC) 2 to the NF-κB/CBP complex by GCs (Figure 1-6 1). This leads to a decrease of acetylation of inflammatory gene promoters and therefore to a less favorable promoter conformation[2, 24, 27]. GCs may also interfere with phosphatidyl-inositol 3-kinase (PI3K), which negatively modulates IKK leading to a reduced NF-κB activity (Figure 1-6 5). Furthermore, cross-repression of GR and NF-κB through protein kinase A (PKA) is possible, suggesting a reciprocal antagonism between GR and NF-κB[24]. Additionally, GR interferes with the phosphorylation of C-terminal domain (CTD) of PTEFb (transcriptional elongation factor) that phosphorylates the CTD of RNA-polymerase II to stimulate transcriptional elongation (Figure 1-6 3)[24].

1.1.3. Nongenomic pathway

The classical genomic pathway cannot explain all of the observed effects of glucocorticoids. The translocation of the ligand-bound GR into the nucleus and the start of gene transcription takes at least 30 min, but more likely hours to days[11]. Therefore, another mode of action for glucocorticoids is discussed, the nongenomic pathway. The nongenomic mode of action was first described by Hans Selye in 1942[30]. He noted fast occurring effects of steroid hormones such as anesthesia in rats minutes after application[13].

Several classifications of the nongenomic pathways were described over the years. Up-to-date is the classification from Buttgereit. There are most likely three possible nongenomic pathways: The cytosolic glucocorticoid receptor (cGR), the membrane-bound GR (mGR) and interaction of GCs with the cellular membrane[5, 11, 16, 19, 16, 18]. If

there are other possible pathways remains to be elucidated. It is possible that direct GC-protein interactions occur.

1.1.3.1.Cytosolic glucocorticoid receptor (cGR)

The cytosolic glucocorticoid receptor (cGR) is identical to the GR. Observations showed that GC effects mediated through the cGR are sensitive to RU486, a GR antagonist, and insensitive to actinomycin D, a transcription inhibitor. Therefore, the GR is involved in the interaction, but not in protein transcription, suggesting another mode of action for the GR. One example for the cGR occurrence is the rapid inhibition of arachidonic acid release after dexamethasone treatment. Arachidonic acid is a precursor of prostaglandins and leukotriens and hence involved in many inflammatory diseases. Upon binding of epidermal growth factor (EGF) to its membrane receptor, cytosolic phospholipase A2 (cPLA2) is activated leading to arachidonic acid release. This pathway might be regulated by chaperones or co-chaperones from the multimeric GR protein complex. Src (tyrosine kinase sarcoma family) was identified to be released rapidly from the Hsp90-GR complex and therefore might be a possible candidate for rapid inhibition of arachidonic acid release after dexamethasone treatment[11, 16, 18, 19].

1.1.3.2.Membrane-bound glucocorticoid receptor (mGR)

The membrane-bound glucocorticoid receptor (mGR) was not identified with usual immunofluorescent imaging techniques. It was rather necessary to apply a more sensitive technique using magnetofluorescent liposomes in order to detect the mGR[11]. Buttgereit et al. identified approximately 10 % of monocytes and B-lymphocytes as mGR positive[12, 31]. The detection was performed using cGR antibodies. Hence, it was hypothesized that mGR is a splice variant of cGR[16, 19]. Overexpression of GR did not lead to an increased number of mGR on the cell surface, suggesting that mGR is not a cGR that is transported to the cell surface. It is more likely that mGRs, like membrane-bound estrogen or progesterone receptors, localize to the cellular membrane after post-translational modifications[32].

Buttgereit et al. identified a correlation between disease activity in rheumatoid arthritis patients and occurrence of mGR-positive monocytes[16, 19]. T-cells display the main target for immunosuppression rendered by glucocorticoids[12]. After stimulation of the T-cell receptor (TCR), lymphocyte-specific protein tyrosine kinase p56lck (Lck) and p59fyn (FYN) are activated and phosphorylate the TCR. Lck and FYN are members of the tyrosine kinase sarcoma family (Src; pp60c-src) and important players of the TCR-

mediated signal transduction. Dexamethasone can inhibit those important mediators within minutes, resulting in GR-dependent immunosuppression. This immuno-suppression was also observed in downstream signaling pathways including p38 MAPKs, protein kinase B (PKB) and protein kinase C[33].

1.1.3.3.Interaction with cellular membranes

For GC concentrations exceeding 30 mg prednisone-equivalent, interactions of GCs with cellular membranes can be detected. GCs can change physicochemical properties of membranes through intercalation. Membrane-associated proteins will be affected and membrane permeability and lipid peroxidation is influenced. The interaction between plasma membrane and GCs in immune cells leads to reduced calcium and sodium transport through the membrane. This is thought to contribute to immunosuppression and reduced inflammation[16]. An example for this kind of interaction is the inhibition of mast cell degeneration in allergic asthma. Upon crosslinking of the IgE receptor by the antigen, exocytosis in mast cells is induced resulting in allergic reactions. GCs reduce Ca^{2+} elevation and therefore inhibit exocytosis of mast cells decreasing the allergic reaction[34].

GCs can also increase the mitochondrial proton leak through interaction with the mitochondrial membrane. The induced proton leak as well as the inhibition of oxidative phosphorylation result in a diminished ATP production. In immune cells, ATP is necessary among others for cytokine synthesis, antigen processing and presentation. The reduction of ATP in immune cells might also lead to anti-inflammatory and immunosuppressive effects of high-dose GCs[11, 16].

1.1.4. Development of glucocorticoid ligands for therapeutic use

Cortisol is the human endogenous glucocorticoid. It has typical structure characteristics such as the α-ketol function at position 17, the α,β-unsaturated keto function at position 3 and the oxygen function at position 11 (Figure 1-7). Synthetic GCs have been developed that are distinguishable by their affinity to the GR or mineralcorticoid receptor, the bioavailability and the biological halftime. Several modification strategies are presented in Figure 1-7. The double bond between C(1) and C(2) increases GR specificity over the mineralcorticoid receptor about 10 times and is absent in endogenous cortisol, but mostly present in synthetic GCs. At C(3) and C(20) the keto function is essential for GR affinity. An increase in GR affinity can be obtained through modifications at C(16), C(17), C(9α) and C(6α). The affinity of the GC to the GR can be

extended through acetalization and ketalization at C(16) and C(17), respectively. Esterification at C(21) causes a complete loss of GR activity and is used for prodrugs that will be activated by esterases inside the human body[35].

With the help of these modifications, GCs became important therapeutic agents used enormously in inflammatory diseases such as rheumatic arthritis, asthma and bowel disease. Long-term treatment with GCs can cause diverse side effects like osteoporosis, diabetes, fat redistribution, weight gain and hypertension[7, 8]. Research is targeted at identification of new glucocorticoids that have distinct mode of actions with a better side effect profile[8]. In the past years, especially GC derivatives were used that exhibited transrepression but no transactivation properties[9]. As it is described in section 1.1.2.2, transactivation can also lead to anti-inflammatory gene expression. For example, the induction of IκB expression inhibits the activation of NF-κB and acts anti-inflammatory. If transactivation is abolished, the GC derivatives do not display a full anti-inflammatory profile like dexamethasone[7]. Specific transrepression and transactivation adverse and beneficial effects are depicted in Figure 1-8[36]. The aim would be to increase beneficial effects like anti-inflammatory and immunosuppressive actions and eliminate adverse side effects like Cushing's syndrome, hypertension and diabetes.

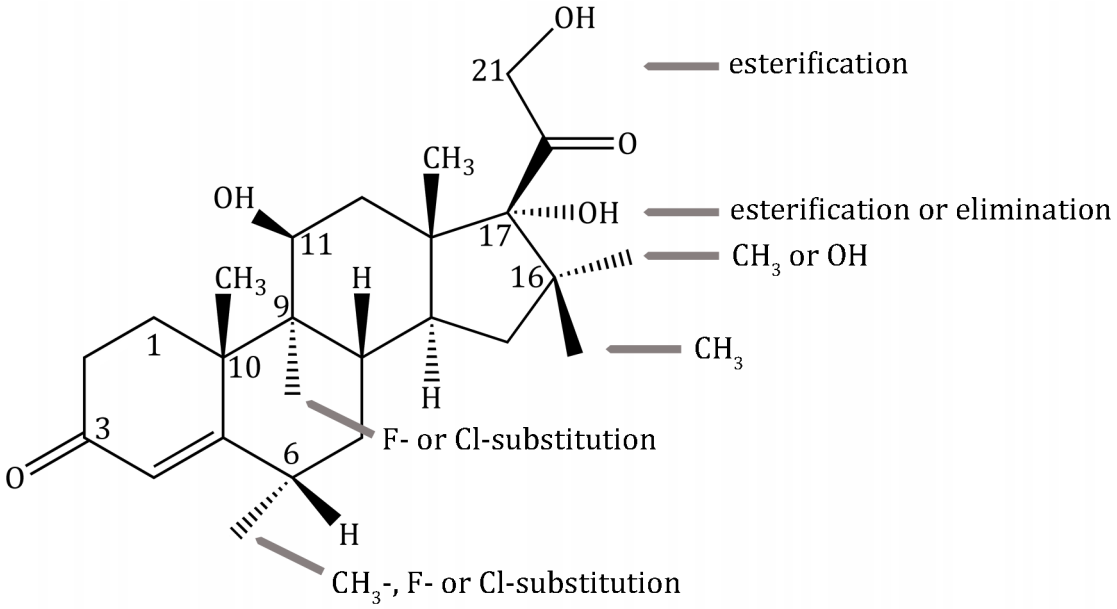

Figure 1-7 Structure activity relationship of GCs: The typical GC characteristics are C(17) α-ketol function, α,β-unsaturated ketofunction at C(3) as well as oxygen function at C(11). The GR affinity is elevated when C(16), C(17), C(9α) and C(6α) are modified. An acetalization or ketalization at C(16) / C(17) leads to an extended GR affinity, whereas an esterification at C(21) causes a complete loss of GR activity. Image modified from Steinhilber[35].

The group of Du et al. found a ginsenoside, Rg1 that shows anti-inflammatory characteristics in acute and chronic inflammatory animal models with an estrogen-like

activity. Unlike dexamethasone, Rg1 does not impair osteoblast differentiation or proliferation that may be due to the estrogen-like activity[7].

Furthermore, nitrosteroids like NO-prednisolone have been developed. NO is additionally released and synergizes in anti-inflammatory potency. In animal models, nitrosteroids induce less osteoporosis[6, 16, 36]. Moreover, liposomal encapsulated GCs were developed. Liposomes will accumulate specifically at inflammation sites leading to less off-target effects. Unfortunately, long cycling polyethyleneglycans result in a hypersensitivity in 10 % of the patients. Hence, the identification of long-cycling GCs will be the next step in identification of selective GR agonists (SEGRA)[6, 16, 18, 31, 36].

Endogenous cortisol displays an ultradian rhythm with an hourly pulsation in expression. In the early morning hours between 3:30 – 9:00 am, GR is expressed the highest. Morbus Addison's patients do not have an endogenous cortisol level and need to substitute cortisol. Patients will take the highest dose in the morning and lower doses midday and in the evening. Due to the non-pulsative application of the GC, a lot of side effects appear. They have a twice-elevated mortality rate compared to healthy humans. For those patients, more selective drugs would be an increase of life outcome. Even more, a pulsatile dosage form would decrease the undesired side effects[37, 38].

Development of improved pulsatile dosage forms and more selective GR ligands would lead to a better awareness of life and life outcome, respectively for patients with rheumatic diseases as well as Morbus Addison.

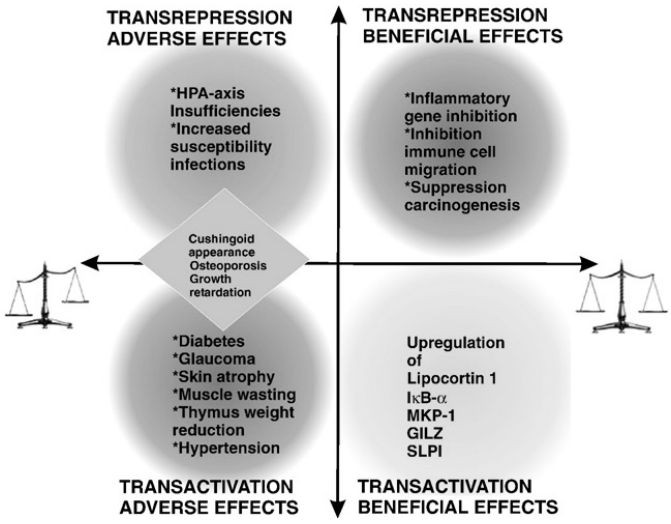

Figure 1-8 Transactivation and transrepression: beneficial vs. adverse effects: The development of new GR agonists will require an increase in transrepression and transactivation beneficial effects like anti-inflammatory and immunosuppressive actions by upregulation of IκB-α. Adverse effects occurring in transrepression and transactivation events like the Cushing's syndrome, diabetes and hypertension should be decreased or abolished. Image taken from De Bosscher[36].

1.2. The target-fishing approach

Most of the active compounds used in modern medicine are small molecules. Although some drugs were used over decades, the exact molecular targets are not yet discovered. Examples for these small molecules are glucocorticoids. In order to identify possible glucocorticoid targets, an appropriate technique had to be developed.

In the 1950s Leonard Lerman was able to purify enzymes with small molecule inhibitors. This was the first step in the development of the target-fishing approach with small molecules[39]. In 1989, Harding et al. carried out the first successful target-fishing approach and were able to identify the target for FK506, the FK506 binding protein (FKBP)[40]. In adjacent years, several other drug-protein interactions were successfully identified that could explain for example liver toxicity of the Parkinson drug tolcapone[41].

1.2.1. Principle of the target-fishing approach

The target-fishing approach in this thesis is a molecular approach and is often referred to as chemical proteomics. For this technique, small molecules are immobilized onto a matrix and incubated afterwards with different cell lysates or tissues (Figure 1-9). After the incubation, immobilized matrices are washed to remove unspecific protein binding and subsequently eluted with an excess of free small molecule or with denaturing conditions[39]. The identification of specific targets from a complex eluate is difficult and requires adequate negative controls.

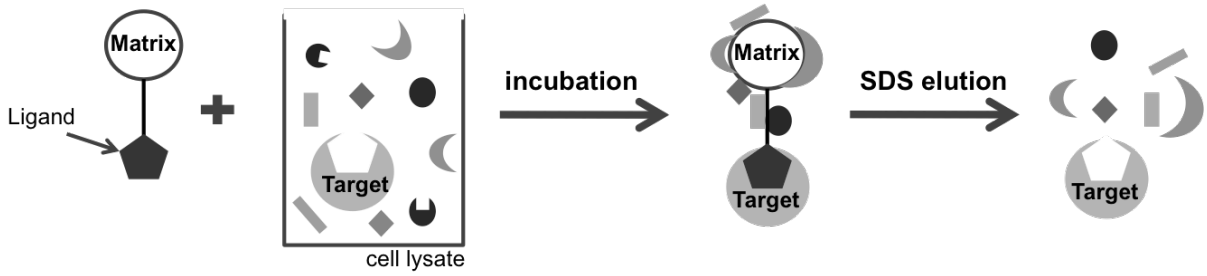

Figure 1-9 Principle of the target-fishing approach: A ligand coupled to a linker is immobilized onto a matrix and incubated with a cell lysate containing several unspecific proteins and the target candidate. After incubation, several proteins attach non-specifically to the matrix and the linker whereas only a few (here: one) proteins bind to the ligand specifically. After SDS elution all proteins are removed from the cell surface and are present in the eluate. The separation of non-specific from specific targets is difficult and requires accurate negative controls.

The advantages of chemical proteomics are an unbiased proteome-wide experimental setting of natural proteins and their binding partners at an endogenous expression level. The setup allows the identification of post-translational protein modifications (PTM). Additionally, the experiment can be carried out in a cellular environment and disease-relevant (primary) cells and tissues can be used (Figure 1-10)[42].

On the other hand, disadvantages are a high background, the chemical modification for immobilization of the drug, especially if an active metabolite for target identification is required[39, 42]. Rix et al. were able to obtain good results with small molecules of at least 300 kDa. The risk of destroying biological important functions of smaller compounds is elevated. If the compound does not contain any functional group for immobilization, an analogue has to be synthesized that still exhibits biological activity. In addition, low abundant proteins such as membrane proteins are hard to identify. Usually, a prefractionation step of the extract such as a membrane isolation is necessary. Furthermore, the choice of an optimal negative control is important to eliminate unspecific matrix-protein or matrix-linker interaction partners. It would be optimal if the negative control was an analogue of the drug that does not exhibit biological activity. In order to eliminate unspecific interaction partners, specific elution with an excess of the free drug can be applied. Usually, high concentrations of the drug have to be used that are often not soluble in aqueous solutions. Therefore, other target identification or quantification techniques need to be applied. (Figure 1-10)[42].

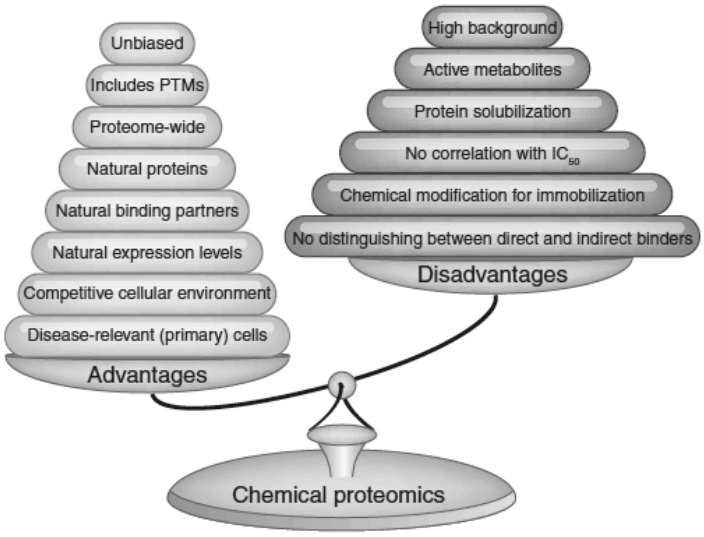

Figure 1-10 Chemical proteomics: advantages and disadvantages: The advantages are an unbiased proteome-wide experimental setting of natural proteins, their binding partners at an endogenous expression level as well as the inclusion of post-translational modifications (PTM). Additionally, the setup is in a competitive cellular environment and disease-relevant (primary) cells can be used. On the other hand, disadvantages are the high background, the chemical modification for immobilization of the drug, especially the choice of an active metabolite. The amount of bound interaction partner does not correlate to the IC_{50} and distinguishing between direct and indirect binders is not possible. Image taken from Rix[42].

1.2.2. Different target identification techniques

In recent years, several other target identification techniques were established like the activity-based protein profiling (ABPP), which is similar to chemical proteomics. In ABPP, the small molecule or the linker contains a reactive group that can covalently attach to the target protein. The linker could contain a photoactivatable, radioactive or biotinylated residue to attach to the target protein[39, 43]. Such approaches based on photoaffinity labeling were synthesized and evaluated from Martin Golkowski (Prof. Ziegler, Eberhard-Karls Universität Tübingen) in the "Promotionsverbund: Identifizierung und Validierung von Arzneistofftargets"[44]. The enhancement of a capture compound approach as described by Fischer et al. is a promising technique. The photoactivatable biotinylated ligand is incubated with a pool of possible target proteins and attaches covalently to its interaction partners. The drug-protein mixture can then be precipitated with its biotinylated tag on streptavidin beads. Elution will only detect covalently bound drug-protein interaction[41]. The catch and release two-photon-process approach has a similar technique but uses other chemical features[45]. For affinity purification techniques like the chemical proteomics and ABPP the main challenge displays the study of the structure activity relationships in order to find the right position for immobilization of the small molecule onto a matrix.

Therefore, Pramod Sawant (Prof. Maier, Eberhard-Karls Universität Tübingen) photo-crosslinked a small molecule onto an affinity matrix to identify protein candidates[46]. No chemical modification is necessary, because the crosslinker forms highly reactive carbens upon UV-light exposure that bind irreversibly to the small molecule[47]. The amount of differently immobilized beads is unknown as well as the exact position where the immobilization and therefore the chemical modification occurred.

Lomenick et al. used an approach to identify novel targets for small molecules by applying the drug affinity responsive target stability (DARTS) technique. A small molecule will stabilize a protein and protect it from protease degradation. Therefore, all non-specific proteins will be eliminated by the protease and only target proteins will remain that can be separated by SDS-PAGE and analyzed with MS. A chemical modification is not necessary and analyzing lower affinity interactions is possible. Several proteins like stress proteins are evolutionary robust against protease digestion and a partial instability against proteases is required for the DARTS technique[39, 48]. A similar technique was developed in 2010 and measures the changes in folding and thermodynamic stability induced by binding of the small molecule to proteins. The rate

of methionine that is oxidized is measured and the technique is named stability of protein from rates of oxidation (SPROX). A drawback of this approach is the requirement of methionine in the peptides analyzed as well as that only the most abundant proteins in a sample can be examined[39].

1.2.3. Quantification possibilities of the target-fishing approach

The amount of bound protein to an immobilized compound compared with the negative control cannot be obtained with the used technique above. Therefore, special techniques can be applied. The isotope-coded affinity tag (ICAT) technology is depicted in Figure 1-11 A. The active (dark grey) and the inactive (light grey) compounds are labeled via ICAT after elution and can be analyzed by mass spectrometry (MS) and bioinformatics. Isobaric tags for relative and absolute quantification (iTRAQ) can be employed for kinase inhibitors (Figure 1-11 B). Kinobeads contain unspecific kinase inhibitors immobilized to a matrix. Different concentrations of free kinase inhibitors are incubated with cell lysate and all non-targeted proteins are then captured by the kinobeads. The non-targeted kinases that did not bind to various concentrations of kinase inhibitor are labeled using iTRAQ and compared with each other. MS and bioinformatics can obtain the quantification of proteins. iTRAQ does not need proliferating cells to incorporate the label and can also be used for tissue samples (Figure 1-11 B)[49, 50].

The stable isotope labeling of amino acids in cell culture (SILAC) technique labels cells proteome-wide before elution. The immobilized compound is incubated in presence or absence of its soluble counterpart with light labeled or heavy labeled cell lysate, respectively. The MS and bioinformatics analysis is performed afterwards (Figure 1-11 C)[42].

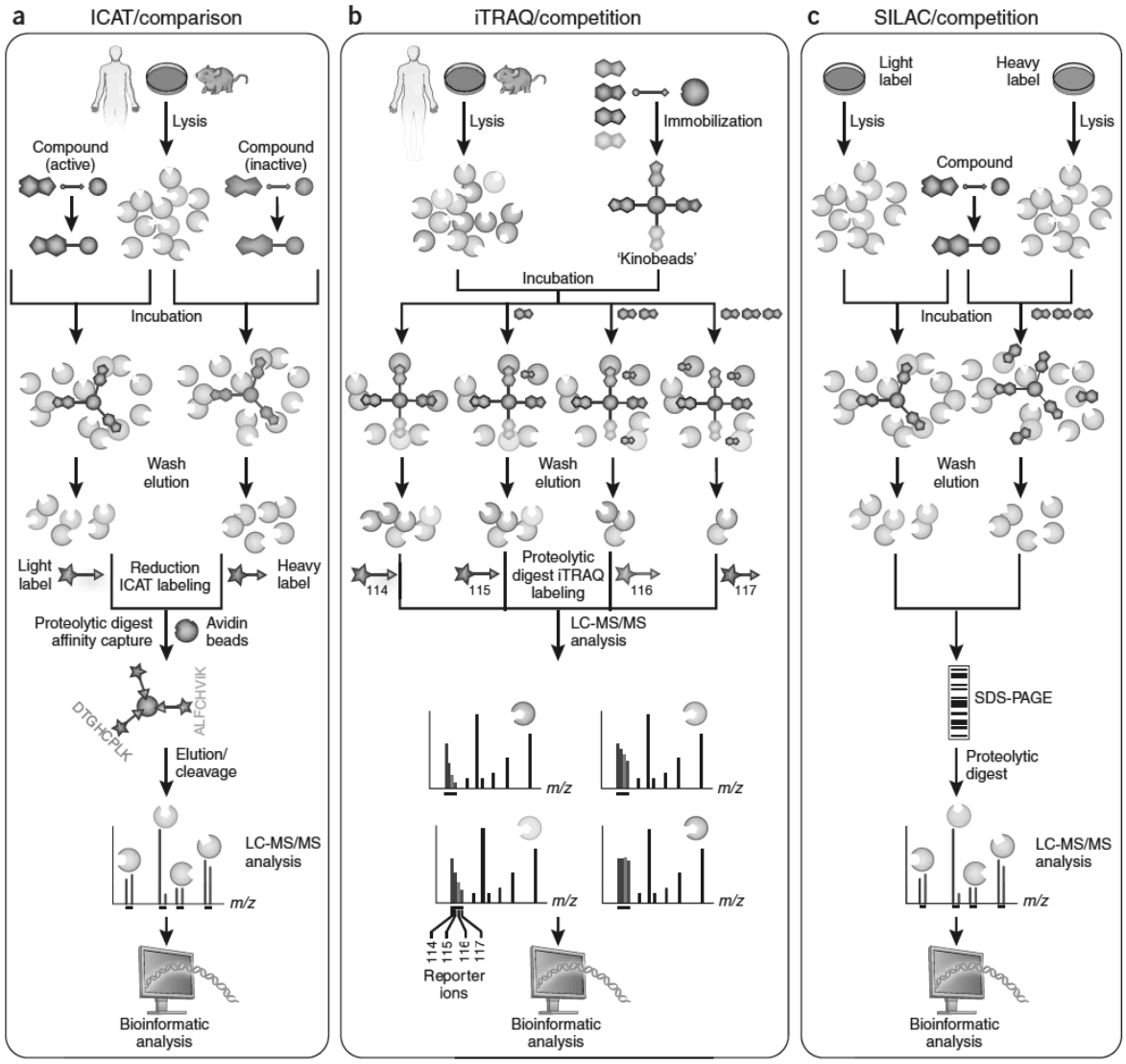

Figure 1-11 Quantification possibilities of the target-fishing approach: A: Comparing active (dark grey) and inactive (light grey) compounds by labeling via the isotope-coded affinity tag (ICAT) technology of the eluted proteins. Samples are labeled with a reactive thiol group containing either heavy or light isotopes. B: Kinobeads contain unspecific kinase inhibitors bound to a matrix. Different concentrations of free kinase inhibitors are incubated with cell lysate and all non-targeted proteins are then captured by the kinobeads. The non-targeted kinases that did not bind to various concentrations of kinase inhibitor are labeled using isobaric tags for relative and absolute quantification (iTRAQ) technique. C: Two different cell populations are grown separately using stable isotope labeling of amino acids in cell culture (SILAC) technique. Afterwards the immobilized compound is incubated in presence or absence of soluble compound with light labeled or heavy labeled cell lysate, respectively. Image taken from Rix[42].

1.3. Aim of this work

The focus of the present thesis was to identify and validate possible target proteins of the glucocorticoids (GC) dexamethasone and hydrocortisone. Glucocorticoids exert a variety of actions and especially the fast occurring nongenomic effects are not yet understood on a molecular basis. A suitable technique for the identification of drug-protein interaction partners is the target-fishing approach. Therefore, GCs had to be first chemically modified to exhibit a reactive group that was then used to immobilize the compound onto a solid matrix. Derivatives, which had proven to exhibit bioactivity in an

in vivo system, were afterwards processed to the target-fishing experiment using the GC-coupled beads as baits for proteins in human cell lysates. Different elution techniques had to be tested and further adjusted. The following identification of possible target proteins had to be performed with proteomic approaches.

A promising candidate, who was assigned for both dexamethasone and hydrocortisone, is peroxiredoxin 1 (Prdx1). An interaction between glucocorticoids and peroxiredoxin 1 had not been described yet and needed to be further investigated by a direct binding assay. Prdx1 is an important scavenger of hydrogen peroxide inside the cell. This peroxidase activity had to be tested in presence or absence of dexamethasone. The other major function of Prdx1 occurs under oxidative stress when Prdx1 decamers exhibit a molecular chaperone function. The influence of GCs on the oligomerization state of Prdx1 had to be elucidated. Furthermore, Prdx1 and GCs both influence the PI3K signaling pathway. Prdx1 protects phosphatase and tensin homologue (PTEN) from inactivation of its Cys residue and therefore negatively regulates Akt phosphorylation[51]. The incubation of GCs leads to a decrease in Akt phosphorylation[52]. The exact molecular target of the GC-induced negative regulation of Akt phosphorylation is unknown and hence had to be addressed in a further experiment. In the end, the detailed characterization of a possible Prdx1-GC interaction should define more precisely the molecular role of Prdx1 in glucocorticoid-induced cellular activities with respect to its peroxidase function, its chaperone activity and its involvement in Akt signaling.

2. Materials and Methods

2.1. Buffer, reagents and compounds

All buffer substances and reagents were purchased from Roth (Karlsruhe, Germany) unless noted otherwise.

Target-fishing approach	
Washing buffer 4.0	0.1 M sodium acetate, 0.5 M NaCl, pH 4.0
Washing buffer 8.0	0.1 M Tris, 0.5 M NaCl, pH 8.0
Lysis buffer	50 mM Hepes, pH 7.4, 200 mM NaCl, 1 mM EDTA, 0.5 % (v/v) Triton X-100, 1:200 protease inhibitor cocktail (Sigma Aldrich, Munich, Germany)
Binding buffer	50 mM Hepes, pH 7.4, 200 mM NaCl, 1 mM EDTA
Molybdate buffer	50 mM Hepes pH 7.4, 200 mM NaCl, 20 mM Na_2MoO_4
Protein analysis	
SDS loading dye	125 mM Tris (pH 6.8), 4 % (w/v) SDS, 10 % (v/v) β-ME, 20 % (v/v) glycerol, 0.02 % (w/v) bromophenol blue
SDS running buffer	25 mM Tris, 192 mM glycine, 0.1 % (w/v) SDS, pH 8.3
Coomassie staining solution	30 % (v/v) ethanol, 10 % (v/v) acetic acid, 0.25 % (w/v) Coomassie Brilliant Blue G-250
Coomassie destaining solution	30 % (v/v) ethanol, 10 % (v/v) acetic acid
Fixation solution	40 % (v/v) ethanol, 10 % (v/v) acetic acid
Sensitizing solution	30 % (v/v) ethanol, 8 mM $Na_2S_2O_3$, 500 mM sodium acetate
Silver solution	30 mM $AgNO_3$
Developing solution	235 mM Na_2CO_3, 0.0185 % (v/v) formaldehyde, 0.0025 % (w/v) $Na_2S_2O_3$
Stopping solution	5 % (v/v) acetic acid
Western blotting buffer	20 mM Tris, 150 mM Glycin, 0.05 % (w/v) SDS, 20 % (v/v) methanol
TBS	100 mM Tris, 100 mM NaCl, pH 7.4
TBS-Tween	TBS, 0.1 % (v/v) Tween 20
PBS	10 mM Na_2HPO_4, 1.8 mM KH_2PO_4, 140 mM NaCl, 2.7 mM KCl, pH 7.4
PBS-Tween	PBS, 0.1 % (v/v) Tween 20
PBS-T	PBS, 0.1 % (v/v) Triton X-100
PBS-ST	PBS, 0.02 % (w/v) SDS, 0.1 % (v/v) Triton X-100
Molecular Biology	
E. coli DH5α (Invitrogen, Darmstadt, Germany)	F- φ80*lac*ZΔM15 Δ((*lac*ZYA-*arg*F)U169 *rec*A1 *end*A1 *hsd*R17(r_k^-, m_k^+) *pho*A *sup*E44 *thi*-1 *gyr*A96 *rel*A1 λ^-
E. coli BL21 (DE3) (NEB, Frankfurt, Germany)	*fhuA2 [lon] ompT gal (λ DE3) [dcm] ΔhsdS λ DE3 = λ sBamHIo ΔEcoRI-B int::(lacI::PlacUV5::T7 gene1) i21 Δnin5*
SOC medium	2 % (w/v) peptone, 0.5 % (w/v) yeast extract, 10 mM NaCl, 2.5 mM KCl, 10 mM $MgCl_2$, 10 mM $MgSO_4$, 20 mM glucose
LB medium	1 % (w/v) peptone, 1 % (w/v) NaCl, 0.5 % (w/v) yeast extract

LB-Amp	LB medium with 100 µg/mL ampicillin
LB-Kan	LB medium with 34 µg/mL kanamycin
LB agar	1 % (w/v) peptone, 1 % (w/v) NaCl, 0.5 % (w/v) yeast extract, 1.5 % (w/v) agar
	Protein Purification
Prdx1 buffer A	10 mM Na_2HPO_4, 20 mM NaCl, 1.8 mM KH_2PO_4
Prdx1 buffer B	10 mM Na_2HPO_4, 1 M NaCl, 1.8 mM KH_2PO_4
Prdx1 SEC buffer	20 mM Tris pH 7.5
TrxR Extraction buffer	20 mM Tris pH 7.5, 10 mM NaCl, 1 mM EDTA, 1:200 protease inhibitor (Sigma Aldrich, Munich, Germany), 5 mM DTT
TrxR buffer A	20 mM Tris pH 7.5, 1 mM EDTA
TrxR buffer B	20 mM Tris pH 7.5, 1 mM EDTA, 500 mM NaCl
TrxR SEC buffer	20 mM Hepes pH 7.0, 1 mM EDTA
His A	20 mM Tris pH 8.0, 100 mM NaCl, 10 mM imidazole
His B	20 mM Tris pH 8.0, 100 mM NaCl, 500 mM imidazole
Trx1 SEC buffer	20 mM Tris pH 8.0, 100 mM NaCl
	Prdx1 activity assay
TrxR activity buffer	50 mM Hepes, pH 7.0, 1 mM EDTA, 200 µM NADPH, 0.8 µM yTrxR, 90 µM oxidized yTrx
Prdx1 activity buffer	50 mM Hepes, pH 7.0, 1 mM EDTA, 200 µM NADPH, 1.5 µM yTrx, 0.8 µM yTrxR
	Akt assay
Akt buffer	50 mM Hepes, pH 7.4, 200 mM NaCl, 1 mM EDTA, 10 µM Na_2MoO_4, 1 mM Na_3VO_4, 10 mM NaF, 2.5 mM sodium pyrophosphate, 1 % (v/v) Triton X-100, 1:200 protease inhibitor cocktail (Sigma Aldrich, Munich, Germany)

2.1.1. Glucocorticoid derivatives

Glucocorticoids (GC) and sex hormones (SH) were purchased from Fagron (Barsbüttel, Germany). Martin Golkowski from the group of Prof. Ziegler (Eberhard-Karls Universität, Tübingen) synthesized the compounds with linker depicted in Figure 2-1. The synthesis is described in his thesis[44]. The denotations of compounds can be found in section 8.1.

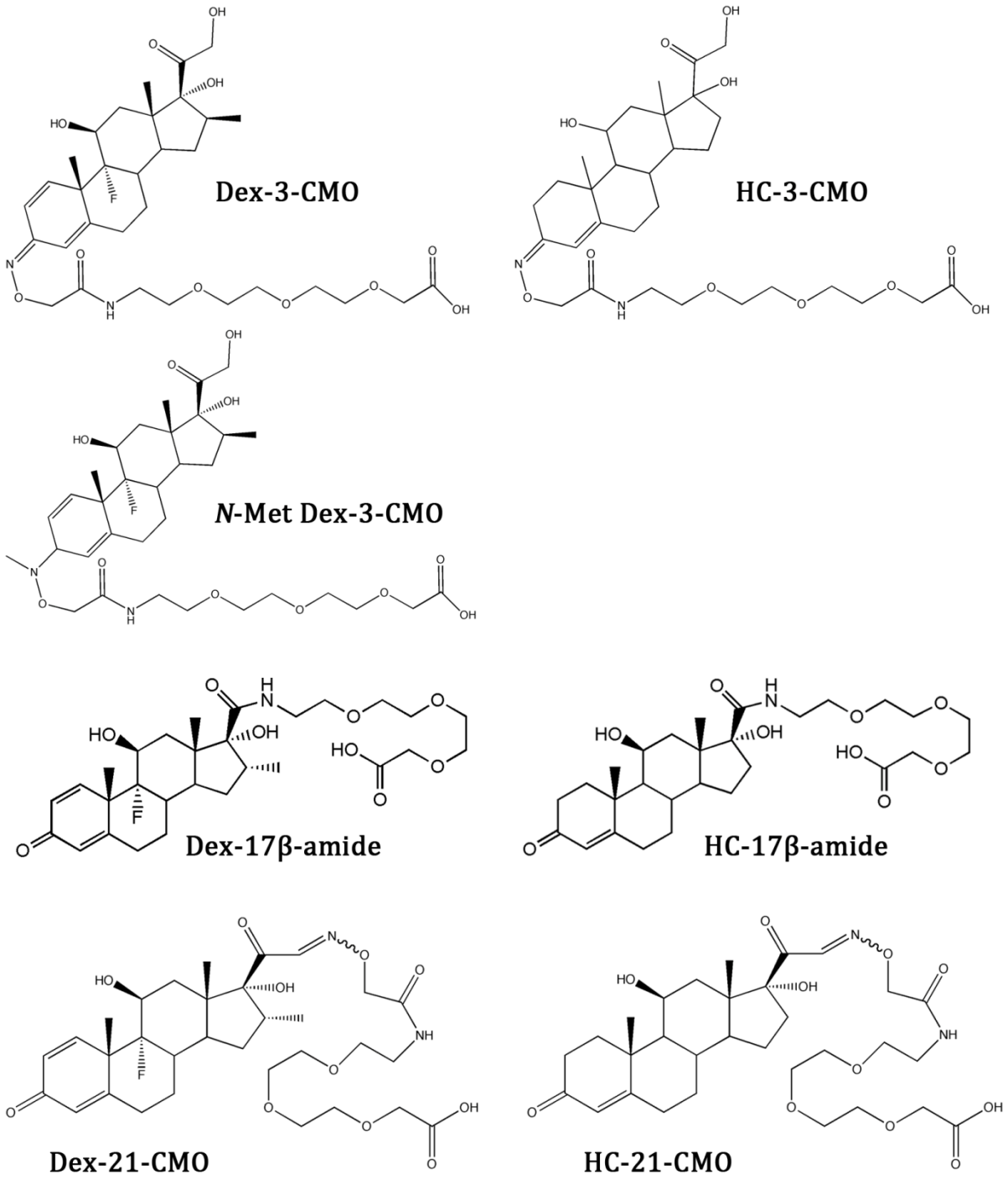

Figure 2-1 Chemical structures of compounds and their abbreviations used in this thesis: denotation of compounds can be found in section 8.1. The synthesis is described in Martin Golkowski's thesis[44].

2.2. Cell biochemistry

All cell culture reagents were purchased from PAA (Paching, Austria), Sarstedt (Nümbrecht, Germany) and BD Biosciences (Heidelberg, Germany) unless indicated otherwise.

2.2.1. Cell lines

Cells were cultured in Dulbecco's modified Eagle's medium high glucose (4.5 mg/mL) (DMEM) supplemented with 10 % fetal calf serum, 2 mM glutamine and 0.1 mM gentamicin (=standard medium). Cells were grown at 37 °C and 8.5 % CO_2.

Thawing of cells from liquid nitrogen was performed at 37°C. Cells were collected in standard medium supplemented additionally with 10 % of fetal calf serum and centrifuged (200*g, 5 min, room temperature). The supernatant was discarded and cells were transferred to 25 cm^2 cell culture flasks with standard medium supplemented additionally with 10 % fetal calf serum. For next 2-3 subpopulations, standard medium supplemented additionally with 10 % fetal calf serum was used.

Subpopulations were obtained after washing cells in 75 cm^2 cell culture flasks with 10 mL Hank's without Ca^{2+}/Mg^{2+} and detachment with 2 mL trypsin containing EDTA. Detachment was followed in a transmitted-light microscope and stopped with standard medium. Cells were transferred to new cell culture flask according to their growth behavior.

Freezing of cells for storage occurs in the gas phase of liquid nitrogen. Cells from 75 cm^2 cell culture flasks were trypsinated, collected in 10 mL standard medium and centrifuged (200*g, 5 min, room temperature). The supernatant was discarded and cells were collected in 3.8 mL standard medium supplemented additionally with 10 % fetal calf serum and 10 % DMSO. 1.9 mL cell suspension per cryovial was used and first frozen at -20°C for 2 h, then overnight at -80°C before long-term storage in the gas phase of liquid nitrogen.

GM5756T are human transformed fibroblasts and were provided by Stephen Gould (John Hopkins University, Baltimore).

A549 (ATCC: CCL-185™) cells are human alveolar adenocarcinoma cells and were used in most experiments. This cell line is widely used to study the biology of GC effects[53]. HEK293T (ATCC: CRL-1573) cells are transformed human embryonic kidney cells. HepG2 (ATCC: HB 8065) cells are human hepatocellular carcinoma cells. All these cells were a gift from Prof. Probst (Eberhard-Karls Universität Tübingen).

2.2.2. Transfection of human cells

Transfections of human A549 cells were performed with jetPEI (polyplus Transfection, Illkirch, France). JetPEI is a lipofection reagent. It consists of positively charged polyethyleneimine molecules that can form complexes with DNA. Cells will incorporate complexes via endocytosis. Inside the cell, the plasmid will be transcribed and translated and the cell will overexpress the desired protein.

Transfections were performed according to manufacturer's instruction. 24 h prior to transfection, cells were seeded onto coverslips in 10 cm^2 dishes. The exact plasmid to jetPEI ratio was 1 µg to 2 µL and cells were incubated with 5 mL DMEM supplemented with 10 % fetal calf serum and 2 mM glutamine for 3-4 h at 37°C and 8.5 % CO_2 before switching to standard medium.

2.2.3. Immunofluorescence microscopy

Immunofluorescence is a visualization method for cellular proteins with the help of antibodies. In this thesis, indirect immunofluorescence was used. First antibodies are directly targeted against the target protein, whereas the second fluorescence-labeled antibody is directed against the first antibody.

24 h after transfection (section 2.2.2) with a GFP tagged glucocorticoid receptor, cells were exposed to glucocorticoid derivatives (Figure 2-1). All compounds were dissolved in 50 % ethanol, the negative control was 50 % ethanol. Dexamethasone derivatives were used at 1 µM. Hydrocortisone exhibits a lower binding affinity to the GR[35] and therefore 25 µM for HC derivatives was used. After 15 min, cells were subjected to immunofluorescence as described earlier.[54] Shortly, cells were fixated with for 20 min 3 % (v/v) formaldehyde prior to permealizing cells for 5 min with 1 % (v/v) Triton X-100. GFP was detected using monoclonal α-AFP antibodies (3E6) (1:250) (QBiogene/MP Biomedicals, Illkirch, France) for 30 min followed by a 10 min incubation with AlexaFluor-488 coupled α-mouse antibodies (1:300) (Molecular Probes/Invitrogen, Darmstadt, Germany). In between, washing steps with Dulbecco's PBS were performed. Immunofluorescence images were acquired using a Zeiss Axiovert 200M fluorescence microscope equipped with an AxioPlanApochromat 1.4 63x oil objective and an AxioCamMRm camera in combination with AxioVision 4.7.2 software. Statistical analysis was performed with Prism, Version 5.0d (GraphPad Software, Inc.).

2.2.4. Stable isotope labeling of amino acids in cell culture

Stable isotope labeling of amino acids in cell culture (SILAC) was first described by Ong et al.[55]. The principle of SILAC is shown in Figure 2-2[56]. The cellular proteome is metabolically labeled with heavy isotopes of essential amino acids. After five cell doublings most (≈ 95 % at least) of the proteins will have incorporated the heavy amino acids. Heavy isotopes do not have a different chemical structure and will display the same characteristics as non-labeled amino acids. After labeling of amino acids, cells were lysed and the classical or the soluble competition SILAC experiment, respectively, was performed. The eluates were mixed and afterwards digested with trypsin and the peptide mixture was subjected to mass spectrometry (MS). In the MS spectra, differences in the m/z ratio become visible, because heavy isotopes will introduce a mass shift.

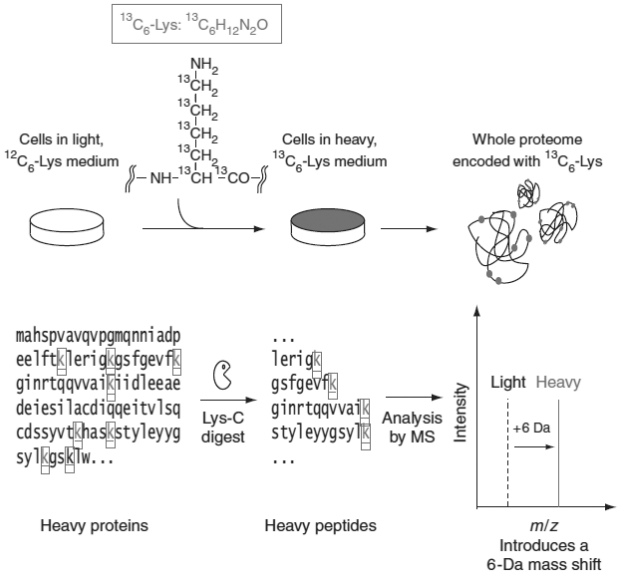

Figure 2-2 SILAC principle: Cells are grown with heavy non-radioactive isotopes of essential amino acids arginine and lysine that will be incorporated by the cell into its proteome. After digestion, heavy polypeptides can be distinguished by a 6 Da mass shift from light to heavy isotopes in a mass spectrum. Image taken from Ong[56].

For SILAC experiments, cells were cultured in Dulbecco's modified Eagle's medium (DMEM) high glucose (4.5 mg/mL) without arginine, lysine and glutamine supplemented with 10 % fetal bovine serum, 1 % L-glutamine and 1 % penicillin/ streptomycin. For heavy labeled cells amino acids were labeled with Lys 8 and Arg 10, for medium with Lys 4 and Arg 6 and for light labeled cells amino acids were not labeled with heavy isotopes (Lys 0 and Arg 0) (Cambridge isotopes, England). Cells were incubated at 37 °C and 8.5 % CO_2.

For all SILAC experiments, an incorporation test was performed prior to each experiment. Cells were grown for five subpopulations in order to check for full incorporation of the heavy isotopes. Cells were harvested from a 7 cm^2 dish with 300 µL containing a mix of 6 M urea and 2 M thiourea for 10 min on ice and afterwards vortexed intermittently for 5 min. Cells were centrifuged (16100*g, 4°C, 10 min) and protein concentration was determined from the supernatant. 30 µg protein of heavy or medium labeled cell lysate were tested by the Proteome Center Tübingen for full incorporation[56].

2.3. Target-fishing

2.3.1. Immobilization of compounds to Toyopearl AF Amino 650M beads

For all pull-down assays, Toyopearl AF Amino 650M beads (Tosoh, Japan) were used. The compounds used for immobilization were usually GC-3-CMO derivatives. 70-130 µmol amino functions are present on 1 mL bead surface. In order to saturate all amino functions, a 3.3 excess of the appropriate compound (Figure 2-1) was used. For the negative control acetic acid was coupled to the beads. All washing steps during immobilization were performed three times with 5 mL solvent. Before use, beads were washed in a sintered glass filter with DMSO (dimethyl sulfoxide). 330 µmol of the GC derivative and 1.5 mmol DIC (*N,N'*-diisopropylcarbodiimide) were added to a total volume of 3 mL bead suspension. The suspension was rotated for 60 h at room temperature. The chemical reaction is depicted in Figure 2-3. Afterwards, beads were washed with DMSO and 50 % (v/v) dioxan. In order to block the remaining free amino groups, 1.5 mmol DIC was added together with 150 µmol acetic acid to 3 mL solvated beads. The beads were rotated for 4 h at room temperature. Next, beads were washed with 50 % dioxan/water mixture, followed by an alternating washing step between Washing buffer pH 4.0 and Washing buffer pH 8.0 to remove unspecific ionic binding. After washing with pure water and 20 % ethanol, beads were stored under 20 % ethanol at 4°C until use.

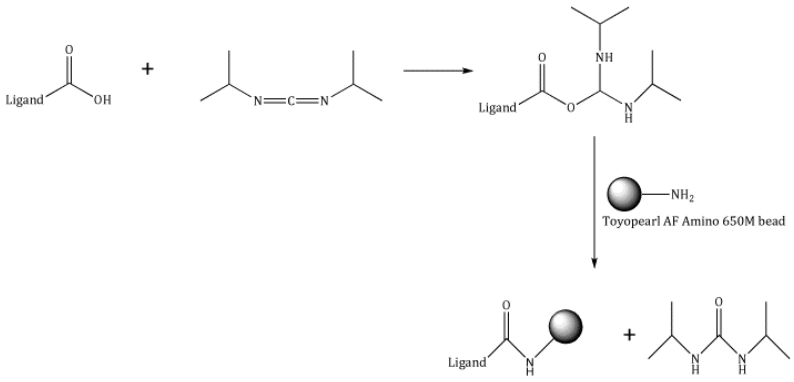

Figure 2-3 Immobilization of ligands to amino functionalized beads using DIC technique: Carboxylic acid function of ligand is activated by incubation with carbodiimide. The immobilization to the bead surface results in an amide.

The reaction with DMSO as a solvent in the immobilization protocol leads to the Pfitzner-Moffatt reaction, an oxidation occurring on primary and secondary alcohols[57]. As the compounds hydrocortisone and dexamethasone both exhibit hydroxyl groups, it is likely that a modification occurred. Therefore, dioxan was used instead in the last experiments. Unless otherwise noted, usually immobilized beads with DMSO were used.

2.3.2. Immobilization capability

In order to test the immobilization capabilities for each of the used compounds, the supernatant of the derivatives after immobilization was collected, 1:100 diluted and then subjected to an UV spectrum. The absorption of the resulting peak was determined and used for calculations. Compounds present in the supernatant did not bind to the bead surface and can be discarded from originally applied compound. The µmol/mL compound loading was calculated with a calibration curve of GC-3-CMO derivatives.

2.3.3. Cell disruption for target-fishing

Cells from two 175 cm^2 cell culture flasks were trypsinated, collected in standard medium and centrifuged for 5 min at 200*g. After discarding the supernatant, cells were washed twice with Hank's with Ca^{2+}/Mg^{2+}. Cells were frozen at -80°C after determination of moist mass (approximately 0.2 g) until further use.

Prior to each fishing experiment the cell lysate was prepared freshly. Five times more Lysis buffer was used than the determined moist mass. Per 200 mg cells, 300 µL glass beads were added. The cell suspension was vortexed 10 times for 30 s and rested in between for 30 s on ice. Afterwards, the suspension was incubated for 15 min on ice for further lysis. A centrifugation was performed at 800*g for 10 min at 4°C to remove the glass beads. The supernatant was transferred to reaction tubes and centrifuged at 16000*g for 30 min at 4°C. The obtained supernatant is referred to as cell lysate.

2.3.3.1. Membrane isolation for target-fishing

For membrane isolation, 9 flasks with 175 cm^2 of confluent cells are required. Cells were washed with 13 mL Hank's without Ca^{2+}/Mg^{2+} and trypsinated. Afterwards, cells were collected in 10 mL DMEM medium and centrifuged at 200*g for 5 min. Subsequently to discarding the supernatant, cells were washed twice with 32 mL Hank's with Ca^{2+}/Mg^{2+}. After determination of moist mass in mg, the five fold amount of Binding buffer with 1:200 protease inhibitor cocktail was used. Per 200 mg cells, 300 µL glass beads were added. The cell suspension was vortexed 10 times for 30 s and rested in between for 30 s on ice. Afterwards, cells were incubated for 15 min on ice for further lysis. After centrifugation at 800*g for 10 min at 4°C, an ultracentrifugation of the supernatant at 100000*g for 1 h was performed. The resulting supernatant was used as the cytosolic fraction. The obtained pellet was resuspended with half of the volume Lysis buffer compared to the supernatant. The resuspended pellet was rotated for 30 min at 4°C and subjected afterwards to ultracentrifugation at 100000*g at 4°C for 1 h. The supernatant displays the solubilized membrane fraction.

A pull-down assay as described in section 2.3.4 was performed separately for cytosol and membrane fractions. 1 mL cytosolic and 0.5 mL membrane fraction were used for target-fishing, respectively.

2.3.4. Target-fishing protocol

For target-fishing, 50 µL of pure immobilized beads (section 2.3.1) were centrifuged at 8000*g at 4°C for 10 min. The beads were washed three times with 500 µL ddH_2O. An appropriate amount of cell lysate corresponding to ≈ 2 mg protein was used for the fishing experiment and filled to 750 µL with Lysis buffer. Incubation was performed for 4 h at 4°C on a rotator. The beads were centrifuged at 6400*g for 10 min at 4°C and washed twice with 1 mL Binding buffer containing 0.1 % (v/v) Triton X-100 and once with 1 mL Binding buffer.

Elution was usually performed with 50 µL 2 x SDS loading dye at 100°C for 5 min. After centrifugation at 16000*g (10 min, 4°C), 45 µL of the supernatant were removed, and aliquots were frozen at -20°C until further use.

For glucocorticoids, different elution techniques were established. Besides the SDS loading dye elution, urea, hydrocortisone and dexamethasone were used for more specific elutions. In case of urea, elution was performed twice with 100 µL 7.2 M urea and the eluates concentrated in a concentrator to 50 µL containing a cutoff of 5 kDa

(Millipore/Merck, Darmstadt, Germany). Hydrocortisone was purchased from Fagron (Barsbüttel, Germany) and dissolved in 50 % ethanol (14 mM), whereas a dexamethasone solution from Jenapharm (10 mg/mL) was used at 25 mM. Elution was performed accordingly to urea.

2.3.5. Binding of the glucocorticoid receptor to glucocorticoid-immobilized beads

In order to validate the binding capacity of GC-coupled beads to its endogenous receptor, a test system was established.

A GR-GFP (pK7-GR-GFP)[58] construct was transfected into A549 or GM5756T cells (section 2.2.2) and cells were harvested after 24 or 48 h. Cells were disrupted and subjected to the target-fishing approach (section 2.3.3 and 2.3.4). In the first experiments the buffer used was Lysis buffer. The results obtained with Lysis buffer were not reproducible. Molybdate secures the binding of the GR to Hsp90 upon an all-around stabilization of the GR[59]. Therefore, Molybdate buffer was used for further GR target-fishing experiments. After elution of proteins with SDS, samples were subjected to SDS-PAGE and Western blotting either with α-GR or α-GFP antibodies (sections 2.5.2.2 and 2.5.2.3).

2.3.6. Direct binding assay

After identification of a possible target protein through MS, it is necessary to confirm a specific interaction between the protein and the drug. The proteins usually get identified in a cellular context, therefore it is ambiguous whether it displays a direct interaction or an indirect interaction mediated through another protein. Hence, a direct binding assay with Prdx1 was performed. Prior to incubation with recombinant Prdx1, 50 µL pure glucocorticoid beads were blocked for 30 min with 0.5 % milk powder in Binding buffer to prevent unspecific binding to the beads. Beads were then incubated with 0.2, 0.5, 1 or 2.4 µg Prdx1 for 4 h at 4°C and washed three times with 1 mL Binding buffer. Elution was performed with 50 µL 2x SDS loading dye at 100°C for 5 min.

Another experimental setup was used for the direct binding assay with soluble competition. The principle of the soluble competition assay is described in section 2.3.8. For the soluble competition, 50 mM dexamethasone (dissolved in Binding buffer) and 10 mM hydrocortisone (dissolved in 50 % (v/v) ethanol) was used. Further, negative control-coupled beads were incubated with ethanol 50 % (v/v) in the presence or absence of 10 mM hydrocortisone. Beads were blocked for 30 min with 0.5 % milk powder in Binding buffer in presence or absence of soluble competitors. Beads were

then incubated with 2.4 µg Prdx1 for 4 h at 4°C and washed three times with 1 mL Binding buffer. Elution was performed with 50 µL 2x SDS loading dye at 100°C for 5 min.

2.3.7. Classical SILAC triple experiment

For the classical SILAC triple experiment, cells were grown for five cell subpopulations. Cell disruption and the target-fishing approach were performed as described in section 2.3.3.

For the GC experiment, 400 µL cell lysates of heavy (H) labeled cells were incubated with 50 µL pure dexamethasone-beads, medium (M) labeled cells with 50 µL pure hydrocortisone-beads and light (L) labeled cells with 50 µL pure negative control (acetic acid) beads. In the SH experiment, cell lysates of heavy (H) labeled cells were incubated with 50 µL pure testosterone-beads, medium (M) labeled cells with 50 µL pure progesterone-beads and light (L) labeled cells with 50 µL pure negative control (acetic acid) beads. Both experiments were performed simultaneously.

After 4 h incubation of GC beads with cell lysate, elution was performed with 100 µL 7.2 M urea followed by a concentration step to 50 µL eluate with a protein concentrator containing a cut-off of 5 kDa (Millipore/Merck, Darmstadt, Germany). 30 µL GC H, M, L extracts were mixed in equal amounts, as were the SH extracts. Afterwards, 30 µL samples were subjected to SDS-PAGE. The whole lane was digested with trypsin and further analyzed by EasyLC nano-HPLC (Proxeon Biosystems/Thermo Scientific, Dreieich, Germany) coupled to an LTQ Orbitrap XL mass spectrometer (Thermo Scientific, Dreieich, Germany) at the Proteome Center Tübingen. Data acquisition was performed with MaxQuant software (v1.0.14.3) by Dr. Mirita Franz-Wachtel[60].

2.3.8. SILAC soluble competition experiment

Ong first described the soluble competition strategy in 2009[61]. Usually, a so-called bead control experiment is performed as described in section 2.3.7. The limitation of such a pull-down assay is the proper use of an appropriate negative control. It should be comparable with the drug, but must lack its activity. Such a molecule is usually hard to design and has to be tested in an activity experiment. A solution to this limitation is the soluble competition technique. Here, for the positive and negative control, the same beads are compared; one in the presence of a 10 times excess of the soluble drug that is also coupled onto the beads and the other one without the soluble drug. In this experiment the negative control has exactly the same matrix and properties and will not

show any differences in activity. The experiment setting ignores all unspecific proteins that bind to the linker or beads and will focus on the important targets of the drug.

In this experimental setup, a second negative control, namely beads coupled with acetic acid, is used as described in section 2.3.1.

For the soluble competition SILAC triple experiment, cells were grown for five cell subpopulations. Cell disruption and the target-fishing approach were performed as described in section 2.3.3. After determination of the protein concentration, 2 mg cell lysate was used. All beads were immobilized with Dioxan instead of DMSO. Heavy (H) labeled cells were incubated with 50 µL pure dexamethasone-beads, medium (M) labeled cells with 50 µL pure dexamethasone-beads and Dex in solution (50 mM) and light (L) labeled cells with 50 µL pure acetic acid negative control beads. After elution with 50 µL 2x SDS loading dye at 100°C for 5 min and 1:1:1 mixing (30 µL each), proteins were subjected to SDS-PAGE and further analyzed as described in section 2.3.7.

The same experiment was performed with the drugs atorvastatin and englerin A for the group of Prof. Maier (Eberhard-Karls-Universität Tübingen), and is described in Pramod Sawant's thesis[46].

2.4. Molecular biology

All restriction enzymes were purchased from Fermentas (Fisher Scientific, St. Leon Roth, Germany). DNA concentrations were measured using their absorbance values at 260 nm with the NanoDrop ND-100 (PeqLab, Erlangen, Germany).

2.4.1. Plasmids

The plasmids used in this thesis are listed in Table 2-1.

Table 2-1: Plasmids used

Plasmid (Number)	Vector backbone	Description (Short form)	Obtained from
pET17b-Prx1 (662)	pET17b (Novagen/Merck, Darmstadt, Germany)	Human peroxiredoxin 1 (=Prdx1)	Kang (EWHA Women University, Seoul, Korea)
pET17b-yTrxR (664)	pET17b (Novagen/Merck, Darmstadt, Germany)	Yeast thioredoxin reductase (=yTrxR)	Kang (EWHA Women University, Seoul, Korea)
pYE1 (669)	pET28a (Novagen/Merck, Darmstadt, Germany)	Yeast thioredoxin 1, N-terminal His_6-tag (=yHisTrx1)	Cloned from pET17b-yTrx1
pk7-GR-GFP (667)	pk7-GFP	Human GR tagged with C-terminal GFP (=GR-GFP)	www.addgene.org (Cambridge, USA)

2.4.2. Transformation and DNA isolation

E. coli DH5α cells were transformed using electroporation. 50 µL of electrocompetent cells were mixed with 100 ng plasmid and pipetted in an electroporation cuvette (Biozym, Hessisch Oldendorf, Germany). After exposure to 2500 V for 6 ms in an electroporator (Eppendorf, Hamburg, Germany), cells were treated immediately with 500 µL warm SOC medium and incubated for 30-45 min at 37°C on a bacterial shaker at 180 rpm. 30 µL cell suspension were plated onto an LB-agar plate with corresponding antibiotics and incubated at 37°C overnight. DNA preparation was performed after inoculation of a single colony to LB-Amp or LB-Kan medium and incubation overnight at 37°C. DNA preparation was carried out using mi-Plasmid Miniprep Kit (Metabion, Martinsried, Germany) or NucleoBond® XtraMidi Kit (Machery-Nagel, Düren, Germany) according to the manufacturer's protocol.

The identity of isolated DNA was controlled by restriction analysis.

Table 2-2 shows the reaction mixture used for digestion of pET17b-yTrx1 and pET28a.

Table 2-2 Restriction analyses mixture: Incubation was performed for 1 h at 37°C.

Component	Amount
DNA	1 µg
*Nde*I	1 µL
*Xho*I	2 µL
Buffer (O)	2 µL
H_2O	ad 20 µL

2.4.3. Cloning

Purification of pET17b-yTrx1 described by Kim et al.[62] was not successful, therefore pET17b-yTrx1 was cloned into a vector containing an N-terminal hexahistidin tag (pET28a)[63]. After transformation of DH5α cells with either pET17b-yTrx1 or pET28a, DNA was isolated and a restriction analysis was carried out at 37°C overnight (

Table 2-2). The yTrx1 fragment and the pET28a vector were separated using agarose gelelectrophoresis. For pET17b-yTrx1 a 1.5 % gel and for pET28a a 0.65 % gel was used. The bands were cut out and DNA was extracted from agarose by centrifugation (16000*g, 15 min, 4°C) using a filter tube (Costar Spin-X®, Corning, Amsterdam, Netherlands).

Ligation was performed using 75 ng of the digested plasmid pET28a and different molar ratios of insert DNA (yTrx1). Molar ratios of insert:vector used in this thesis were 5:1, 10:1 and 20:1. 1 µL of ligase was added, together with 2 µL of ligase buffer and

supplemented with water to a total volume of 20 µL. Ligation mixtures were incubated for 16 h at 16°C in a thermocycler (Biometra, Göttingen, Germany).

Before transformation and restriction (see section 2.4.2), samples were dialyzed for 20 min against water on a nitrocellulose filter (0.025 µm VSWP; Millipore/Merck, Darmstadt, Germany).

Prior to use, plasmids were sequenced for confirmation at Eurofins MWG Operon, Ebersberg, Germany. The plasmid is depicted in section 8.5.

2.5. Protein preparation and protein analysis

2.5.1. Purification of proteins

Protein purification was performed on a ÄKTA Purifier system (GE Healthcare, Munich, Germany) with Unicorn 5.01 software. Size exclusion chromatography was carried out with either a Pharmacia LKB system (GE Healthcare, Munich, Germany) or an FPLC BioLogic DuoFlow system (Bio-Rad, Munich, Germany).

Proteins were recombinantly expressed in *E.coli* BL21 (DE3) cells with a plasmid containing the target protein and an antibiotic resistance. 4 mL of an overnight pre-culture was used to inoculate 400 mL of LB-medium with the appropriate antibiotic. Cells were grown until optical density at 600 nm was 0.6. All plasmids are based on the lac operon, which can be regulated by the addition of isopropyl-β-thiogalactopyranoside (IPTG). Therefore, 1 mM IPTG was added to induce protein expression. The bacterial cells were incubated overnight on a bacterial shaker with 180 rpm at 37°C. Cells were harvested by centrifugation at 8000*g for 10 min at 4°C. For protein purification, cells were lysed with a sonicator (Branson Digital Sonifier®; PGC scientifics, Palm Desert, USA) or a French Press (Emulsiflex, Avestin, Mannheim, Germany). After lysis and centrifugation, cells were loaded onto ion exchange or His-tagged columns (GE healthcare, Munich, Germany) for further purification steps. Additionally, proteins were purified using size exclusion chromatography.

2.5.1.1. Peroxiredoxin 1

Cells were grown in 800 mL LB-Amp medium as described in section 2.5.1. Cells were resuspended in a 10 fold excess of Prdx1 buffer A to determined moist mass in g, typically 3 g. Cell lysis was performed using a French Press. After centrifugation (12000*g, 1 h, 4°C), the supernatant was filtrated (0.45 µm) and typically 30 mL loaded onto a 1 mL HiTrap FF SP column. Prdx1 was eluted with Prdx1 buffer B using the

protocol listed in Table 2-3. The obtained fractions were analyzed for Prdx1 by SDS-PAGE and Coomassie staining and fractions containing the desired protein were pooled.

Table 2-3 Protocol for elution of Prdx1

Step	Concentration Prdx1 buffer B (%)	Column Volume
Washing 1	0	20
Elution 1	0-100	20
Elution 2	100	20

2.5.1.2. Thioredoxin reductase

Cells were grown in 1.6 L LB-Amp medium as described in section 2.5.1. The cell pellet was resuspended in a 10 fold excess of TrxR Extraction buffer to determined moist mass typically 4 g. Cell lysis was performed using ultrasonication (40 % amplitude, 1 s on, 4 s off). After centrifugation (12000*g, 30 min, 4°C), the supernatant was treated with 1 % (w/v) streptomycin for 30 min on ice and centrifuged (12000*g, 30 min, 4°C). The supernatant was filtrated (0.45 µm) and typically 40 mL loaded onto a 1 mL DEAE FF column. TrxR was eluted with TrxR buffer B using the protocol listed in Table 2-4 ion exchange chromatography (IEX) I. The obtained fractions were analyzed for TrxR with SDS-PAGE and Coomassie staining. Fractions containing the desired protein were pooled and subjected to size exclusion chromatography on a Superdex™ 200 60/16 with TrxR SEC buffer. The obtained fractions were analyzed for TrxR with SDS-PAGE and Coomassie staining. Fractions containing the desired protein were pooled and subjected again to DEAE FF column using the protocol in Table 2-4 IEX II.

Table 2-4 Protocol for elution of TrxR

Step	Concentration TrxR buffer B (%)	Column Volume
IEX I		
Washing 1	0	20
Elution 1	0-100	40
Elution 2	100	20
IEX II		
Washing 1	0	20
Elution 1	10	10
Elution 2	20	20
Elution 3	30	30
Elution 4	40	40
Elution 5	50	50
Elution 6	100	20

2.5.1.3. Thioredoxin 1

Cells were grown in 1.6 L LB-Kan medium as described in section 2.5.1, but induction of protein expression through IPTG was carried out only for 3 h at 37°C. The cell pellet was resuspended in a 10 fold excess of His A buffer to determined moist mass typically 3 g. Cell lysis was performed using ultrasonication (40 % amplitude, 1 s on, 4 s off). After centrifugation (12000*g, 30 min, 4°C), the supernatant was filtrated (0.45 µm) and typically 30 mL loaded onto a 1 mL HisTrap column. Trx1 was eluted with His B using the protocol listed in Table 2-5. The obtained fractions were analyzed for yHisTrx1 with SDS-PAGE and Coomassie staining. Fractions containing the desired protein were pooled and subjected to size exclusion chromatography on a Superdex™ 75 with Trx1 SEC buffer.

Table 2-5 Protocol for elution of Trx1

Step	Concentration His B (%)	Column Volume
Washing 1	0	20
Elution 1	0-100	25
Elution 2	100	35

2.5.2. Protein analysis

2.5.2.1. Determination of protein concentration

Protein concentrations of the purified fractions were measured with a NanoDrop ND-100 (Peqlab, Erlangen, Germany) with the help of ε_{280} values obtained with the software ProtParam (Table 2-6)[64, 65].

Table 2-6 Extinction coefficients at 280 nm and molecular masses

Protein	ε_{280} [$M^{-1}cm^{-1}$]	M_r [kDa]
Prdx1	18700	22.1
yTrxR	24410	34.2
yHisTrx1	10095	13.4

For the determination of protein concentration of other samples, a Bradford assay was performed[66]. The Coomassie Protein assay Kit was purchased from Thermo Scientific (Dreieich, Germany) and was used according to manufacturer's instructions.

2.5.2.2. SDS-PAGE

A complex mixture of proteins can be separated by sodium dodecyl sulfate polyacrylamide gel electrophoresis (SDS-PAGE)[67]. Proteins are complexed and denaturated with the detergent SDS in a constant mass ratio of 1.4 $mg_{SDS}/mg_{protein}$. SDS incubated samples are loaded onto an acrylamide/bisacrylamide gel and separated according to protein masses.

In this thesis, protein fractions were tested for purity or the evaluation of pull-down assays was performed with SDS-PAGE. All SDS-PAGE gels contain a 12 % separating gel and a 5 % stacking gel, unless noted otherwise. All gels were run with 20 mA per gel for 1 h. Afterwards either a Coomassie or silver staining or a Western blotting was performed (section 2.5.2.3).

For Coomassie staining, gels were heated with a Coomassie staining solution and afterwards incubated for 10 min. The Coomassie destaining solution was heated and incubated for an additional 10 min.

For silver staining, gels were fixated for 30 min in Fixation solution followed by a 30 min sensitizing step with Sensitizing solution. After washing three times for 5 min with water, gels were incubated with Silver solution for 30 min. The Developing solution was applied for 2-5 minutes and the process was ended with Stopping solution.

2.5.2.3. Western blotting

In order to identify specific proteins with antibodies, proteins are transferred after the SDS-PAGE onto a membrane. After blocking the membrane with milk powder, the membrane is decorated with the first antibody targeted against a specific protein. Subsequent, a horseradish peroxidase (HRP) coupled secondary antibody is applied. When the membrane is exposed to H_2O_2 and luminol, photons are generated, that will darken a light-sensitive film.

In this thesis, for all membranes polyvinylidene fluorid (PVDF) was used unless noted otherwise. Before blotting in a semidry blotting chamber (Bio-Rad, Munich, Germany) with Western blotting buffer, the PVDF membrane was activated with pure methanol. Proteins were transferred for 1 h at 20 V and room temperature. All antibody incubation steps were performed at room temperature unless noted otherwise (Table 2-7).

Table 2-7 Antibodies used

Antibodies	Blocking solution	First antibodies	Secondary antibodies	Washing steps after incubation with antibodies
α-Prdx1; rabbit (Abcam, Cambridge, UK)	10 % (w/v) milk powder in PBS-Tween over night at 4°C	1:2000 5 % (w/v) milk powder in PBS-T 2 h	1:15000 α-rabbit (Sigma Aldrich) 5 % (w/v) milk powder in PBS-T 1 h	3x 10 min with 10 mL PBS-T
α-AktP; rabbit (Ser473, Cell signaling/NEB, Frankfurt, Germany)	5 % (w/v) milk powder in TBS-Tween 1 h	1:5000 5 % bovine serum albumin in TBS-Tween over night at 4°C	1:15000 α-rabbit (Sigma Aldrich) 5 % (w/v) milk powder in TBS-Tween 1 h	3x10 min with 10 mL TBS-Tween
α-Akt; rabbit (Cell signaling/ NEB, Frankfurt, Germany)	5 % (w/v) milk powder in TBS-Tween 1 h	1:5000 5 % (w/v) bovine serum albumin in TBS-Tween over night 4°C	1:15000 α-rabbit (Sigma Aldrich) 5 % (w/v) milk powder in TBS-Tween 1 h	3x10 min with 10 mL TBS-Tween
α-GFP; rabbit (Torrey Pines, Carlsbad, USA)	10 % (w/v) milk powder in PBS-ST 2 h	1:5000 5 % (w/v) milk powder in PBS-ST 2 h	1:15000 α-rabbit (Sigma Aldrich) 5 % (w/v) milk powder in PBS-ST 1 h	3x10 min with 10 mL PBS-ST
α-GR; rabbit (Bioworld Technology, Minneapolis, USA)	5 % (w/v) milk powder in PBS 1 h	1:500 5 % (w/v) milk powder in PBS over night 4°C	1:15000 α-rabbit (Sigma Aldrich) 5 % (w/v) milk powder in PBS-T 1h	3x10 min with 10 mL PBS-T

2.6. Peroxiredoxin activity assay

In order to characterize the role of Dex on Prdx1, a 2-Cys Prdx activity assay was performed. The principle of 2-Cys Prdx assay was described by Kim et al. (Figure 2-4)[62].

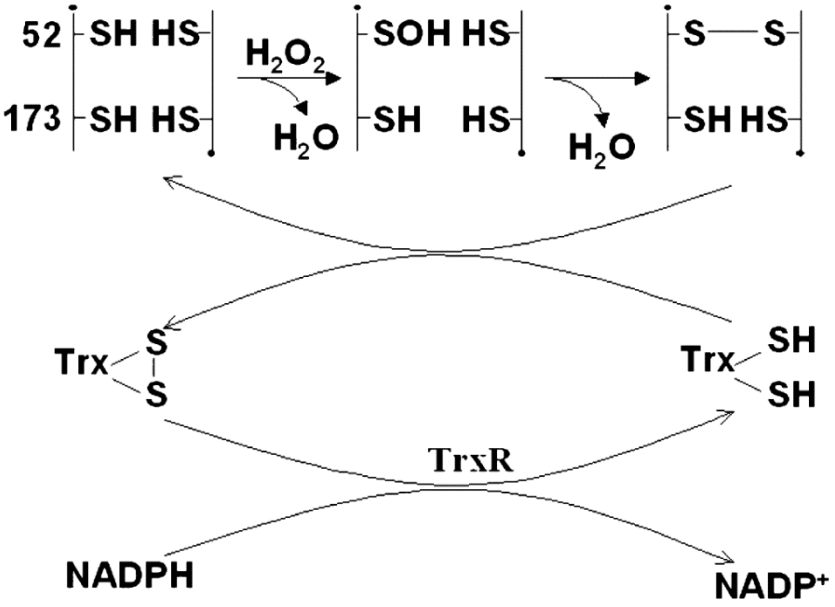

Figure 2-4 Principle of Prdx1 activity assay: Prdx1 is oxidized by H_2O_2 and forms dimers via an intermolecular disulfide bond. Thioredoxin 1 (Trx1) can reduce the oxidized Cys groups forming an intramolecular disulfide bond itself. Trx1 can be reduced by thioredoxin reductase (TrxR), which oxidizes NADPH to $NADP^+$ leading to a decrease of NADPH absorption at 340 nm. Image taken from Kim et al.[62].

Shortly, thiol groups of Prdx1 are oxidized in the presence of H_2O_2. This inactivation can be compensated with Trx1 that reduces Prdx1 and is itself oxidized. TrxR reduces in turn Trx1 and oxidizes NADPH. The reduction of NADPH to $NADP^+$ can be visualized with an ELISA reader (Tecan infinite 200, Tecan, Männedorf, Switzerland) at 340 nm.

All proteins were expressed and purified as described earlier (section 2.5.1.1-2.5.1.3). TrxR activity was tested before use as reported by Kim et al.[62]. For the Prdx1 activity assay, 1.5 µM yHisTrx1, 0.8 µM yTrxR, 200 µM NADPH, 100 µM H_2O_2 and different concentrations of Prdx1 and dexamethasone were used. Dexamethasone and Prdx1 were incubated prior to addition of yHisTrx1, yTrxR, NADPH and H_2O_2 for 15 minutes at 30°C. After addition of the above-mentioned proteins and mixing, the decrease of NADPH absorption at 340 nm was monitored every 30 s for 10 minutes. The evaluation was performed using MS Office 2008 and Prism 5.0d (GraphPad, Inc.).

2.7. Assay to investigate the signaling of Akt

For determination of the phosphorylation state of the serine/threonine kinase Akt a cell-based assay was performed. 3.84 x 10^5 cells were seeded in each well of a six-well plate 16 h prior to experiments. Cells were incubated for 15 min at 37°C, 8.5% CO_2 in presence of 1 µM dexamethasone or 25 µM hydrocortisone (in early experiments: 1 µM), 100 µM ascorbic acid (control), 2.3 nM IGF1 (positive control) or with ethanol as a negative control. Afterwards 200 µM of H_2O_2 was applied to each well (except the negative control without H_2O_2) and incubated at 37°C, 8.5 % CO_2 for 15 min. Cells were harvested in two different fashions. The experiments without phosphatase inhibitor were performed using trypsination as harvesting method, then cells were washed twice with Hanks with Ca^{2+}/Mg^{2+} and disrupted with 30 µL of cold water and frozen at -20°C until further use. For the phosphatase inhibitor experiments, cells were harvested after washing with Hanks without Ca^{2+}/Mg^{2+} with 150 µL Akt buffer that was applied for 10 min at 4°C with gentle shaking. Cells were scraped off dishes with a cell scraper (GBO, Nürtingen, Germany). Cell suspensions were vortexed several times and centrifuged (16100*g, 15 min, 4°C). 100 µL supernatant was boiled with 33 µL 4x SDS loading dye and frozen until further use. Protein concentration was determined using a Bradford assay (section 2.5.2.1). 5 µg for Akt and 1 µg for AktP or 12.5/25 µg for both were subjected to SDS-PAGE and Western blotting. Quantification was obtained with Aida Image Analyzer software (v4.19.029, 2007; raytest Isotopenmessgeräte GmbH, Straubenhardt, Germany).

2.8. Oligomerization of peroxiredoxin 1 in the presence of dexamethasone

Prdx1 looses its peroxidase activity when exposed to high H_2O_2 concentrations. It will form decamers and act as a chaperone[51]. The role of Dex on oligomerization of Prdx1 was analyzed with this experiment.

In a total volume of 40 µL, 10 µM of Prdx1 was incubated with 40 µM Dex (Dexamethasone 21-phosphate disodium salt; Sigma Aldrich, Munich, Germany) in the presence of PBS for 15 min at 37°C and was then exposed to different concentrations of H2O2. The incubation with H2O2 was performed for 15 min at 37°C. Afterwards, to 40 µL sample, 13 µL 4x SDS loading dye without β-ME was added. Samples were incubated at 60°C for 5 min and 15 µL were subjected to SDS-PAGE and Western blotting against Prdx1.

3. Results

Glucocorticoids (GC) exhibit anti-inflammatory, anti-allergenic and immunosuppressive properties. They are extensively used in inflammatory diseases such as rheumatic arthritis[1-3]. Due to their broad spectrum of actions inside the human body, they exert severe side effects such as osteoporosis, hypertension and fat redistribution[1, 6-10]. Not all of the GC actions are understood, yet. The genomic mode of action was studied extensively over the years. GCs will enter the cell where they bind to a multimeric complex containing heat shock proteins (Hsp) and the glucocorticoid receptor (GR). This multimeric complex is than translocated into the nucleus where the GR can act among others as a ligand-dependent transcription factor. The effect on gene transcription will take at least 30 min before changes in protein expression can be noticed. However, GCs exert fast occurring effects within in seconds to minutes that cannot be explained by the regulation of transcription. Therefore, an additional nongenomic pathway was hypothesized that still remains to be elucidated[5, 11].

In this thesis, target proteins for glucocorticoids were studied to clarify the nongenomic pathway. Direct protein interaction partners for GCs were searched for and the possibility of being a GC target in the nongenomic pathway was investigated. For this reason, different glucocorticoids were immobilized onto methacrylate beads. The differently linked GC derivatives were tested for their biological activity. Afterwards, appropriate beads were incubated with different cell lysates and the proteins bound to GC-immobilized beads were identified by mass spectrometry. The amount of unspecific bead-protein interactions in a pull-down assay is immense. Therefore, specific elution techniques were tested. Due to the random identification of proteins via SDS-PAGE band patterns, a more systematic approach was used, namely the stable isotope labeling of amino acids in cell culture (SILAC). With the help of the SILAC approach, several promising drug target candidates were identified. The evaluation of one of these proteins, peroxiredoxin 1 (Prdx1), was followed up. Prdx1 reduces hydrogen peroxides and thus is an important protein in the stress response of the cell. The interaction between Prdx1 and Dex was further studied, by elucidating the direct drug protein interaction in a cell-free system. Prdx1 exhibits distinct activity characteristics. It can either act as a peroxidase reducing hydrogen peroxides or in the presence of high levels of oxidative stress it acts as a decameric chaperone. The influence of Dex on the two

Prdx1 properties was investigated. Both Dex and Prdx1 have an effect on Akt phosphorylation, therefore the phosphorylation state of the serine/threonine kinase Akt was studied after Dex treatment.

3.1. Glucocorticoid bioactivity assay

As described in section 1.1.2.2, GCs pass the cellular membrane and enter the cytosol binding to a multimeric protein complex composed of several heat shock proteins and a glucocorticoid receptor. This GR complex translocates into the nucleus to influence gene transcription.

Different modifications of the glucocorticoid scaffold will influence the glucocorticoid activity and thus the localization of the GR within the cell. The modified compounds namely GC-3-CMO, GC-17β-amide and GC-21-CMO are depicted in Figure 3-1. In order to test whether the compounds synthesized by Martin Golkowski (group of Prof. Ziegler, Eberhard-Karls Universität Tübingen) (Figure 2-1) are still biological active, a GC bioactivity assay, based on the translocation of the GR into the nucleus, was developed.

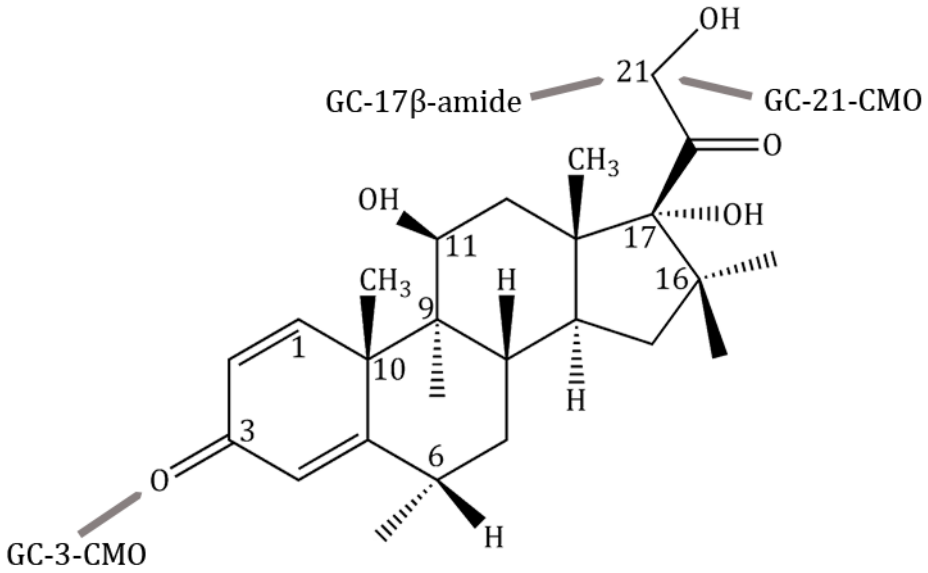

Figure 3-1 Schematic view of GC scaffold: Modifications in compounds performed by Martin Golkowski are shown with grey lines, namely GC-3-CMOs, GC-17β-amides and GC-21-CMOs. The denotations of compounds is noted in section 8.1.

For better protein detection of the GR, a GFP (green fluorescent protein) tagged GR was transiently expressed in A549 cells. A549 cells are widely used for studying GC actions inside cells[53]. After 24 h, cells were exposed to appropriate glucocorticoid derivatives for 15 min and subjected to immunofluorescence analysis with α-GFP antibodies.

Glucocorticoids will trigger the translocation of the GFP tagged GR into the nucleus to regulate gene transcription. In the absence of GC activity, the GR will remain in the cytosol (Figure 3-2 A: ctrl). The presence or absence as well as the localization of GFP

was determined for each of approximately 1000 cells and is displayed in % of cells with a nuclear GR-GFP staining in relation to transfected cells (Figure 3-2 B).

HC and Dex served as positive controls and displayed a nearly 100 % (92-93 %) nuclear location rate of GFP. The negative control ethanol translocated the glucocorticoid receptor into the nucleus in 13 % of the cells.

HC-3-CMO displays the same translocation activity of GR-GFP into the nucleus as HC with 92 %. Dex-3-CMO shows a lower (63 %) translocation activity than HC-3-CMO. A reason for this might be the possibility, that Dex-3-CMO is oxidation sensitive to metabolic enzymes and especially in presence of transition metals like copper. A decrease in cellular uptake of Dex-3-CMO is also discussed. HC-3-CMO translocation activity is not decreased, the reason for this fact remains to be elucidated. An *N*-methylated Dex-3-CMO derivative was synthesized to test whether a chemical modification is the reason for a decreased chemical stability (for details see Golkowski's thesis[44]). The activity of the *N*-methylated Dex-3-CMO derivative was 16 %, which is comparable to the negative control ethanol. Therefore, for all further experiments, 3-CMO derivatives without *N*-methylation were used. The substances were used immediately after synthesis to reduce the possibility of acid decomposition, which was observed by Golkowski[44].

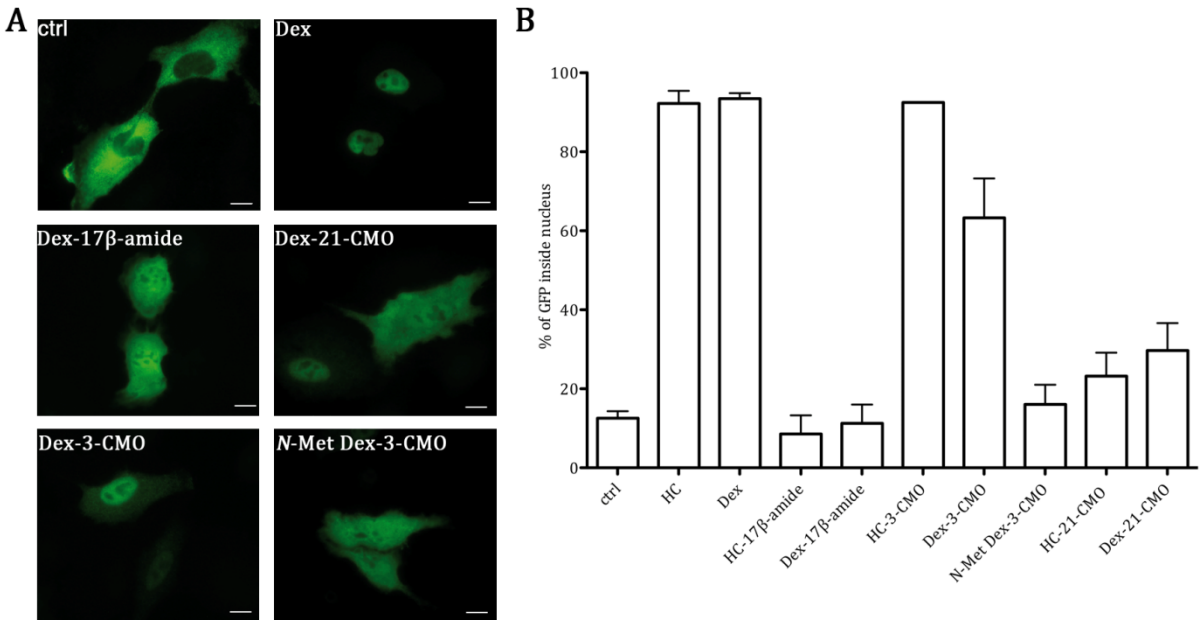

Figure 3-2 Biological activity assay for GC-17β-amides, 3-CMOs and 21-CMOs: A549 cells transiently expressing GR-GFP were exposed for 15 min either to 25 µM HC derivatives, 1 µM Dex derivatives or 50 % ethanol, respectively, before subjecting cells to immunofluorescence analysis. A: Immunofluorescence images of indicated Dex derivatives. B: Mean +/- SD of A for nuclear localized GFP that was compared to transfected cells of at least 1000 counted cells. Bar = 10 µm; n ≥ 3. Abbreviations of the used compounds can be found in section 8.1.

3.2. Target-fishing results

The target-fishing approach is a technique for identifying drug-target interactions. Immobilized GC-3-CMOs were incubated with appropriate cell lysates. Cells were lysed with glass beads and 2 mg of cell lysate was incubated for 4 h with immobilized drugs. After elution with SDS, urea, Dex or HC, proteins were subjected to SDS-PAGE and silver staining. Different elution pattern in the SDS-PAGE could be detected. However, problems with this approach are especially non-specific drug-target interactions. Proteins will not only bind specifically to the drug immobilized to the matrix, but also to the matrix and the linker. It is possible to overcome these problems with special techniques. One example is the application of different elution techniques. This approach will be discussed in section 3.2.3.

Felix Behnke (group of Prof. Werz, Friedrich-Schiller-Universität Jena) and Thomas Kutter (group of Prof. Ziegler, Eberhard-Karls Universität Tübingen) developed an UV-cleavable linker[68]. After attachment of all specific or unspecific proteins in the target-fishing experiment, the linker can be cleaved with UV light. Thus proteins bound to either linker or matrix are eliminated and only proteins bound to the drug will remain for detection. This approach was successfully used together with Marc Weißer (group of Prof. Laufer, Eberhard-Karls Universität Tübingen) to discover new drug-target interactions of metamizol[69].

The most important part of the target-fishing approach is the identification of proteins bound specifically to the drug. The identification was performed using mass spectrometry (MS). The analysis was carried out by the proteome center Tübingen. Results will be discussed in sections 3.2.5 and 3.3.

3.2.1. Verifying the immobilization capability

The amount of GC derivatives immobilized onto the matrix surface was calculated from the amount of GCs present in the flow through after the coupling reaction. The solution was subjected to UV spectroscopy and the amount of GC bound to the beads was determined with a calibration curve. The results are presented in Table 3-1 and show the percentage of coupled GCs to the free amino functions of the bead surface.

The coupling of the compounds either with DMSO or Dioxan was successful. More than 50 % of the derivatives bound to the surface of the amino functionalized beads. It is noticeable, that HC-3-CMO immobilizes 113 % onto the bead surface. This is possible, because the manufacturer of the matrix only declares a range of the free amino functions

on the bead surface, namely 70-130 µmol. For the calculation of the immobilization capability, 100 µmol as an arithmetic average was used.

The immobilization with Dioxan was performed for the SILAC experiment with soluble competition. If not noted otherwise, for all other experiments, DMSO as a coupling agent was used. Through the immobilization technique, about half of the surface was immobilized with the GC-3-CMO derivatives.

Table 3-1 Immobilization capability of glucocorticoid derivatives in %, n = 1

Compound	Compound immobilized to the matrix [%]
Immobilization with DMSO	
HC-3-CMO	113
Dex-3-CMO	70
Immobilization with Dioxan	
HC-3-CMO	60
Dex-3-CMO	57

3.2.2. Binding of the glucocorticoid receptor to glucocorticoid-immobilized beads

In order to characterize GC derivatives besides their bioactivity function, the binding of the compounds to the GR was investigated. If the synthesized GC derivatives are still able to bind the GR with the target-fishing approach, the compounds should be valid for use in all further experiments.

To analyze the binding of the GR to GC beads, A549 cells were harvested and lysed with lysis buffer prior to performing a target-fishing approach.

Dex-3-CMO and HC-3-CMO bind to endogenous GR as depicted in Figure 3-3. Unfortunately, this experiment could not be reproduced, probably due to the low endogenous expression level of the GR.

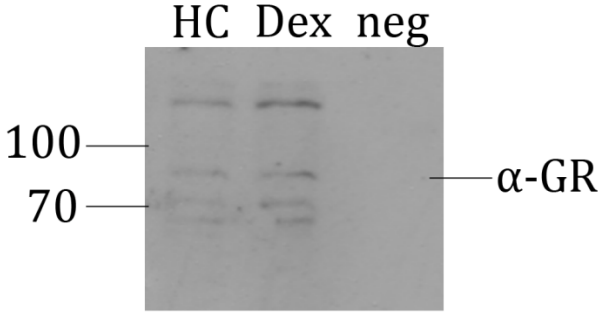

Figure 3-3 Binding of GR to GC-3-CMO beads (immobilization with DMSO): approximately 2 mg A549 cells were lysed with glass beads and Lysis buffer and a target-fishing approach with GC-coupled beads was performed. After SDS elution, 20 µL samples were separated by SDS-PAGE and additionally, Western blotting with an α-GR antibody was carried out. The position of the GR is marked; n = 1.

In order to raise the level of GR inside the cell, GM5756T cells were transfected with a plasmid coding for GR-GFP. After 24 h, cells were harvested, lysed with Molybdate buffer and utilized for the target-fishing approach. The use of molybdate salts in GR binding studies was described by Modarress et al. and was used for lysis[59]. Although GR-GFP could be found in the lysate and the supernatant, a binding of GR-GFP to the beads was not detected (Figure 3-4).

Unfortunately, an interaction between the GR and GC could not be shown in this experiment. However, as nongenomic targets of GCs were elucidated in this thesis, it may not be necessary that these GC compounds also display a GR binding. Thus, a reduced GR-binding ability does not exclude a possible nongenomic effect of the GC-derivatives used.

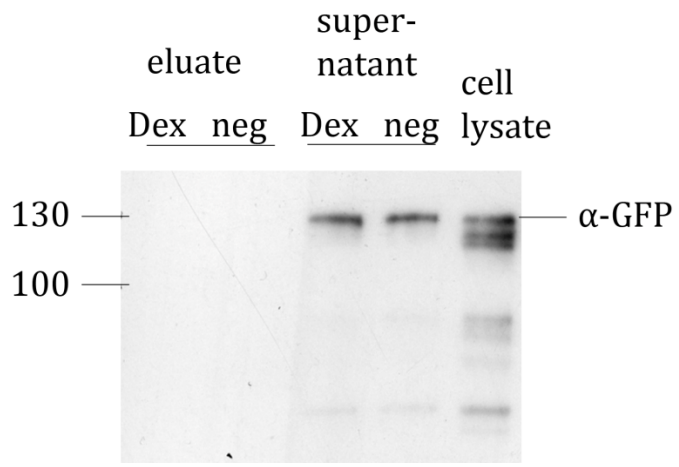

Figure 3-4 Binding of GFP-GR to GC-3-CMO beads (immobilization with Dioxan 50 %): GM5756 cells were transfected with a plasmid coding for GFP tagged GR for 24 h. Afterwards, cells were harvested and lysed with glass beads and Molybdate buffer before performing a target-fishing. After SDS elution, 15 µL of the eluate and 7.5 µL of the supernatant (+2.5 µL 2x SDS loading dye) were separated by SDS-PAGE and additionally, Western blotting with an α-GFP antibody was carried out. The position of the GR-GFP is marked.

3.2.3. Improvement of elution techniques

Elution of proteins with the detergent SDS elutes all proteins bound to bait, matrix and linker in a target-fishing approach. Therefore, it is quite impossible to distinguish between specific and non-specific bound proteins. In order to elute more specifically, elution with SDS, HC, Dex and urea were compared (Figure 3-5). SDS elutes by far the most proteins, followed by urea and the least proteins were eluted by HC and Dex. Specific elution with HC and Dex leads to less protein abundance than SDS or urea, because only specific bound proteins are eluted due to competition with the soluble drug. Because of the low amount of eluted proteins, proteins seem to be specific. In Figure 3-5 A, only a slight difference between HC and Dex elution is observable, probably due to similar scaffolds.

The band pattern for the different elution techniques is diverse. A prominent band between 40 and 50 kDa (Figure 3-5 point) is visible for all elution compounds and probably displays actin. In Figure 3-5 A the elution pattern for HC, Dex and urea has some similarities. For example between 20 and 25 kDa HC, Dex and urea elute a noticeable band for HC and Dex beads (Figure 3-5 asterisk). Whether this protein is also eluted with SDS is not visible, due to the enormous amount of eluted proteins. The protein between 20 and 25 kDa is more abundant in the eluate of HC than Dex beads, indicating that HC was immobilized more onto the beads than Dex. The higher immobilization capability of HC-3-CMO was also seen with the experiment described in section 3.2.1.

In further experiments the elution with HC and Dex was not used, because the amount of proteins was insufficient. For the chemical proteomics approach with the membrane fraction (section 3.2.5), SDS elution was utilized due to the low amount of membrane proteins. Urea elution was employed for the classical SILAC experiment, because a protein determination after elution was necessary. A protein determination was no longer necessary for the SILAC approach with soluble competition. The SILAC approach will distinguish between specific and non-specific elution itself, therefore no specific elution is necessary. Hence, SDS elution was used.

3.2.4. Comparison of different cell lines used in the target-fishing approach

Three different cell lines were utilized in the comparison of protein elution patterns. Cells were disrupted as described in section 2.3.3 and approximately 2 mg of each cell lysate was used to perform a target-fishing approach (Figure 3-5 A-C).

Target-fishing with HepG2 cells resulted in a lot of proteins eluted in all four elution techniques (Figure 3-5 A). A549 cells (Figure 3-5 B) are not able to elute as many proteins. HEK293T cells (Figure 3-5 C) elute by far less proteins than HepG2 and A549, but also exhibit the actin band between 40 and 50 kDa (Figure 3-5 point).

Depending on the cell line, it could be easier to isolate bands with specific or non-specific elution. For further research, mostly A549 cells were employed, because they can be handled quite easily and grow fast. In addition, A549 cells are appropriate for studying GC effects[53].

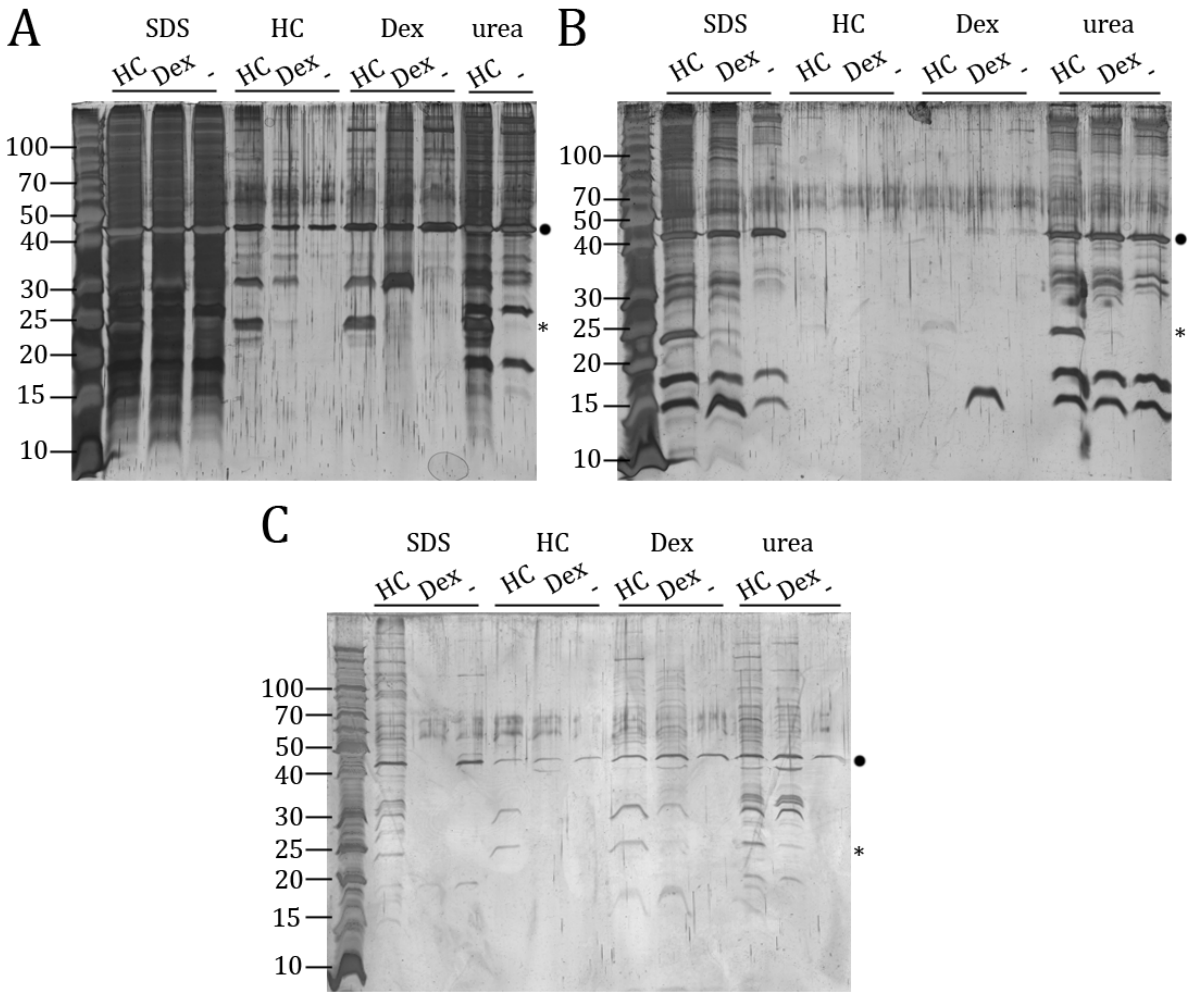

Figure 3-5 Target-fishing approach with specific elution techniques and different cell lines: A: HepG2 cells; B: A549 cells; C: HEK293T cells. Cells were lysed with glass beads and Lysis buffer prior to target-fishing. The elution was performed either with 50 µL 2x SDS loading dye, 7.2 M urea, 14 mM HC or 25 mM Dex. 5 µL for SDS and 10 µL for Dex, HC and urea samples were separated on a 12 % SDS-PAGE and visualized by silver staining.

3.2.5. Membrane isolation and mass spectrometry analysis

One problem of the target-fishing approach is the identification of low abundant proteins. Especially membrane proteins are expressed at lower levels and are hard to identify with the target-fishing approach. One solution could be a membrane isolation. Therefore, cells were disrupted with glass beads in Hepes binding buffer without detergent and subjected to ultracentrifugation to separate cytosol and membranes. The pellet was resuspended with a detergent-containing buffer (Lysis buffer) to isolate membrane proteins. In order to concentrate membrane proteins, they were resuspended in a smaller volume. In the current work, membrane isolation was performed with HepG2 cells. The Proteome Center Tübingen carried out the identification of the bands with mass spectrometry.

The membrane isolation from HepG2 cells is shown in Figure 3-6 A. The membrane fraction shows a somehow distinct protein pattern compared to the cytosolic fraction.

Band number 1 on the right hand side of A shows a higher concentration in the cytosol than in the membrane fraction. This band was identified as Prdx1, which is expressed highly in the cytosol. It was also identified in the membrane fraction, because a complete depletion of cytosolic proteins from the membrane is difficult. Band number 2 was identified as adenine nucleotide translocator (ANT) a protein that is located in the inner membrane of mitochondria. It was not possible to identify this protein in the cytosolic fraction, because too many proteins, that were more abundant, overlay the MS signal.

ANT has an important function in the transport of ATP and ADP and is involved in the proton gradient across mitochondrial membrane. It has been described that after dexamethasone treatment in rats, the proton leak of the mitochondria is increased[70]. The reason for this increase was neither found in the modification of the membrane surface nor in the phospholipid composition of the mitochondria. Rather the 100 % raise of the ANT content displays a major factor of mitochondrial proton leak in dexamethasone-treated rats. Treatment with glucocorticoids in general leads to a growth in known ATP consuming pathways like gluconeogenesis, proteolysis and lipolysis. The increase of ADP input capacity and of ATP output through ANT meets the ATP consuming requirements. ANT mediates the obtained raise in the basal proton leak[70].

Two prominent components of the multimeric GR receptor complex Hsp70 (number 3) and Hsp90 (number 4) were identified in the cytosolic fraction[20]. Further bands were subjected to MS and could be identified, but will not be discussed.

GM5756 cells were used in the target-fishing approach (Figure 3-6 B). There is a prominent band between 25 and 20 kDa, could be identified as peroxiredoxin 1 (Figure 3-6 B asterisk). Therefore, it can be assumed that the band in Figure 3-5 A-C, which was discussed above, displayed Prdx1, too. Using the membrane isolation of HepG2 cells Prdx1 was identified as interaction partner both for Dex and HC. Nevertheless, Prdx1 bound more to HC than Dex beads. As mentioned earlier, about twice as much HC is immobilized to the matrix as is Dex. Therefore, it is likely that HC is able to pull-down more Prdx1 than Dex.

The target-fishing approach led to the identification of Hsp70, Hsp90 and ANT that are known interaction partners of GCs. Hence, the target-fishing approach is a valid technique for the identification of drug-target interaction. It is likely, that the other identified protein Prdx1 is also an important protein in GC signaling. Prdx1 will be investigated further to elucidate the relationship between Prdx1 and Dex.

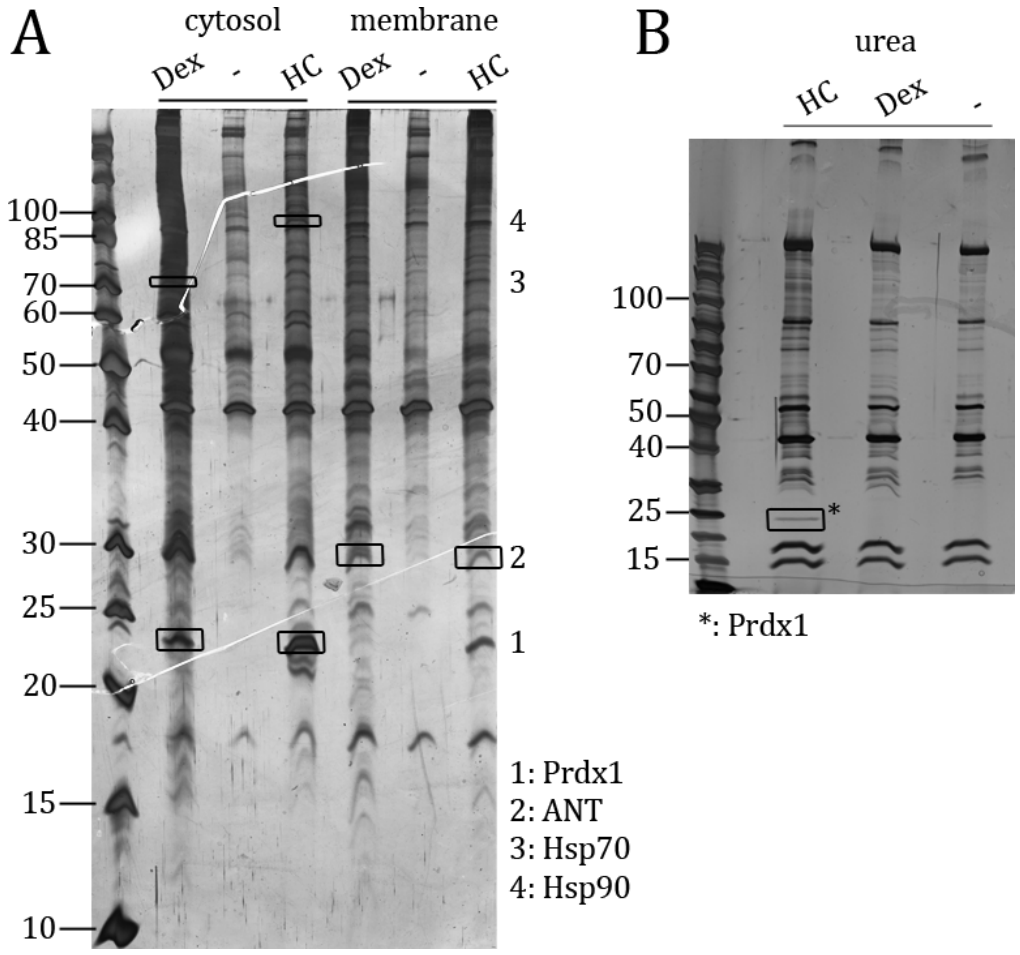

Figure 3-6 MS identification of pull-down proteins of different cell lines: A: HepG2 cells were harvested and a membrane isolation by ultracentrifugation (section 2.3.3.1) was performed prior to target-fishing. Elution was carried out with SDS. The encircled proteins were subjected to MS. Proteins identified are 1: Prdx1, 2: adenine nucleotide translocator (ANT), 3: Hsp70, 4: Hsp90; B: GM5756 cells were harvested and lysed, additionally the cell lysate was subjected to target-fishing. Elution was performed with urea. Proteins identified are: *: Prdx1. 10 µL of samples were separated on a 12 % SDS-PAGE and visualized by silver staining.

3.3. Stable isotope labeling of amino acids in cell culture

The excision of bands from a 1D SDS-PAGE as described in section 3.2.5 is biased and can only detect high abundant proteins. In order to overcome this biased approach, stable isotope labeling of amino acids in cell culture (SILAC) was applied. SILAC is a technique to label the cellular proteome metabolically. Cells are grown in heavy, medium or light isotope medium and will incorporate the heavy or medium amino acids of lysine and arginine into their proteome. Afterwards, a pull-down assay with the labeled cell lysate is performed. In the classical SILAC experiment, heavy, medium and light samples are incubated with three different kinds of immobilized beads. The classical experimental setup was performed for glucocorticoids (GC) and sex hormones (SH) respectively. For the soluble competition (SC), heavy and medium labeled cell lysates were incubated with (medium) or without (heavy) soluble drug that competed

with the beads for protein binding. The SC experimental setup was carried out with dexamethasone beads. After elution with urea for the classical SILAC experiment and SDS for the soluble competition experiment, proteins were mixed 1:1:1 (v/v/v). In the experimental setting all proteins obtained are compared to controls. Therefore, SILAC experiments display a systemic technique for identification of drug target candidates.
The following sections describe the incorporation test for all experiments as well as the evaluation of the classical SILAC approaches for dexamethasone (GC experiment), progesterone and testosterone (both SH experiment) and additionally the evaluation of the soluble competition assay for dexamethasone (Dex experiment). The tables obtained after the evaluation of all four (GC-Dex, SH-testosterone, SH-progesterone and Dex) experiments display ratios for the explained experiment together with the other three ratios for comparison.

3.3.1. Incorporation test

The incorporation test was performed to determine the amount of heavy and medium isotopes labeled in the cellular proteome. This test was carried out for each experiment separately. For the classical triplet SILAC experiment the incorporation rate for both heavy and medium labeled A549 cells reached 98.6 %, for the soluble competition experiment it was 98.4 %. HEK293T cells were employed for the englerin A and atorvastatin SILAC experiment from the group of Prof. Maier (Eberhard-Karls Universität, Tübingen) and displayed an incorporation rate for heavy labeled cells of 96.6 % and for medium labeled cells of 97.0 %, respectively. An incorporation rate above 95 % is sufficient for SILAC experiments.

3.3.2. Classical SILAC experiment of glucocorticoids – dexamethasone

For the classical SILAC experiment, heavy (H) labeled cells were incubated with dexamethasone-coupled beads, medium (M) labeled cells with hydrocortisone-coupled beads and light (L) labeled cells with negative control (acetic acid)-coupled beads. Mass spectrometry identified 667 possible target proteins.
In order to validate possible targets, proteins have to be limited. In this thesis, a scatter plot was prepared to narrow down the number of possible target proteins. Subsequently, proteins were compared to a bead proteome to eliminate possible contaminants. Furthermore, proteins with a high intensity and ratio were excluded. The obtained list of proteins was compared to the other steroids that are known to lack cross-reactivity for

the receptor. The list achieved was subjected to a network search and chosen proteins will be discussed.

First, the log_2 ratios of H/L were plotted against the number of proteins (Figure 3-7 A). A line was drawn through the linear part of the plot and the intersection was determined (Figure 3-7 A grey line). The intersection point of Figure 3-7 A, together with the log_2 enrichment M/L, plotted against the number of proteins (Figure 8-2), was the point of origin (both protein 70) in the scatter plot (Figure 3-7 B). The scatter plot displays protein ratios of H/L and M/L in a log_{10} scale. Specific proteins are present in one of the four squares. Due to the same scaffold of the glucocorticoids Dex and HC do not exhibit a distinct mode of action. Therefore, it is not possible to use just one square of the scatter plot (Figure 3-7 B). In the upper right square proteins are represented, that bind to hydrocortisone and dexamethasone with high affinity. Hydrocortisone has a 25 times lower affinity to the glucocorticoid receptor than dexamethasone[35], hence the lower right square is also considered to be important. It is feasible to take the above-mentioned Top 70 H/L scores, because these proteins are represented in the two right squares.

The frequency distribution of the protein ratios can be displayed in a histogram. The histogram of H/L and M/L frequency distribution can be found in the appendix (Figure 8-1 A). It is noticeable, that the histogram displays a Gaussian-like distribution. Proteins on the edgeways are most likely specific for dexamethasone.

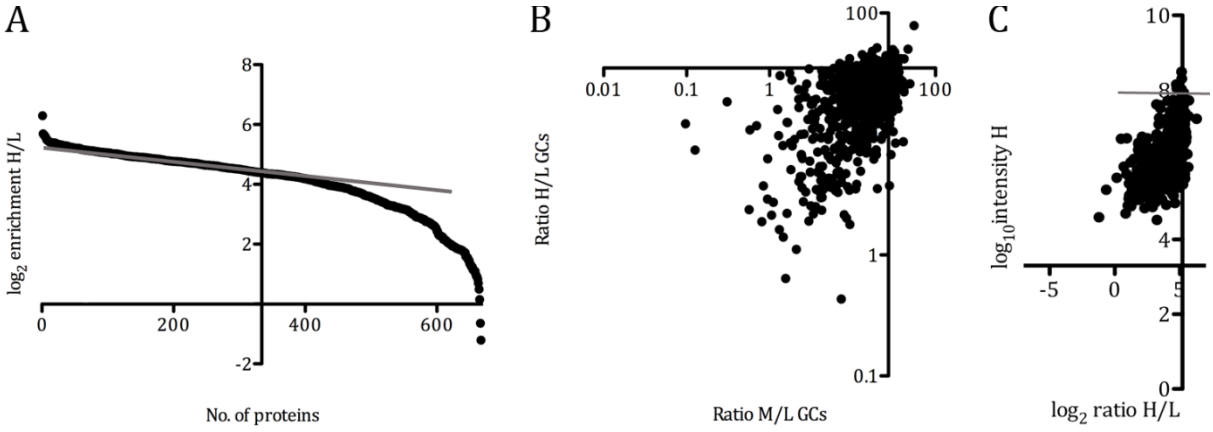

Figure 3-7 SILAC evaluation GC: A: The log_2 enrichment of H/L was plotted against the number of proteins. A line was drawn through the linear part of the graph and intersects at protein 70. B: Scatter plot with determined intersections of A (H/L and M/L both protein 70). C: The log_{10} intensities (H) were plotted against the log_2 ratios (H/L). Proteins identified above the line are most likely unspecific.

The obtained proteins were compared to a bead proteome[71]. Trinkle-Mulcahy et al. performed several SILAC experiments with sepharose beads and identified the most common non-specific proteins (marked in Table 8-1-Table 8-3 in dark grey) and called it

bead proteome. The beads used in this thesis were methacrylate beads, which have different properties, but the bead proteome is a good indication for discrimination of specific and non-specific interaction partners.

The comparison of these 70 proteins with the list of Mulcahy-Trinkle et al.[71] led to 31 possible contaminants. Heat shock proteins were not excluded from the drug target candidates due to their importance in glucocorticoid receptor complex assembly. Additionally, peroxiredoxin 1 was not excluded, because it was identified twice in earlier experiments. Furthermore, 14-3-3 proteins display an interesting class of proteins and were not eliminated.

In a more recent paper, Boulon et al. were able to refine the bead proteome research by creating a protein frequency library. They generated a software, which is able to compare the frequency of proteins identified in over 150 SILAC experiments and helps to detect the most commonly identified and thus probably unspecific proteins[72]. The idea of the paper was applied by plotting the $\log_{10}$ intensity of H against the $\log_2$ ratio of H/L to determine the probable contaminants of the experiment (Figure 3-7 C). Most of the proteins accumulate around zero, when normalized according to the MaxQuant software[60]. The glucocorticoid samples could not be normalized, because the negative control differs from the glucocorticoids in its hydrophobicity. Accordingly, they do not accumulate around zero, but rather around the digit obtained from the diagram of the $\log_2$ ratios plotted against the amount of proteins. The proteins with the highest intensities and top ratios have an exalted probability to be most abundant within the cell and are therefore able to bind non-specifically to the beads. A threshold was applied to exclude the proteins with the highest $\log_{10}$ intensities (H) that were plotted against the $\log_2$ ratios (H/L) (Figure 3-7 C, above grey line). Three proteins were identified as possible contaminants. One was previously excluded with the bead proteome (Plectin 1); heat shock protein 90 and peroxiredoxin 1 were the other two, but not excluded due to the reasons mentioned above.

In another classical SILAC experiment progesterone and testosterone were used. Testosterone does not cross-react with the GR like progesterone and can therefore be applied as a negative control with the same scaffold. Hence, all proteins in the Top 100 of testosterone were excluded from the GC and progesterone experiment. After elimination of the Top 100 testosterone-identified proteins, four more proteins were excluded (Table 8-1-Table 8-3 marked in light grey).

Two more SILAC experiments were performed in collaboration with Prof. Maier (Eberhard-Karls Universität Tübingen); one with atorvastatin and the other with englerin A. All of the proteins of the SILAC experiment performed in this thesis were cross-examined with the results of these two compounds. They display a different chemical structure compared to the steroids and should not have the same target proteins (Table 8-1-Table 8-3 marked in lighter grey). One protein was also found with atorvastatin and therefore left out.

After the elimination of all possible contaminants, a list of 33 proteins remained (Table 3-2), the full list is displayed in Table 8-1. Ratios for all three different SILAC experiments are displayed in Table 3-2. If no ratios are listed in the table, the protein was not identified in the experiment. The table was arranged with the ratio H/L GC. The No Dex to the right of ratio H/L GC corresponds to the original hit list of proteins depicted in Table 8-1. Normalization was performed for classical SILAC experiment of the sex hormones. During normalization, protein-mixing errors are adjusted with MaxQuant software. For details see Cox et al.[60].

In order to display all possible drug candidates in a network, the obtained proteins were subjected to STRING (Search Tool for the Retrieval of Interacting Genes/Proteins) database[73]. STRING is an open source database that presents known and predicted protein-protein interactions (for a review see von Mehring et al.[74]). The results are depicted in Figure 3-8. Abbreviations and a short summary about the protein function are obtained in section 8.3.1.

Table 3-2 Protein hit list of classical SILAC evaluation GC – dexamethasone: The protein list is arranged by highest ratios for GC H/L. The other ratios in this table represent results from the different SILAC experiments (part 2 SH experiments: section 3.3.3 and 3.3.4, part 3 SC experiment Dex: section 3.3.5) performed in this thesis. H represents the intensity of identified heavy peptides of the corresponding protein. M and L behave accordingly. Bold printed proteins will be discussed.

Protein Names	Gene Names	Ratio M/L GCs	No HC	**Ratio H/L GCs**	No Dex	No	Ratio H/M GCs	Ratio M/L SH	No Prog	Ratio H/L SH	No Testo	Ratio H/M norm SH	No SH H/M norm	Ratio M/L Dex	Ratio H/L Dex	No H/L	Ratio H/M Dex	No H/M	Ratio H/M Norm Dex
Nuclear pore glycoprotein p62	NUP62	32,4	45	**47,55**	6	1	1,18		537		537		537			167		173	
Thymidylate kinase	DTYMK	13,1	365	**45,25**	7	2	1,92	10,3	178	0,47	455	0,107	484			421		424	
14-3-3 protein epsilon	YWHAE	25,3	130	**44,42**	8	3	1,84	21,5	64	6,39	127	0,657	376			228		234	
Heat shock 40 kDa protein 4	DNAJA1	15,8	306	**43,66**	10	4	2,62	18,7	83	4,81	161	0,76	325			367		372	
Splicing factor 3A subunit 3	SF3A3	30,7	60	**42,86**	11	5	0,97		540		540		540			178		184	
Cleavage and polyadenylation specificity factor subunit 3	CPSF3	18,1	249	**42,02**	14	6	1,72		605		605		605			317		322	
Delta-1-pyrroline-5-carboxylate synthetase	ALDH18A1	9,23	449	**42,02**	15	7	2,51		691		691		691			498		501	
Importin subunit beta-1	KPNB1	18,3	246	**41,91**	17	8	2,27	9,78	192	4,74	162	0,693	363			314		319	
Tetratricopeptide repeat protein 9C	TTC9C	17,2	273	**41,74**	19	9	2,2		617		617		617			337		342	
Serine/threonine-protein phosphatase 2A catalytic subunit	PPP2CA	14,9	331	**41,73**	20	10	2,1		643		643		643			389		392	
Protein arginine N-methyltransferase 1	PRMT1	16,2	299	**40,71**	23	11	2,35		627		627		627			360		365	
Programmed cell death protein 2-like	PDCD2L	20,3	210	**40,35**	25	12	1,18		585		585		585			287		292	
BAG family molecular chaperone regulator 2	BAG2	22,5	166	**39,87**	28	13	1,56	18,5	87	7,22	111	0,886	263			250		255	
RuvB-like 1	RUVBL1	16,9	283	**39,86**	29	14	1,96	9,51	200	1,56	353	0,458	437			345		350	
C-1-tetrahydrofolate synthase, cytoplasmic	MTHFD1	16,9	282	**39,13**	33	15	1,88	8,59	218	3,58	204	0,486	432			344		349	
Heat shock protein HSP 90-beta	HSP90AB1	20,4	208	**39,09**	34	16	1,76	9,82	190	3,46	212	0,505	427	0,917	0,087	101	0,083	99	0,126
Exocyst complex component 3	EXOC3	16,5	296	**39,1**	35	17	2,7		624		624		624	357		368			
Capping protein (Actin filament) muscle Z-line, beta	CAPZB	13,7	352	**38,9**	37	18	2,5	11,7	161	5,08	153	0,774	315			409		412	
Abhydrolase domain-containing protein 14B	ABHD14B	21,7	182	**38,89**	38	19	1,64		572		572		572			263		268	
C-terminal-binding protein 1	CTBP1	6,99	514	**38,34**	41	20	1,7		731		731		731			556		559	
Uridine phosphorylase 1	UPP1	17,3	269	**37,99**	43	21	1,8		615		615		615			333		338	
Heat shock protein HSP 90-alpha	HSP90AA1	13,8	351	**37,76**	44	22	2,22	5,81	280	2,3	279	0,634	386			408		411	
NADH dehydrogenase [ubiquinone] iron-sulfur protein 2, mitochondrial	NDUFS2	9,15	452	**37,64**	45	23	1,8		694		694		694			501		504	
T-complex protein 1 subunit theta	CCT8	8,64	468	**37,19**	49	24	1,95	8,14	223	1,26	388	0,828	287			514		517	
DNA-directed RNA polymerases I, II, and III subunit	POLR2E	11,3	403	**36,82**	57	25	1,72		669		669		669			456		459	
Programmed cell death protein 6	PDCD6	20,8	203	**36,77**	58	26	1,76		583		583		583			282		287	
T-complex protein 1 subunit delta	CCT4	8,91	455	**35,99**	60	27	2,09		695		695		695			504		507	
DnaJ homolog subfamily A member 2	DNAJA2	15,4	315	**35,82**	61	28	2,37	30,7	16	7,42	108	0,617	391			376		381	
DnaJ homolog subfamily C member 10	DNAJC10	21,3	189	**35,7**	62	29	1,4		577		577		577			270		275	
Heat shock 70 kDa protein 1	HSPA1A	19,9	221	**35,46**	65	30	1,56	10,1	182	4,93	157	1,061	186			297		302	
Peroxiredoxin-1	PRDX1	23,9	144	**35,35**	67	31	1,41	21,5	65	2,86	245	0,222	478	7,033	1,202	25	0,149	86	0,323
Trifunctional enzyme subunit alpha, mitochondrial	HADHA	17	278	**35,3**	68	32	1,58	28,5	23	4,87	158	0,425	451			341		346	
14-3-3 protein zeta/delta	YWHAZ	21,2	191	**35,2**	70	33	1,82	13,6	141	5,91	138	0,72	344	0,21	0,59	35	2,27	28	17

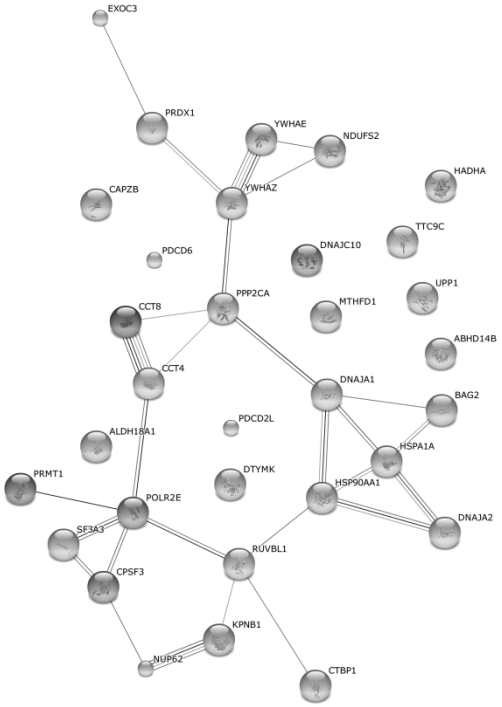

Figure 3-8 GC dexamethasone network of identified possible drug targets analyzed with STRING software[73]. Abbreviations of genes are explained in **Table 3-2** and in section 8.3.1 a little description of the corresponding protein function is given.

Some protein-protein interactions displayed in Figure 3-8 are noteworthy; for example the different heat shock proteins (Hsp). The glucocorticoid receptor complex consists of several Hsps that are essential for the complex formation, such as Hsp90 (HSP90AA1), Hsp70 (HSP1A1) and Hsp40 (DNAJA1, DNAJA2). Therefore, this SILAC experiment was able to identify GR related proteins and displays a valid approach for the identification of GC target proteins. Furthermore nucleoporin 62 (NUP62) is an essential protein for glucocorticoid receptor translocation into the nucleus after ligand binding. As nucleoporin 62, importin β was also described to interact with the GR directly (see section 1.1.2)[22].

Whether dexamethasone is able to bind directly to one of the above-mentioned proteins remains to be elucidated. Dexamethasone-coupled beads seem to resemble similar binding properties as free dexamethasone. Otherwise these interaction partners of the glucocorticoid receptor complex would not have been identified in the experiment with dexamethasone.

Further biochemical analyses were performed with peroxiredoxin 1, that will be described in detail in section 3.4.

3.3.2.1. Serine/threonine-protein phosphatase 2A and dexamethasone

The catalytic subunit of serine/threonine-protein phosphatase 2A (PP2A = PPP2) was identified with dexamethasone. Effects of PP2A on the GR have been reported. PP2A belongs to the phosphoprotein phosphatase family of Ser/Thr phosphatases (PPP) that include seven enzymes (PPP1-7)[75, 76]. About 30 PPPs dephosphorylate cellular proteins that were previously phosphorylated by 428 different Ser/Thr protein kinases[75]. GR is dephosphorylated by PP1, PP2A and PP5, leading to nuclear translocation of the GR. PP5 is also a component of the multimeric GR complex[77].

PP2A is considered to be one of the most abundant enzymes, displaying up to 1 % of total cellular proteins in some tissues[76]. PP2A plays an important role in a lot of different cellular processes such as cell cycle regulation, DNA replication, RNA splicing, apoptosis and many more. During apoptosis, PP2A does not only affect the regulation, but also influences the cellular response to pro-apoptotic stimuli[78].

It was described, that dexamethasone induces cell death in insulin-secreting cells through activation of calcineurin. Calcineurin dephosphorylates Bad and promotes apoptosis[79, 80]. Calcineurin is also known as PPP2B (=PPP3). It belongs to the same phosphatase family as PP2A, but PP2A and PPP2B have nevertheless distinct mode of actions[81]. Calcineurin and PP2A are both able to dephosphorylate Bad[78, 79], suggesting a possible interaction between dexamethasone and PP2A. Additionally, effects of PP2A on GR have been reported. The GC-induced inhibition of translation of p70 S6K dephosphorylation might be due to an interaction between PP1 and PP2A with GCs[82]. Further research is necessary to elucidate the impact of the interaction between dexamethasone and PP2A.

3.3.3. Classical SILAC experiment of sex hormones – testosterone

In the SILAC experiment for sex hormones, testosterone was incubated with heavy (H) labeled cell lysate, progesterone with medium (M) labeled and the negative control (acetic acid) with light (L) labeled cell lysate. Mass spectrometry identified 480 possible target proteins. A normalized ratio H/M could be used for the sex hormones, because testosterone (H) and progesterone (M) have similar hydrophobic properties.

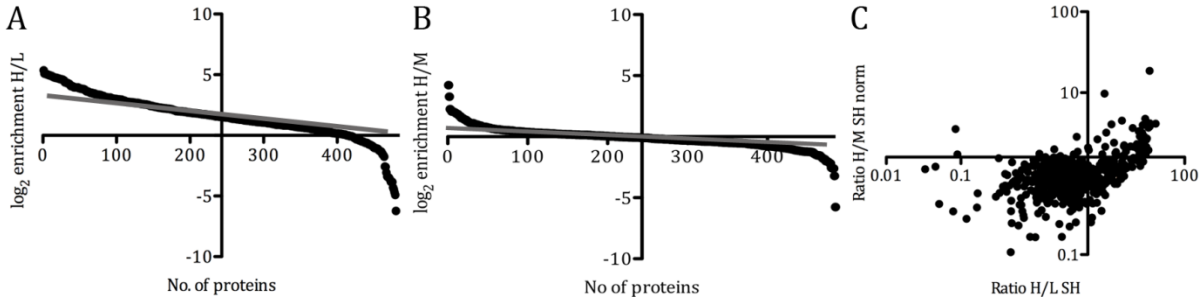

Figure 3-9 SILAC evaluation SH- testosterone: A: The log_2 enrichment of H/L was plotted against the number of proteins. A line was drawn through the linear part of the graph (light grey) and intersects at protein 155; B: The log_2 enrichment of H/M was plotted against the number of proteins. A line was drawn through the linear part of the graph (light grey) and intersects at protein 54. C: Scatter plot with determined intersections (H/L protein 155; H/M protein: 54).

The diagram of the log_2 enrichment of normalized H/M was plotted against the number of proteins (Figure 3-9 B). The proteins above the line (intersection: protein 54) resemble proteins most likely specifically identified by testosterone. This evaluation was also performed with the log_2 enrichment of H/L and protein 155 was the limit (Figure 3-9 A). The obtained data was used to determine the intersection in the scatter plot (Figure 3-9 C). The important square is on the upper right. Here, the ratios from both H/M and H/L are high and resemble specific testosterone interaction partners. In this square, 43 proteins were present. Nine of those proteins were eliminated due to the list from Mulcahy-Trinkle et al.[71] .

All proteins identified in the Top 100 of progesterone, hydrocortisone or dexamethasone were excluded from the testosterone experiment, because they may not cross-react with testosterone targets. Hence, eight more proteins were excluded. 15-Hydroxyprostaglandin dehydrogenase was not left out, because it is an important protein in inflammation and testosterone influences inflammation, too. Peroxisomal trans-2-enoyl-CoA reductase and alkyldihydroxyacetonephosphatesynthase are not excluded either, because there were other peroxisomal proteins identified by testosterone. The peroxisomal proteins and their interaction with testosterone will be discussed in section 4.2.2.2.

As described in section 3.3.2, the evaluation of the log_{10} intensities (H) plotted against the log_2 ratios (H/M) led to 15 proteins (Figure 3-10 B).

After the elimination of all possible contaminants, a list of 27 proteins was extracted (Table 3-3). The full list can be found in the appendix (Table 8-2).

The network of the remaining 27 proteins was investigated by subjecting proteins to the STRING database[73]. The results are depicted in Figure 3-10 A. Abbreviations and a short summary about the protein function are given in section 8.3.2.

The interaction between Pex1 and Pex6 shown in Figure 3-10 will be further discussed in section 4.2.2.2.

There is also an interaction described for Dolichyl-diphosphooligosaccharide-protein gylceroltransferase 48 kDa subunit (DDOST) with Dolichyl-diphosphooligosaccharide-protein gylceroltransferase subunit 1 (RPN1). The two proteins display different subunits of the same enzyme. The N-oligosaccharyl transferase enzyme catalyzes the transfer of mannose oligosaccharides to polypeptide chains.

Analyzing the SILAC table of identified proteins of testosterone, it is noteworthy, that seven enzymes are involved in lipid metabolism. Acyl-protein thioesterase 2, acyl-CoA desaturase, acylglycerol kinase, acyl-CoA thioesterase, alkyldihydroxyacetone-phosphate synthase, peroxisomal trans-2-enoyl-CoA dehydrogenase and short chain specific acyl-CoA dehydrogenase are these enzymes. Most of those enzymes exhibit an acyl-binding site, suggesting a common structure that could be addressed by testosterone. The exact binding mechanism of testosterone to those enzymes remains unclear. One of the enzymes, acylglycerol kinase, is overexpressed in prostate cancer leading to an increased cell growth, which is due to elevated level of lysophosphatidic acid (LPA). LPA is able to transactivate the epidermal growth factor receptor and to activate the MAPK pathway[64, 83]. Testosterone levels in prostate cancer are increased, which could be an explanation for acylglycerol kinase overexpression[84].

Another protein identified in the SILAC experiment of testosterone was visfatin. It is a protein involved in nicotinamide adenine dinucleotide biosynthesis and was also identified by Felix Behnke[68]. He was able to detect a direct interaction of testosterone and visfatin and showed an additional phosphorylation capability of the kinase ERK by the combination of visfatin and testosterone. Thus, visfatin was identified with two different methods.

The frequency distribution of H/L can be found in Figure 8-1 B and shows a Gaussian-like assignment.

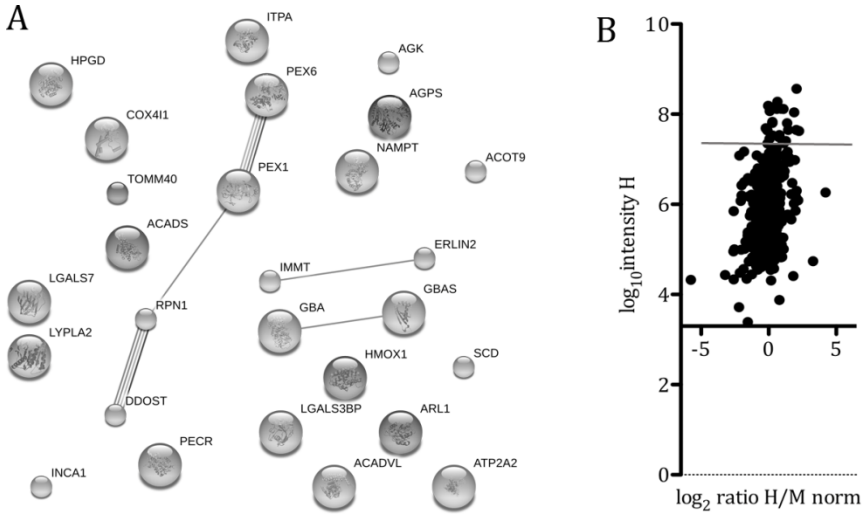

Figure 3-10 Network of possible testosterone target candidates: A: The SH testosterone network of identified target proteins is displayed. The analysis was performed with STRING[73]. Abbreviations of genes are explained in **Table 3-3** and in section 8.3.1 a little description of the corresponding protein function is given. B: The $\log_{10}$ intensities (H) were plotted against the $\log_2$ ratios (H/M normalized). Proteins identified above the grey line are most likely unspecific.

Table 3-3 Protein hit list of classical SILAC evaluation SH– testosterone: The protein list is arranged by highest ratios for SH H/M norm. The other ratios in this table represent results from the different SILAC experiments (part 2 SC experiment Dex: section 3.3.5; part 3 GC experiment: section 3.3.2) performed in this thesis. H represents the intensity of identified heavy peptides of the corresponding protein. M and L behave accordingly. Bold printed proteins will be discussed.

Protein Names	Gene Names	Ratio M/L SH	No Prog	Ratio H/L SH	No Testo	**Ratio H/M norm SH**	No SH H/M norm	Ratio M/L Dex	Ratio H/L Dex	No H/L	Ratio H/M Dex	No H/M	Ratio M/L GCs	No HC	Ratio H/L GCs	No Dex
Acyl-protein thioesterase 2	LYPLA2	2,6	393	33,9	4	**18,6**	1			974		974		971		968
Acyl-CoA desaturase	SCD	1,61	444	8,44	93	**9,735**	2			1226		1226		1226		1225
Acylglycerol kinase, mitochondrial	AGK	0,96	468	14,4	52	**4,517**	4			901		901		898		895
Dolichyl-diphosphooligosaccharide--protein glycosyltransferase subunit 1	RPN1	3,07	371	10,4	73	**4,059**	8			615		618	4,34	580	29,9	153
Cytochrome c oxidase subunit 4 isoform 1, mitochondrial	COX4I1	11,4	167	27,4	16	**3,978**	9			757		757		753		749
Protein NipSnap homolog 2	GBAS	13,1	147	34	3	**3,842**	10	7,38	3,36	17	0,67	46	40,1	10	27,2	200
Acyl-Coenzyme A dehydrogenase, very long chain variant	ACADVL	16,8	107	32,8	5	**3,7**	11	3,11	7,08	14	1,88	30	18	254	38,2	42
Galectin-7	LGALS7	0,02	497	0,09	471	**3,553**	13	0,03		1157		1157		1157		1154
Peroxisome biogenesis factor 1	PEX1	6,16	268	24,1	27	**3,345**	14			1308		1308		1308		1307
Peroxisomal biogenesis factor 6	PEX6	1,7	440	26,9	17	**3,183**	16			1223		1223		1223		1222
Mitochondrial import receptor subunit TOM40 homolog	TOMM40	12,3	152	28,4	14	**2,911**	17			634		637	3,55	605	9,45	537
Mitofilin	IMMT	9,83	189	25,1	23	**2,9**	18	0,59	15,6	9	9,71	10	19,1	234	32,6	109
Sarcoplasmic/endoplasmic reticulum calcium ATPase 2	ATP2A2	2,33	406	6,78	114	**2,653**	21			1118		1118		1117		1114
Erlin-2	ERLIN2	16,4	116	30,6	10	**2,624**	22			971		971		968		965
15-hydroxyprostaglandin dehydrogenase [NAD+]	HPGD	21,8	61	28,9	13	**2,588**	23			203		209	27,7	94	27,1	207
Acyl-coenzyme A thioesterase 9, mitochondrial	ACOT9	16,1	122	26,2	20	**2,405**	25			213		219	26	112	33,4	95
Glucosylceramidase	GBA	11,7	162	15,5	46	**2,248**	27			313		318	18,3	245	17,8	406
Visfatin	NAMPT	13,7	140	15,4	48	**2,181**	28			216		222	25,9	115	26,4	223
Alkyldihydroxyacetonephosphate synthase, peroxisomal	AGPS	17,9	94	20,8	30	**2,152**	30			338		343	17,1	274	20,3	348
ADP-ribosylation factor-like protein 1	ARL1	4,96	301	8,61	92	**2,15**	31			1161		1161		1161		1158
Heme oxygenase 1	HMOX1	3,74	343	5,05	155	**2,095**	33			565		568	6,67	525	11,4	507
Dolichyl-diphosphooligosaccharide--protein glycosyltransferase 48 kDa subunit	DDOST	4,44	319	5,2	151	**1,955**	37			599		602	5,13	561	15,5	443
Protein INCA1	INCA1	9,37	203	32,6	6	**1,954**	38			674		677	1,75	650	31,9	120
Galectin-3-binding protein	LGALS3BP	11,5	164	12	62	**1,853**	42			943		943		940		937
Inosine triphosphate pyrophosphatase	ITPA	17,2	103	11,8	63	**1,789**	43			898		898		895		892
Peroxisomal trans-2-enoyl-CoA reductase	PECR	21,6	63	30	11	**1,743**	45			424		427	12,7	368	16,3	427
Short-chain specific acyl-CoA dehydrogenase, mitochondrial	ACADS	10,3	179	7,87	102	**1,743**	46			981		981		978		975

3.3.4. Classical SILAC experiment of sex hormones – progesterone

In the SILAC experiment for sex hormones, testosterone was incubated with heavy (H) labeled cell lysate, progesterone with medium (M) labeled and the negative control (acetic acid) with light (L) labeled cell lysate. Mass spectrometry identified 480 possible target proteins. For the sex hormones a normalized ratio H/M could be used because testosterone and progesterone have similar hydrophobic properties.

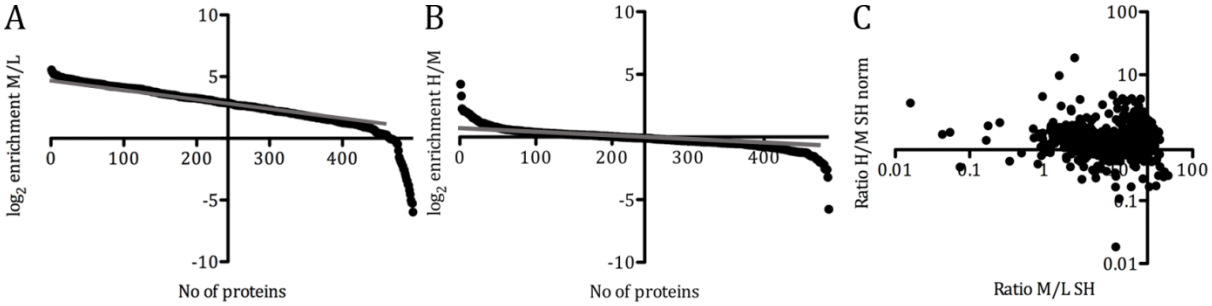

Figure 3-11 SILAC evaluation SH- progesterone: A: The log_2 enrichment of M/L was plotted against the number of proteins. A line was drawn through the linear part of the graph (light grey) and intersects at protein 40. B: The log_2 enrichment of H/M was plotted against the number of proteins. A line was drawn through the linear part of the graph (light grey) and intersects at protein 380. C: Scatter plot with determined intersections (M/L protein 40; H/M protein: 380).

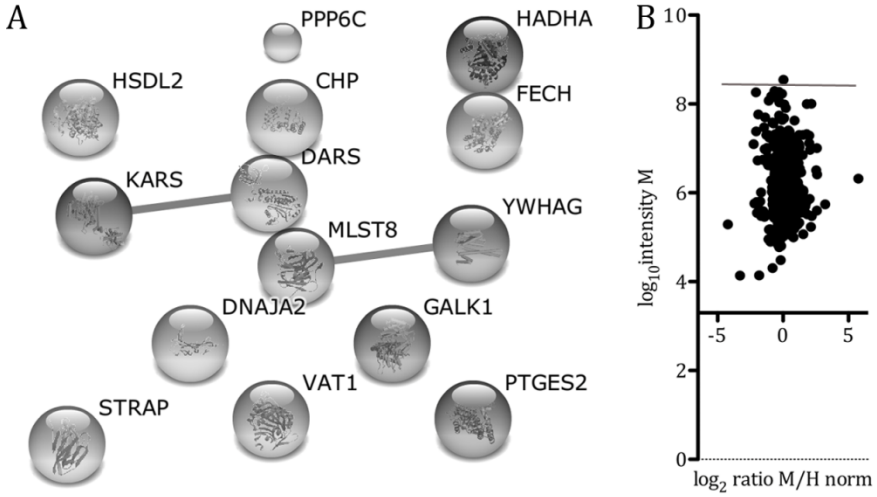

Figure 3-12 Network of possible progesterone target candidates: A: The SH progesterone network of identified target proteins is displayed. The analysis was performed with STRING[73]. Abbreviations of genes are explained in **Table 3-4** and in section 8.3.3 a little description of the corresponding protein function is given. B: The log_{10} intensities (M) were plotted against the log_2 ratios (M/H normalized). Proteins identified above the line are most likely unspecific.

The diagram of the log_2 enrichment of H/M is plotted against the number of proteins (Figure 3-11 B). The proteins below the line (intersection: protein 380) resemble proteins most likely specifically identified by progesterone. When this evaluation was performed with M/L, protein 40 was the limit (Figure 3-11 A). The obtained data were used to determine the intersection in the scatter plot (Figure 3-11 C). The important square is on the lower right. Here, the ratio from H/M is low and the ratio from M/L is

high and therefore proteins resemble specific progesterone interaction partners. In this square, 15 proteins were present. One protein was eliminated, because it was also found with atorvastatin.

The evaluation of the $\log_{10}$ intensities (M) plotted against the $\log_2$ ratios (H/M) led to one protein, calcium binding protein p22 (Figure 3-12 B). Even though it was also identified with testosterone, it will not be excluded.

After the elimination of all possible contaminants, a list of 14 proteins was left (Table 3-4). The full list can be found in the appendix (Table 8-3).

The network of the remaining 14 proteins was investigated by subjecting the proteins to the STRING database[73]. The results are depicted in Figure 3-12 A. Abbreviations and a short summary about the protein function can be found in section 8.3.3.

An interaction between DARS aspartyl-tRNA synthetase (DARS) and lysyl-tRNA synthetase (KARS) was identified by STRING (Figure 3-12 A). These two proteins both catalyze the attachment of an amino acid to their corresponding tRNA.

MLST8 (subunit of mTORC1 and mTORC2) and YWHAG (14-3-3 protein gamma) display another interaction in the progesterone network. MLST8 will be described in section 3.3.4.1.

The phosphoprotein phosphatase PPP6C will be further discussed in section 3.3.4.2.

The histogram of the M/L frequency distributions shows a Gaussian-like assignment and is given in the appendix (Figure 8-1 B).

Table 3-4 Protein hit list of classical SILAC evaluation SH– progesterone: The protein list is arranged by lowest ratios for SH H/M norm, which corresponds to highest ratios for progesterone. The other ratios in this table represent results from the different SILAC experiments (part 2 SC experiment Dex: section 3.3.5; part 3 GC experiment: section 3.3.2) performed in this thesis. H represents the intensity of identified heavy peptides of the corresponding protein. M and L behave accordingly. Bold printed proteins will be discussed.

Protein Names	Gene Names	Ratio M/L SH	No Prog	No	Ratio H/L SH	No Testo	Ratio H/M norm SH	No SH H/M norm	Ratio M/L Dex	Ratio H/L Dex	No H/L	Ratio H/M Dex	No H/M Dex	Ratio M/L GCs	No HC	Ratio H/L GCs	No Dex	Ratio H/M GCs
Synaptic vesicle membrane protein VAT-1 homolog	VAT1	26,14	33	1	2,26	283	0,17	481			1087		1087		1086		1083	
Hydroxysteroid dehydrogenase-like protein 2	HSDL2	32,33	11	2		481	0,17	480			625		628	4,02	595	4,75	608	1,53
Prostaglandin E synthase 2	PTGES2	40,75	3	3	2,09	300	0,24	476			148		154	35,6	20	30,3	143	0,81
Ferrochelatase, mitochondrial	FECH	46,84	1	4	5,56	145	0,25	474			365		370	16	304	28,8	173	1,8
Lysyl-tRNA synthetase	KARS	34,78	9	5	3,49	211	0,25	473			186		192	29,2	74	34,8	78	1,09
Serine/threonine-protein phosphatase 6 catalytic subunit	PPP6C	42,14	2	6	5,74	142	0,29	470			286		291	20,4	209	31,9	119	1,23
Target of rapamycin complex subunit LST8	MLST8	36,45	4	7	7,7	107	0,35	462			254		259	22,3	170	19,5	371	0,88
Aspartyl-tRNA synthetase, cytoplasmic	DARS	28,13	26	8	0,61	442	0,41	456			141		147	42,3	4	25	248	0,69
Trifunctional enzyme subunit alpha, mitochondrial	HADHA	28,47	23	9	4,87	158	0,42	451			341		346	17	278	35,3	68	1,58
Galactokinase 1	GALK1	26,04	34	10	6,67	119	0,44	444			481		484	9,87	432	34,2	84	1,41
Serine-threonine kinase receptor-associated protein	STRAP	33,05	10	11	4,57	170	0,45	440			352		357	16,6	291	29,8	157	1,4
Calcium-binding protein p22	CHP	35,94	6	12	8,62	90	0,54	416	0,3	7,208	13	16,8	4	24,4	137	33,5	93	1,26
14-3-3 protein gamma	YWHAG	25,61	37	13	6,59	121	0,56	411			401		404	14,2	343	35	72	1,75
DnaJ homolog subfamily A member 2	DNAJA2	30,7	16	14	7,42	108	0,62	391			376		381	15,4	315	35,8	61	2,37

3.3.4.1. Mammalian target of rapamycin and progesterone

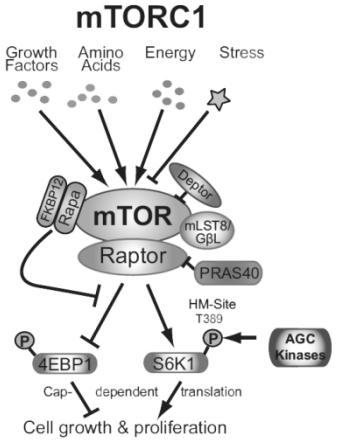

Figure 3-13 mTORC1 complex and signaling partners. Raptor (regulatory associated protein of mTOR), an mTORC1 regulatory partner, links - as a scaffolding protein - mTOR kinase to mTORC1 substrates. In this complex, deptor functions as an inhibitory partner. mTORC1 notices changes of extra- and intracellular signals and varies cell growth and proliferation. Image taken from Foster[85].

The mammalian target of rapamycin (mTOR) is a Ser/Thr protein kinase and forms the catalytic core of two complexes, mTORC1 and mTORC2. The complex of mTORC1 is shown in Figure 3-13. Raptor (regulatory associated protein of mTOR), an mTORC1 regulatory partner, links - as a scaffolding protein - mTOR kinase to mTORC1 substrates. In this complex, deptor functions as an inhibitory partner. Several other proteins are associated with mTOR, for example MLST8 that was identified with progesterone in the SILAC experiment. As depicted in Figure 3-13, mTORC1 notices changes of extra- and intracellular signals and varies cell growth and proliferation[85]. mTORC1 is involved in protein synthesis, autophagy, cell growth, cell cycle, nerve function and obesity and is also an essential target in cancer therapy for renal cell cancer[86, 87].

The exact role for progesterone in mTORC1 signaling remains unclear and requires further research.

3.3.4.2. Serine/threonine-protein phosphatase PPP6 and progesterone

The catalytic subunit of the phosphatase PPP6 was identified by progesterone. The description of Ser/Thr phosphoprotein phosphatases can be found in section 3.3.2.1. PPP6 is similar to PP2A that was also described in section 3.3.2.1. In transcription, translation, morphogenesis and cell-cycle regulation the involvement of PPP6 was described[75]. The N-terminal domain of PPP6 induces a cell cycle rest in the G_1 phase. Moe et al. described a cell density reduction in Ishikawa cells upon supraphysiological progesterone treatment. The reason for cell density reduction is cell cycle retardation and induction of apoptosis. It could be shown that high concentrations of progesterone

induced G_1/G_0 cell cycle arrest. An extranuclear signaling is suggested, because the concentration of progesterone is above the saturation of the progesterone receptor[88]. Other research suggests a G_2/M cell cycle arrest by down-regulation of cyclin B1[89]. An explanation for the two different modes of actions may lie within the role of PPP6 in cell cycle arrest. PPP6 analoga of *S. cerevisiae* and *S. pombe*, Sit4 and Ppe1 respectively, might act in the arrest in G_2/M as well as in G_1/S transition states of the cell cycle[90]. Therefore, an interaction between PPP6 and progesterone seems possible.

3.3.5. Soluble competition SILAC experiments of glucocorticoids – dexamethasone

As mentioned earlier (section 2.3.1) DMSO performs a Pfitzner-Moffatt oxidation and probably partially destroys dexamethasone on the bead surface. It is possible that dexamethasone cannot bind to its usual interaction partners, because the hydroxyl function on position 11 may be oxidized. Consequently, another SILAC experiment with Dioxan as a solvent that cannot execute a Pfitzner-Moffatt oxidation (section 2.3.1) was performed. In order to meet the advance of science, a soluble competition (SC) SILAC experiment was carried out. It overcomes the usual problems concerning the choice of an optimal negative control. Soluble drug competes for target proteins with the drug immobilized to the beads and prevents the interaction of target protein and beads[61].

For the SILAC experiment, heavy (H) labeled cells were incubated with Dex, medium (M) labeled cells with Dex in the presence of soluble Dex and light (L) labeled cells with the negative control (acetic acid). Mass spectrometry identified 139 possible target proteins. The number of proteins identified might be small, but the identified proteins could display important dexamethasone interaction partners.

This SILAC was performed as a soluble competition assay. A 10-fold excess of soluble dexamethasone competes for proteins in solution with dexamethasone-immobilized beads. Specific interaction partners bind to the dexamethasone excess in solution. Therefore, specific proteins are found in the supernatant. The immobilized dexamethasone beads in presence (M) or absence (H) of dexamethasone in solution have the same experimental settings and can be compared. A discrimination of probable contaminants is no longer necessary, because all proteins identified with H/L and not with H/M bind specific to dexamethasone-immobilized beads and have an influence on dexamethasone.

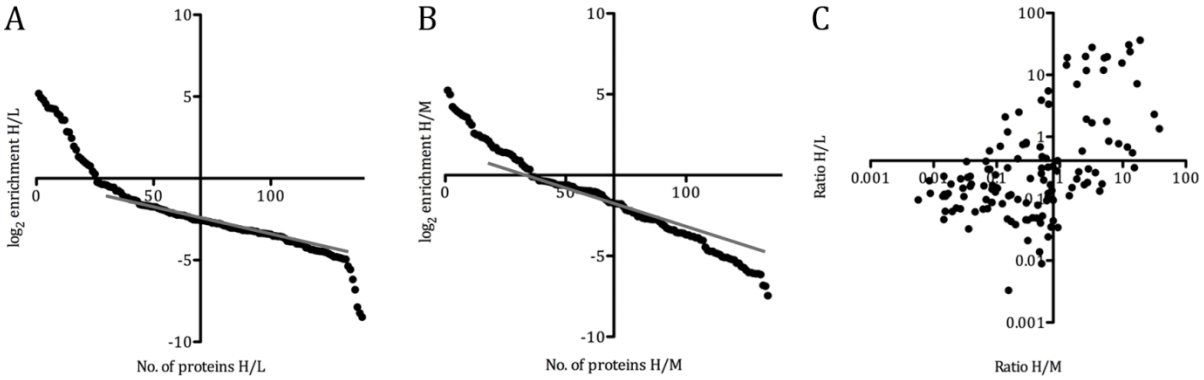

Figure 3-14 SILAC evaluation dexamethasone: A: The log_2 enrichment of H/L was plotted against the number of proteins. A line was drawn through the linear part of the graph (light grey) and intersects at protein 40. B: The log_2 enrichment of H/M was plotted against the number of proteins. A line was drawn through the linear part of the graph (light grey) and intersects at protein 40. C: Scatter plot with determined intersections (H/L protein 40; H/M protein: 40).

In order to discover specific target proteins, a diagram of the log_2 enrichment of H/L (Figure 3-14 A) and H/M (Figure 3-14 B) respectively was plotted against the number of proteins. Proteins above the line resemble most likely specific interaction partners of dexamethasone (intersection: protein 40 for H/L and H/M). Figure 3-14 A and B were used to determine the intersection in the scatter plot (Figure 3-14 C). Proteins in the upper right are important, because the ratios from both H/M and H/L are high and resemble specific dexamethasone interaction partners. In this square 26 proteins remain and are presented in Table 3-5.

The histogram of the frequency distribution from H/L and H/M (Figure 8-1 C) can be found in the appendix. It is noticeable, that both histograms display a bimodal-like distribution.

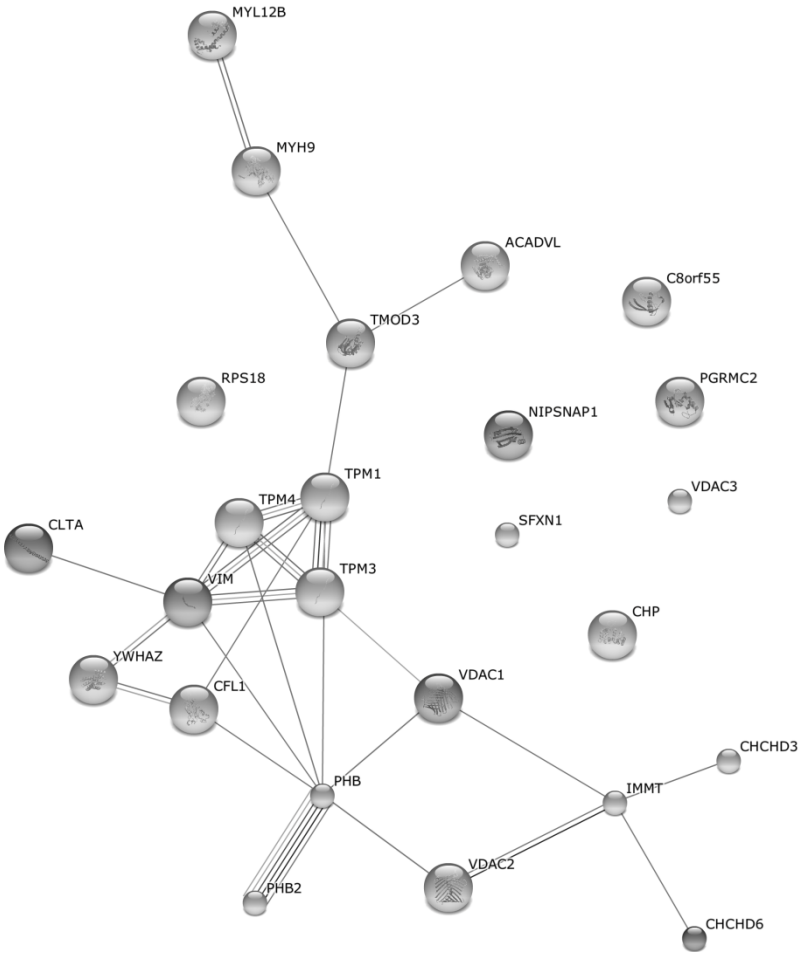

Figure 3-15: Network of possible dexamethasone target candidates: A: The dexamethasone network of identified target proteins is displayed. The analysis was performed with STRING[73]. Abbreviations of genes are explained in **Table 3-5** and in section 8.3.4 a little description of the corresponding protein function is given.

The network of the remaining 26 proteins was investigated by subjecting proteins to the STRING database[73]. The results are depicted in Figure 3-15. Abbreviations and a short summary about the protein function can be found in section 8.3.4.

It is noteworthy that three different tropomyosin isoforms were isolated. They all interact with each other (Figure 3-15). Additionally, vimentin as an intermediate filament was found to interact with some tropomyosin isoforms. Tropomyosins are a group of proteins that will be discussed in section 4.2.2.1.

A steroid receptor was also identified in this SILAC experiment. It is the progesterone receptor membrane component 2 (PGRMC2) that will be discussed in section 4.2.2.3.

Table 3-5 Protein hit list of soluble competition SILAC evaluation dexamethasone: The protein list is arranged by highest ratios for Dex H/M. The other ratios in this table represent results from the different SILAC experiments (part 2: GC experiment section 3.3.2; part 3 SH experiments: section 3.3.3 and 3.3.4) performed in this thesis. H represents the intensity of identified heavy peptides of the corresponding protein. M and L behave accordingly. Bold printed proteins will be discussed.

Protein Names	Gene Names	Ratio M/L Dex	Ratio H/L Dex	No H/L	**Ratio H/M Dex**	No H/M	Ratio M/L GCs	No HC	Ratio H/L GCs	No Dex	Ratio H/M GCs	Ratio H/M norm GCs	No GC H/M norm	Ratio M/L SH	No Prog	Ratio H/L SH	No Testo	Ratio H/M Norm SH	No SH H/M norm
Tropomyosin-3	TPM3	0,03	1,349	24	**38,0**	1		673		668			751	1,1	462	0,496	450	0,78	313
Myosin regulatory light chain 12B	MYL12B	0,06	2,306	19	**31,6**	2	4,26	583	2,35	654	0,536	0,472	665	2,727	389	1,065	407	0,804	299
Prohibitin	PHB	1,81	36,28	1	**18,8**	3	30,3	65	37	52	1,135	1,179	330	30,12	17	24,2	26	1,414	79
Calcium-binding protein p22	CHP	0,3	7,208	13	**16,8**	4	24,4	137	33,5	93	1,262	0,985	465	35,94	6	8,615	90	0,543	416
Myosin-9	MYH9	0,02	0,551	36	**14,2**	6	18	251	9,2	545	0,528	0,843	572	7,427	238	3,54	208	0,979	220
Prohibitin-2	PHB2	1,92	23,76	4	**13,0**	7	23,2	157	34,4	81	1,142	1,241	301	34,81	8	25,46	22	1,242	113
Coiled-coil-helix-coiled-coil-helix domain-containing protein 3, mitochondrial	CHCHD3	2,49	30,62	2	**12,5**	8	25,5	124	29,9	152	1,021	0,96	487	28,22	24	24,74	25	1,734	48
Tropomodulin-3	TMOD3	0,04	0,683	33	**11,9**	9	3,38	610	2,18	656	0,67	0,884	546	2,169	421	1,143	395	0,795	307
Mitofilin	IMMT	0,59	15,58	9	**9,71**	10	19,1	234	32,6	109	1,348	1,439	236	9,826	189	25,12	23	2,9	18
Clathrin light chain A	CLTA	0,05	0,771	29	**8,60**	11	3,05	619	5,97	597	1,967	2,031	87	1,066	463	0,412	458	0,597	396
Vimentin	VIM	0,11	0,849	26	6,00	12	8,67	464	19,2	382	1,508	1,638	169	3,143	366	0,648	440	0,411	457
Sideroflexin-1	SFXN1	2,77	19,6	6	**5,64**	13		674		669			795		498		498		498
Tropomyosin-1	TPM1	0,08	1,774	22	5,57	14	2,1	643	1,11	665	0,594	0,788	599	1,232	459	0,556	447	0,746	336
Voltage-dependent anion-selective channel protein 3	VDAC3	3,21	18,76	8	**5,08**	15		675		670			676	11,36	169	34,18	2	4,188	6
Coiled-coil-helix-coiled-coil-helix domain-containing protein 6	CHCHD6	1,01	11,9	11	**4,94**	16	10,2	426	8,82	555	0,924	1,044	408	23,03	51	15,66	43	1,28	104
Voltage-dependent anion-selective channel protein 1	VDAC1	8	27,83	3	**3,25**	20	29,4	73	27,7	191	0,92	0,858	563	23,41	47	30,68	9	2,136	32
Tropomyosin-4	TPM4	0,02	1,679	23	3,24	21		676		671			758	0,908	471	0,449	456	0,714	349
Stomatin-like protein 2	STOML2	0,73	1,927	21	**2,64**	24	15,3	320	27	209	1,17	1,527	198	26,01	35	24,81	24	1,507	64
Mesenchymal stem cell protein DSCD75	C8orf55	2,98	11,78	12	**2,64**	25		677		672			796		499		499		499
Membrane-associated progesterone receptor component 2	PGRMC2	6,7	19,81	5	2,56	26		678		673			797		500		500		500
14-3-3 protein zeta/delta	YWHAZ	0,21	0,588	35	**2,27**	28	21,2	191	35,2	70	1,823	1,691	156	13,62	141	5,909	138	0,723	344
Acyl-Coenzyme A dehydrogenase, very long chain variant	ACADVL	3,11	7,077	14	**1,88**	30	18	254	38,2	42	1,803	1,953	100	16,81	107	32,79	5	3,7	11
Voltage-dependent anion-selective channel protein 2	VDAC2	12,8	19,1	7	**1,32**	34	29,2	76	6,75	586	0,536	0,692	631	19,09	80	31,19	8	2,722	20
Protein NipSnap homolog 1	NIPSNAP1	10,8	14,41	10	**1,28**	35	23,2	155	9,74	531	0,787	0,771	609	19,96	74	41	1	4,151	7
40S ribosomal protein S18	RPS18	0,45	0,411	40	**0,92**	37	31,9	50	39,8	30	1,142	1,039	412	36,21	5	14,2	53	0,937	244
Cofilin-1	CFL1	0,9	0,478	37	**0,53**	56	3,31	613	9,06	548	2,134	1,77	136	1,217	460	0,331	462	0,578	403

3.3.6. Atorvastatin and englerin A

The SILAC experiments for englerin A and atorvastatin were performed in collaboration with the group of Prof. Maier (Eberhard-Karls Universität, Tübingen). The evaluation was performed by Pramod Sawant and can be found in his dissertation[46]. He identified acylglycerol kinase as possible target for atorvastatin lactone and prohibitin for englerin A.

3.4. Peroxiredoxin 1

3.4.1. Introduction

Peroxiredoxin 1 (Prdx1) belongs to the superfamily of peroxidases that reduce peroxides[51, 91]. These enzymes can be found in all three life kingdoms. Unlike catalase, superoxide dismutases or selenocysteine-containing glutathione peroxidases, peroxiredoxins do not need heme, selenium, flavin or metal ions as redox factors[92, 93].

Peroxiredoxins exhibit a dual function. Under normal conditions, yeast Prdx1 (cPrx1) forms dimers and tetramers that are in equilibrium with doughnut- and ball-shaped decamers (Figure 3-16 A). Decamers are generated by five dimers that are linked by disulfide bonds and/or hydrophobic interactions, respectively. Dimers and tetramers function as peroxidases detoxifying hydrogen peroxides, whereas decamers act as protein chaperones. Upon heat shock or oxidative stress treatment, reactive oxygen species (ROS) occur that will overoxidize cPrx1 to sulfinic or sulfonic acid forming dodecahedrons (12 decamers) that can act as super-chaperones[94-97]. Aran et al. showed, that overoxidation of Prdx1 can lead to high molecular weight species that are no longer soluble. ATP and Mg^{2+} act as cofactors for those species. In high concentrations of ATP and Mg^{2+}, an aggregation can be detected that is neutralized upon chelating Mg^{2+} or ATP removal[97, 98]. The functions of hyperoxidation of 2-Cys Prdxs are protection of hydrogen peroxide signaling molecules and the increase in chaperone activity[99]. The floodgate model can explain the protection of hydrogen peroxide signaling molecules. It describes the hyperoxidation as part of the 2-Cys Prdx cycle that is sufficient for H_2O_2 signaling[100, 101]. Another example for specific H_2O_2 accumulation due to inactivation of 2-Cys Prdxs is the specific phosphorylation of lipid raft-associated 2-Cys Prdxs at Tyr194. This phosphorylation leads to a loss of peroxidase activity resulting in an increase in H_2O_2 that can perform signaling whereas the global redox potential is not disturbed[93]. Unlike the phosphorylation at Tyr194, the phosphorylation at Thr90 induces structural changes resulting in higher molecular weight species that leads to a

switch to chaperone function[102]. Other factors promoting molecular chaperone functions are high concentrations of calcium, high or low ionic strength or a low pH[103].

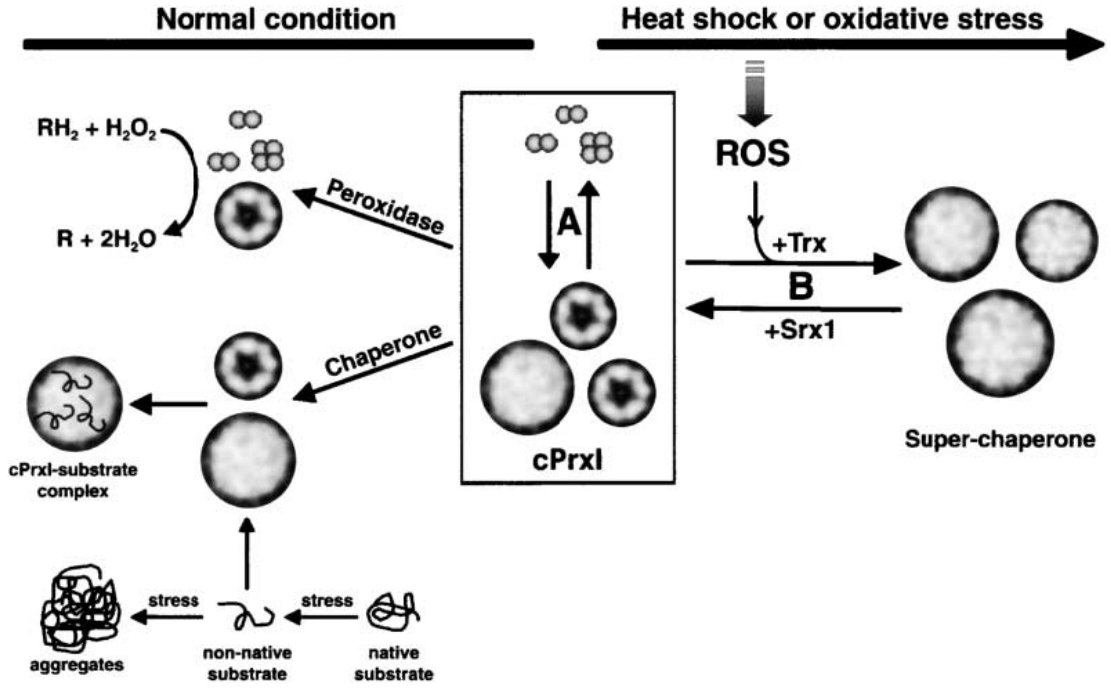

Figure 3-16 Model of functional switching of Prdx1: Under normal conditions, cPrx1 (= yeast Prdx1) exhibits both low molecular weight species such as dimers and tetramers that act as a peroxidase and in addition it forms higher molecular weight species that act as chaperones. A: Formation of high to low molecular weight species is H_2O_2 insensitive and in an equilibrium state. B: Upon heat shock or oxidative stress reactive oxygen species (ROS) overoxidize Prdx1 forming super-chaperones that can be reduced with sulfiredoxin 1 (Srx1). Image taken from Jang[94].

Prdx1 was first identified in *Saccharomyces cerevisiae* and named thiol-specific antioxidant. In the following years, six human peroxiredoxin family members were identified. They can be classified into three groups. 2-Cys peroxiredoxins contain two active cysteine residues, the peroxidatic cysteine (C_P) and the resolving cysteine (C_R). Prdx1-4 belong to the typical 2-Cys family, Prdx5 to the atypical 2-Cys and Prdx6 to the 1-Cys peroxiredoxins. Prdx1, 2 and 6 are mainly located inside the cytosol, whereas Prdx3 is hindered in mitochondria, Prdx4 in the endoplasmic reticulum and Prdx5 is present either in the cytosol, mitochondria or peroxisomes[93, 99]. The molecular mechanism of peroxide detoxification is depicted in Figure 3-17. Typical 2-Cys peroxiredoxins form an intermolecular disulfide bond after reduction of peroxides whereas atypical 2-Cys peroxiredoxins form an intramolecular disulfide bond (Figure 3-17 A and B). 1-Cys peroxiredoxins do not form a disulfide bond (Figure 3-17 C). Upon oxidation by hydrogen peroxide, the obtained sulfenic acid will be reduced by GSH. Disulfide bonds of 2-Cys peroxiredoxins can be reduced by the thioredoxin (Trx) / thioredoxin reductase (TrxR) / NADPH system to regain detoxifying activity[51, 91, 92].

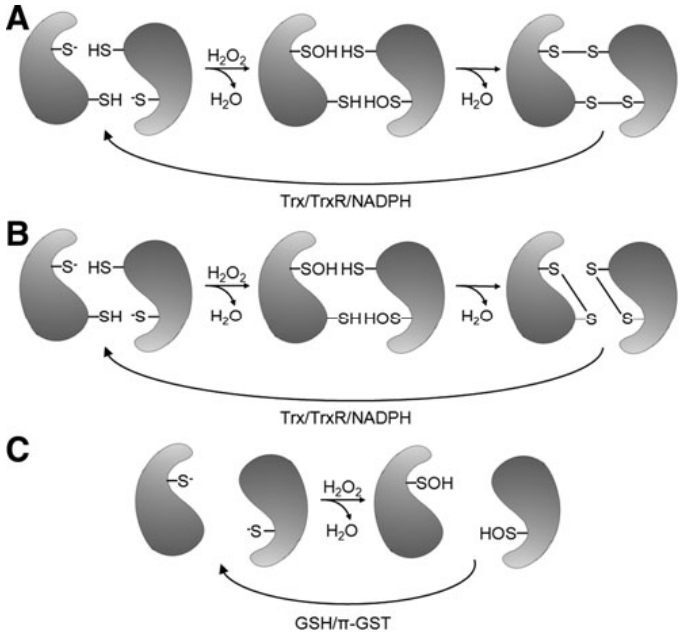

Figure 3-17 Reaction mechanism of peroxiredoxins: A: The reduction of peroxides by typical 2-Cys peroxiredoxins is displayed. After oxidation of C_P (peroxidatic cysteine), the C_R (resolving cysteine) of a neighboring peroxiredoxin molecule forms an intermolecular disulfide bond. Reduction of oxidized peroxiredoxin can be performed with the thioredoxin (Trx) / thioredoxin reductase (TrxR) / NADPH system. B: The reduction of peroxides by atypical 2-Cys peroxidases is displayed. After oxidation of C_P, C_R of the same peroxiredoxin molecule forms an intramolecular disulfide bond. Reduction of oxidized peroxiredoxin can be performed with the Trx/TrxR/NADPH system. C: The reduction of peroxides by 1-Cys peroxiredoxins is displayed. After oxidation of C_P, the obtained sulfenic acid is reduced by GSH, but not Trx. Image taken from Rhee[91].

Mice lacking Prdx1 display an increased cellular level of ROS and will die prematurely of cancer[104, 105].

As described earlier in section 3.2.5 and 3.3.2, peroxiredoxin 1 was identified in three individual experiments via MS. Peroxiredoxin 1 is an important protein in the oxidative stress pathway. An interaction between glucocorticoids and peroxiredoxins has not been described yet. Therefore, interaction studies were performed. First, the direct interaction of recombinantly purified Prdx1 with HC and Dex was investigated. Whether Dex has an influence on Prdx1 activity was tested using an enzyme activity assay with the thioredoxin (Trx) / thioredoxin reductase (TrxR) / NADPH system peroxidase recovering system. The oligomerization of Prdx1 is important for its function as a peroxidase or chaperone respectively, therefore the effect of Dex on Prdx1 oligomerization was examined. The influence of Dex and Prdx1 on the serine/threonine kinase Akt was described[52, 106], hence, the impact of Dex on Akt phosphorylation was investigated.

3.4.2. Purification of recombinant peroxiredoxin 1 (human)

Prdx1 was purified in order to test the interaction of GCs with Prdx1. For the purification procedure, Prdx1 was expressed in *E. coli* and cell lysis was performed using a French press. After centrifugation, the supernatant was subjected to a HiTrap FF SP column (1 mL) for cation exchange chromatography.

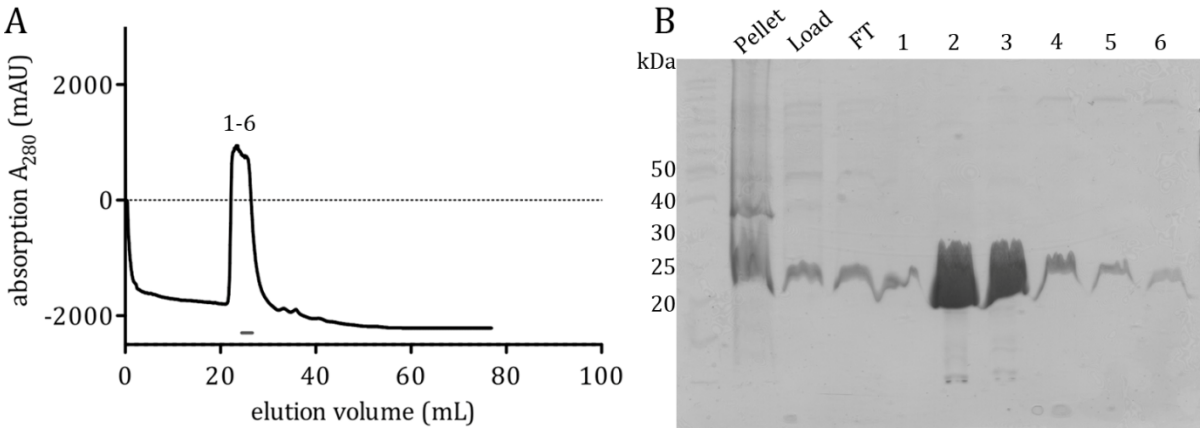

Figure 3-18 Purification and SDS-PAGE analysis of Prdx1: A: Cation exchange chromatography with a HiTrap FF SP column. Elution was performed with a linear gradient of NaCl, according to **Table 2-3**. Fractions marked with a grey bar were used for further analysis. B: 15 µL of samples from cation exchange chromatography were subjected to SDS-PAGE. Nearly pure Prdx1 can be detected at 22 kDa. FT: flow through

The cation exchange chromatogram is displayed in Figure 3-18 A. Purification of *E. coli* cell lysate results in one major peak. Fractions 1-6 were subjected to SDS-PAGE analysis (Figure 3-18 B). The grey bar indicates the pooled fractions that were used for further analysis (Figure 3-18 A) and contain almost pure Prdx1. Expression of Prdx1 from 800 mL LB-medium resulted in approximately 35 mg pure protein.

A partial degradation of recombinant Prdx1 was observed when stored at -80°C. This became evident when the protein was used for the Prdx activity assay (section 3.4.4).

3.4.3. Recombinant peroxiredoxin 1 directly binds to glucocorticoids

A direct interaction of Prdx1 to GC-immobilized beads was tested to examine whether the interaction needs other factors present in the cell lysate. Different concentrations of recombinantly purified Prdx1 were incubated with HC, Dex or negative control (acetic acid) beads for 4 h. The eluate and supernatant fractions are shown in Figure 3-20. For HC and Dex immobilized beads the amount of Prdx1 in the eluate increases from 200 to 1000 ng Prdx1. In the negative control no Prdx1 is eluted at all three concentrations. In conclusion, Prdx1 is able to bind directly to HC- and Dex-immobilized beads in a concentration-dependent manner.

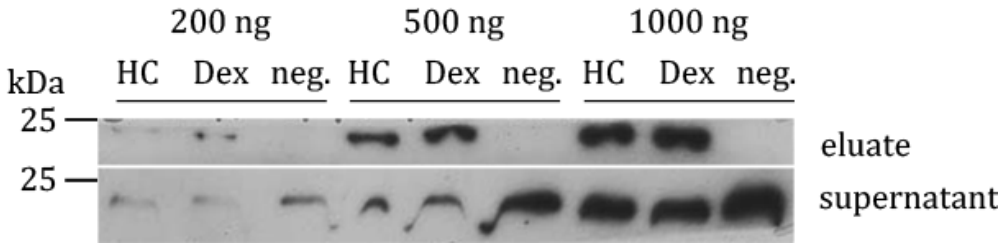

Figure 3-19 A representative Western blot of the direct binding assay of Prdx1 with increasing concentrations of Prdx1: HC-3-CMO, Dex-3-CMO or negative control beads (immobilized with DMSO) were blocked with 0.5 % milk powder in Binding buffer for 30 min and incubated with 200, 500 or 1000 ng Prdx1 for 4 h. 10 % of the eluate and 2 % of the supernatant were subjected to SDS-PAGE and Western blotting with an α-Prdx1 antibody (1:1000 in PBS-Triton 0.1 %). n = 6

In addition, a different method to analyze the binding of Prdx1 to GC-immobilized beads was used. As described for the SILAC experiment with soluble competition (section 3.3.5), HC or Dex immobilized beads were incubated for 4 h with or without soluble dexamethasone or hydrocortisone in the presence of 2.4 µg Prdx1. The excess of soluble Dex / HC compared to immobilized Dex / HC on beads was calculated with the help of in section 3.2.1 obtained results. The eluate is shown in Figure 3-20. Dex and HC immobilized beads are incubated in the presence (SC) or absence (-) of soluble HC / Dex. For Dex a rather slight band is visible, which disappears in the presence of soluble dexamethasone (excess: ≈10). In the negative control no Prdx1 is visible.

For HC Prdx1 is more eluted in the presence of HC in solution (excess: ≈2), indicating that the soluble competition did not work properly. Therefore, negative (acetic acid) beads were incubated in ethanol 50 % in the presence (SC) or absence (-) of HC in solution and subjected to the direct binding assay (Figure 3-20 (right)). The Western blot showed that Prdx1 was bound to the negative control in presence of 50 % ethanol, which was increased when HC was present. This observation explains the increasing amount of Prdx1 present in HC SC (Figure 3-20 left). Ethanol might lead to a decreased stability of Prdx1 resulting in an increased detected amount in the Western Blot.

In conclusion, the soluble competition with dexamethasone was successful. This indicates a direct interaction of Dex and Prdx1 that can be abolished in the presence of a soluble excess of dexamethasone.

The soluble competition with HC was unsuccessful, due to the solvent ethanol. For further analysis, water-soluble HC should be used and the SC experiment has to be repeated.

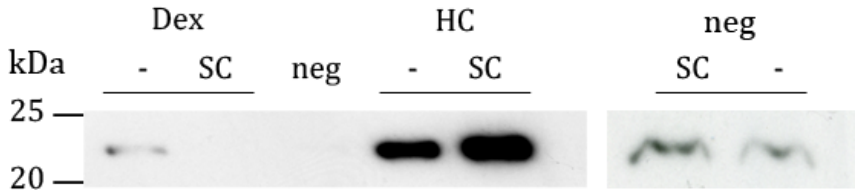

Figure 3-20 A representative Western blot of the direct binding assay of Prdx1 with soluble competition: HC-3-CMO, Dex-3-CMO or negative control beads (immobilized with Dioxan 50 %) were blocked with 0.5 % milk powder in Binding buffer for 30 min. The incubation was performed with (SC) or without (-) the presence of 50 mM Dex or 10 mM HC (solubilized in ethanol 50 %) respectively as soluble competition (SC). Negative control beads on the right were incubated with ethanol 50 % in presence (SC) or absence (-) of 10 mM HC. In all experiments, beads were incubated with 2.4 µg Prdx1 for 4 h and afterwards 5 % of the eluate was subjected to SDS-PAGE and Western blotting with an α-Prdx1 antibody (1:1000 in PBS-Triton 0.1 %). n = 3, right n = 1

3.4.4. Peroxiredoxin activity assay

As described in section 3.4.3, a direct interaction between hydrocortisone-/ dexamethasone-immobilized beads and Prdx1 was shown. In order to test the influence of dexamethasone on Prdx1, a 2-Cys Prdx activity assay was established. The principle of the 2-Cys-Prdx activity assay is depicted in Figure 3-21. 2-Cys peroxiredoxins contain two cysteine residues, located at position 52 and 173. These cysteines are oxidized upon exposure to H_2O_2 (substrate) forming dimers via an intermolecular disulfide bridge. This process can be reversed by thioredoxin 1 (Trx1) by reducing oxidized Prdxs and forming an intramolecular disulfide bridge itself. Trx1 is reduced by thioredoxin reductase (TrxR), which oxidizes NADPH to $NADP^+$. The decrease of NADPH absorption at 340 nm can be visualized with an ELISA reader[62].

The proteins required for this test were recombinantly expressed and purified as described in section 3.4.4.1 and 3.4.4.2.

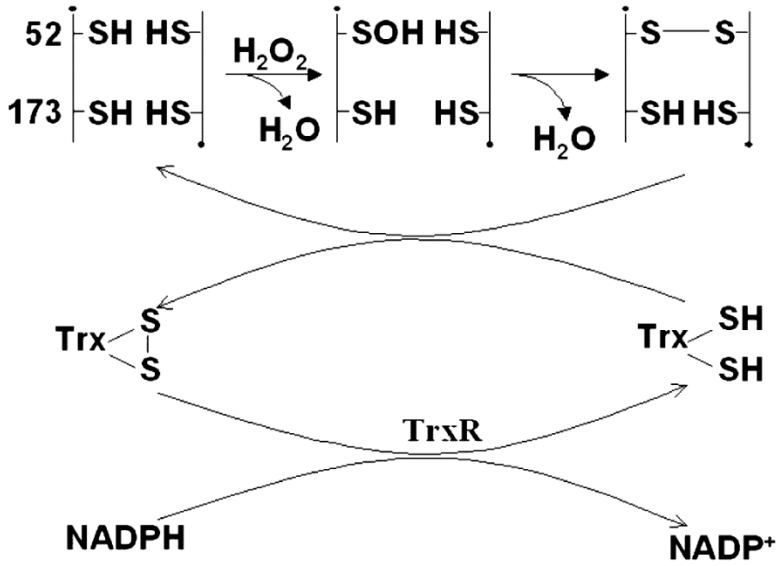

Figure 3-21 Prdx1 activity assay: Prdx1 is oxidized by H_2O_2 and forms dimers via an intermolecular disulfide bond. Thioredoxin 1 (Trx1) can reduce the oxidized Cys groups forming an intramolecular sulfide bond itself. Trx1 can be reduced by thioredoxin reductase (TrxR), which oxidizes NADPH to $NADP^+$ leading to a decrease of NADPH absorption at 340 nm. Image taken from Kim[62].

3.4.4.1.Purification of Thioredoxin Reductase (yeast)

Yeast thioredoxin reductase (yTrxR) was expressed in *E.coli* after induction with IPTG overnight. Cell lysis was performed by sonication followed by anion exchange chromatography, size exclusion chromatography (SEC) and a second anion exchange chromatography. The procedure was modified from Kim et al.[62].

The chromatogram of the first anion exchange chromatography is shown in Figure 3-22 A. The grey bar indicates the fractions used for SEC. The resulting purity (Figure 3-22 B) was not satisfactory, therefore SEC fractions were pooled and subjected to a second anion exchange chromatography with a different NaCl gradient (Figure 3-22 A). The SDS-PAGE of the purified yTrxR protein is shown in Figure 3-23 B. Fractions marked with a grey bar in Figure 3-23 A were pooled and used for 2-Cys Prdx activity assay.

Expression of yTrxR in 1.6 L LB-medium resulted in approximately 7 mg pure protein.

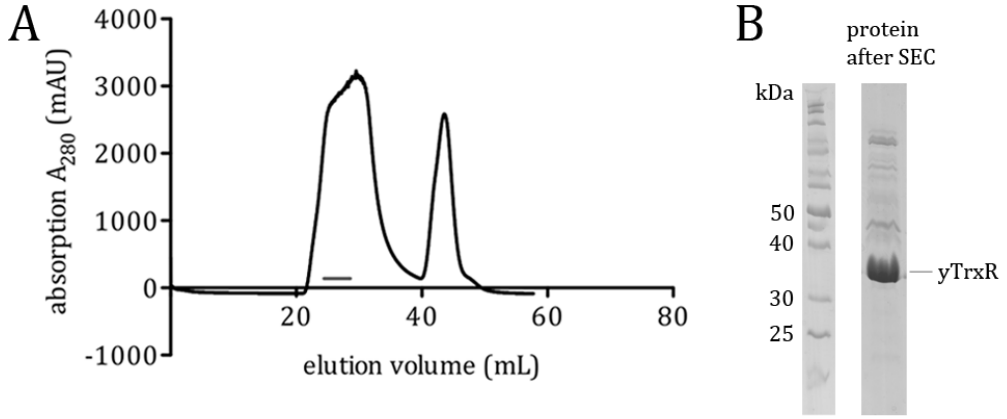

Figure 3-22 Anion exchange chromatography and SDS-PAGE analysis of yTrxR SEC: A: yTrxR was purified with a 1 mL HiTrap DEAE FF anion exchange chromatography column. The elution was performed with a linear gradient combined with a step gradient of NaCl, according to **Table 2-4** IEX I. Fractions marked with a grey bar were used for SEC. B: Protein analysis of 15 µL samples after SEC was performed. yTrxR can be detected at 35 kDa.

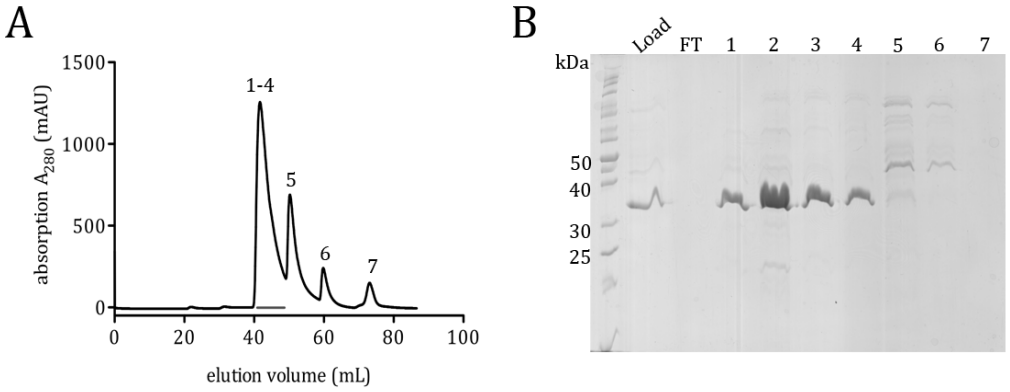

Figure 3-23 Purification and SDS-PAGE of yTrxR: A: yTrxR was purified with a 1 mL HiTrap DEAE FF anion exchange chromatography column. The elution was performed with a step gradient of NaCl, according to **Table 2-4** IEX II. Fractions marked with a grey bar were used for the Prdx activity assay. B: 15 µL of samples from the second anion exchange chromatography were subjected to SDS-PAGE. Nearly pure yTrxR can be detected at 35 kDa. FT: flow through

3.4.4.2.Purification of His-Thioredoxin 1 (yeast)

Kim et al. described a procedure to purify yTrx1 by anion exchange chromatography[62]. Following this procedure, no pure protein could be isolated.

Therefore, the yTrx1 gene was cloned into the pET28a vector resulting in yHisTrx1 with an N-terminal His-tag. yHisTrx1 was transformed in *E. coli* and induced with IPTG for 3 h prior to harvesting cells. Cell lysis was performed using a sonicator. Purification was carried out with a HiTrap Ni^{2+} column (1 mL). The chromatogram is shown in Figure 3-24 A. The grey bar indicates the fractions that were pooled and used for SEC. The SEC chromatogram is depicted in Figure 3-24 B. The SDS-PAGE of the purified yHisTrx1 protein shows nearly pure yHisTrx1 protein in fractions 2-8 (Figure 3-24 C). Fractions marked with a grey bar in Figure 3-24 B were pooled and used for the 2-Cys Prdx activity assay.

Expression of yHisTrx1 in 1.6 L LB-medium resulted in approximately 5 mg pure protein.

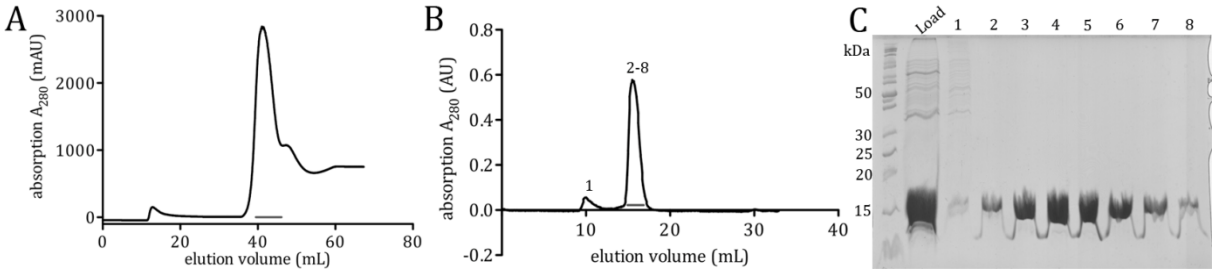

Figure 3-24 Purification and SDS-PAGE analysis of yHisTrx1: A: yHisTrx1 was purified with a 1 mL HisTrap Ni^{2+} column. The elution was performed with a linear gradient of HisB listed in **Table 2-5**. Fractions marked with a grey bar were used for SEC. B: chromatogram of SEC. Fractions marked with a grey bar were used for Prdx activity assay. C: 15 µL of samples from SEC were subjected to SDS-PAGE, whereas load resembles combined fractions from Ni^{2+} column chromatography indicated by the grey bar in A. Nearly pure yHisTrx1 can be detected at 15 kDa .

3.4.4.3. 2-Cys peroxiredoxin activity assay

In order to test the ability of the purified proteins for use in the 2-Cys Prdx activity assay, yTrxR activity was determined. yHisTrx1 was oxidized with H_2O_2, and NADPH decrease was measured in the presence of yTrxR. Specific activity was obtained after 3.5 min, because the reaction was linear up to 3.5 min. The yTrxR specific activity was 40 - 55 µmol NADPH oxidized x min^{-1} x mg^{-1} protein. Kim et al. were able to determine a specific activity of yTrxR of 1.8 µmol NADPH oxidized x min^{-1} x mg^{-1} protein. The enzyme prepared here had a much higher specific activity and was therefore appropriate for further use[62].

To determine the assay conditions of the Prdx activity assay, the absorption of different Prdx1 concentrations was monitored over time (Figure 3-25 A). The absorption was measured in 30 s intervals. The reaction remained linear for 10 min with all concentrations of Prdx1 used. In addition, a linear dependency between µmol of NADPH

oxidized x min^{-1} to the amount of protein was achieved with these assay conditions (Figure 3-25 B).

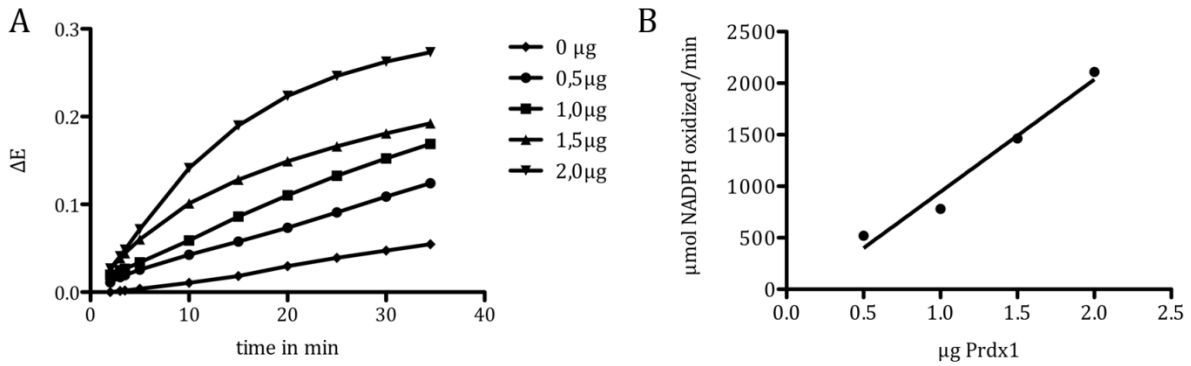

Figure 3-25 Time and protein-dependency of the 2-Cys Prdx activity assay: A: The change in absorption (ΔE) was plotted against the time in min. Growing concentrations of Prdx1 resulted in an increase of ΔE. A linear relationship is visible up to 10 min. B: The specific activity at 10 min in µmol NADPH oxidized x min^{-1} was plotted against µg of Prdx1. Growing concentrations of Prdx1 resulted in a nearly linear increase in µmol NADPH oxidized x min^{-1}.

3.4.4.4.Influence of dexamethasone on peroxiredoxin 1 activity

The Prdx activity assay was now used to determine the influence of dexamethasone on Prdx1 activity. Prior to the assay, Prdx1 was incubated with different dexamethasone concentrations for 15 min at 30°C. The decrease of NADPH at 340 nm was monitored after addition of yHisTrx1, yTrxR, NADPH and H_2O_2 in 30 s intervals for 10 min. The µmol NADPH oxidized x min^{-1} x mg^{-1} protein was determined and is depicted Figure 3-26.

The result of three independent triplet experiments is displayed. The incubation of dexamethasone with Prdx1 15 min prior to measurement does not have any influence on Prdx1 activity. The 2-Cys Prdx activity of Prdx1 in presence of dexamethasone is not significantly altered.

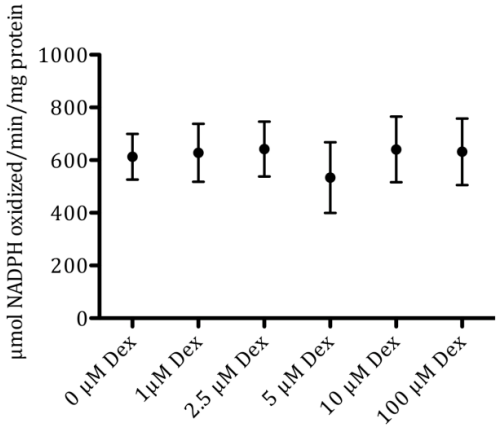

Figure 3-26 2-Cys Prdx activity in µmol of oxidized NADPH x min^{-1} x mg^{-1} protein in the presence or absence of dexamethasone: 15 min prior to measurements, 2.4 µg Prdx1 was incubated with different concentrations of Dex. Afterwards yHisTrx1, yTrxR, NADPH and H_2O_2 were added and the decrease of NADPH absorption at 340 nm was measured every 30 s for 10 min. The amount of µmol NADPH oxidized x min^{-1} x mg^{-1} protein was determined and is shown in the graph. Mean ± SD; n = 3

3.4.5. Influence of dexamethasone on the oligomerization of peroxiredoxin 1

As discussed in section 3.4.4, dexamethasone does not have an influence on Prdx1 activity. Another possibility to influence Prdx1 characteristics could be a change in Prdx1 oligomerization. The function as a molecular chaperone of Prdx1 is discussed in section 3.4.1. Formation of oligomers results in different Prdx1 properties. Prdx1 dimers and tetramers can be reduced to monomers and act as enzymes to detoxify hydrogen peroxide. Decamers rather exhibit molecular chaperone functions[94]. Therefore, the oligomerization state of Prdx1 was analyzed in presence or absence of Dex.

In order to determine the amount of H_2O_2 that oxidizes Prdx1 appropriately, a dilution series was used. The oligomerization states of Prdx1 in presence of different H_2O_2 concentrations in the absence of β-ME are displayed in Figure 3-27. 40 µM Prdx1 was incubated with appropriate amounts of H_2O_2 for 15 min at 37°C. Growing concentrations of H_2O_2 led to an increase in trimers and tetramers and a decrease in monomers and dimers, marked on the right (Figure 3-27).

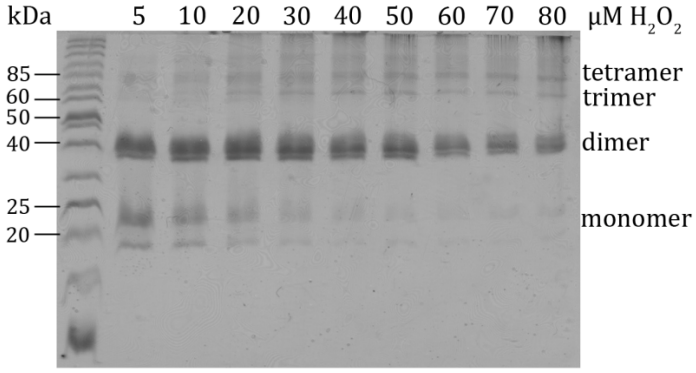

Figure 3-27 Prdx1 oligomerization in presence of H_2O_2: 40 µM Prdx1 was incubated in presence of Prdx1 SEC buffer with appropriate concentrations of H_2O_2 for 15 min at 37°C, Oligomers are marked on the right. A 12 % SDS-PAGE without β-ME in SDS loading dye was used for separation and the gel was stained with Coomassie.

In a more sensitive setting, 5.5 µM Prdx1 were exposed to different concentrations of H_2O_2 for 15 min and subjected to SDS-PAGE under non-reducing conditions and than analyzed via Western blotting. Two Western blots of Prdx1 without β-ME in SDS loading dye show different oligomerization states of Prdx1, which are marked on the right (Figure 3-28). Increasing concentrations of H_2O_2 were incubated with Prdx1 in the absence (Figure 3-28 A) or presence (Figure 3-28 B) of dexamethasone. Prdx1 was incubated with Dex prior to H_2O_2 treatment for 15 min at 37°C. Accidently, at 15 µM H_2O_2 the double amount of Prdx1 was used (indicated by *). This lane was ignored. For increasing concentrations of H_2O_2, the amount of dimers and tetramers slightly increased, whereas the amount of trimers decreased. At 0 µM H_2O_2 more monomers and less trimers and tetramers were visible than at higher concentrations. Decamers were

not visible in this experimental setting. It was shown that five dimers linked together by hydrophobic interactions form one decamer[94]. Therefore, an increase in the amount of dimers could point to an elevated level of decamers.

The difference between Figure 3-27 and Figure 3-28 becomes apparent especially in the change in oligomerization with growing concentrations of H_2O_2. It is possible, that Prdx1 needs distinct concentrations of H_2O_2 for the oligomerization, independent from its own concentrations. By scaling down the protein amount (from Coomassie gel to Western blotting) the amounts of H_2O_2 used may not be adequate for oligomerization studies. Furthermore, the amount of monomers is lower in the second experiment, which may be due to the aging of the protein. There was a difference of about one year between the first (Coomassie) and the second (Western blotting) experiment. Aging of Prdx1 is discussed to influence the oligomerization state[107].

In the presence of Dex (Figure 3-28 B) the oligomerization state slightly changed compared to no Dex treatment (Figure 3-28 A). Dexamethasone was able to decrease the amount of tetramers (and somewhat dimers) and increase the amount of monomers and trimers present after H_2O_2 treatment. Dex cannot intercept the effect of H_2O_2, but can attenuate it.

The exact mode of action of Dex on Prdx1 besides its elevation of Prdx1 monomers remains to be elucidated.

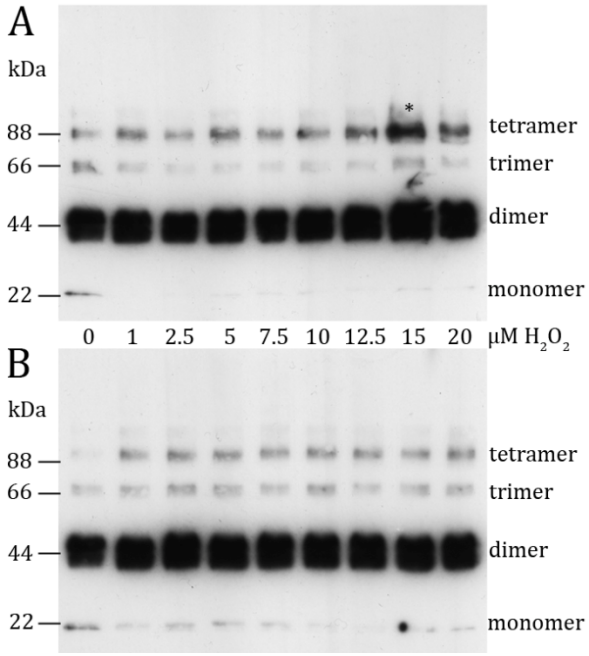

Figure 3-28 Western Blot of oligomerized Prdx1 in presence of appropriate amounts of H_2O_2, 8 % SDS-PAGE gel, without β-ME in SDS loading dye, concentrations for H_2O_2 apply for A and B, oligomers are marked on the right; A: 5.5 µM Prdx1 was incubated for 15 min at 37°C in presence of marked H_2O_2 concentrations without Dex. * indicates a higher amount of Prdx1 used by accident. B: 5.5 µM Prdx1 was treated with 40 µM Dex for 15 min at 37°C for 15 min prior to incubation with marked concentrations of H_2O_2 for 15 min at 37°C

3.4.6. Assay to investigate the signaling of Akt

Prdx1 and Dex both influence Akt phosphorylation. A relationship between those two was not reported yet. Therefore, an assay to investigate the signaling of Akt was developed.

Akt is a serine/threonine kinase and exhibits important functions in cellular signaling, particularly in survival, proliferation and growth. Akt consists of an N-terminal pleckstrin homology (PH) domain, a central catalytic domain as well as a short C-terminal regulatory domain[108]. A dysregulation in Akt signaling can lead to an increase in cell proliferation and a reduced cell apoptosis resulting in tumor development[104]. The PI3K (Phosphatidylinositol 3-kinases) signaling pathway, that also involves Akt, is depicted in Figure 3-29. Upon activation of the receptor tyrosine kinase (RTK), the receptor dimerizes and phosphorylates the insulin receptor substrate (IRS). The PI3K heterodimer, which consists of the regulatory subunit p85 and the catalytic subunit p110, localizes to the cellular membrane. PI3K binds to phosphatidylinositol (4,5)-bisphosphate (PIP_2), which is phosphorylated upon binding to phosphatidylinositol (3,4,5)-trisphosphate (PIP_3). PIP_3 can be dephosphorylated by the phosphatase and tensin homolog (PTEN) to PIP_2. PIP_3 on the other hand can bind to PH domains of for example Akt, which is then phosphorylated at Thr308 through phosphoinositide-dependent protein kinase-1 (PDK1) and at Ser473 through phosphoinositide dependent protein kinase-2 (PDK2). Phosphorylated Akt (AktP) can decrease the phosphorylation of BAD (Bcl-2-associated death promoter), FKHR (forkhead transcription factor), GSK3β (Glycogen synthase kinase 3) and increases the phosphorylation state of mTOR (mammalian target of rapamycin), MDM2, and NF-κB. Through these mechanisms, Akt is involved in apoptosis, cell cycle arrest, and DNA repair as well as cell growth[108].

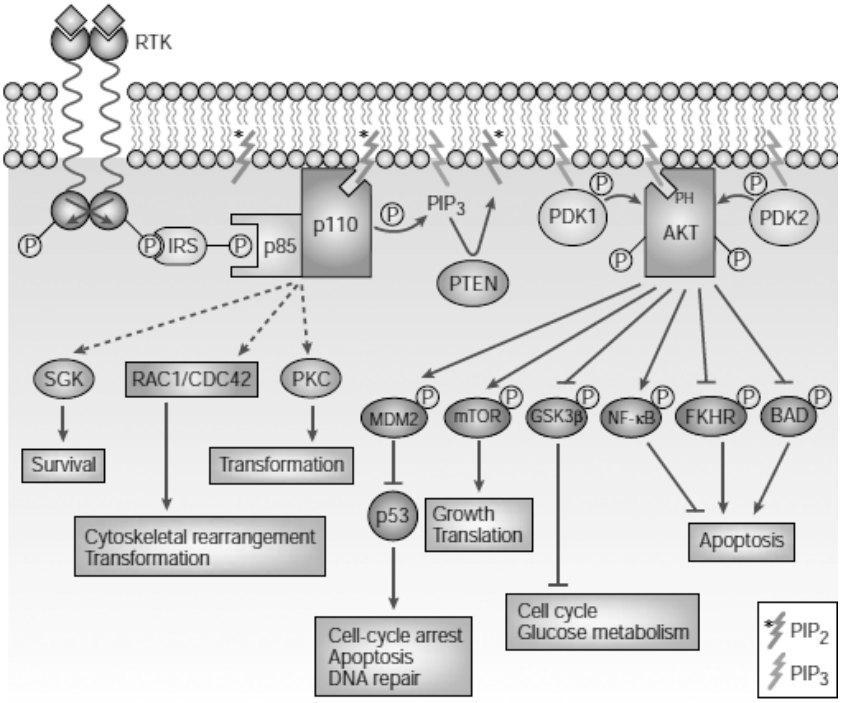

Figure 3-29 The PI3K (Phosphatidylinositol 3-kinase) signaling pathway: Upon activation of receptor tyrosine kinase (RTK), insulin receptor substrate (IRS) is phosphorylated. PI3K heterodimer p85 (regulatory subunit) and p110 (catalytic subunit) localize to membrane and bind to phosphatidylinositol (4,5)-bisphosphate (PIP_2), which is phosphorylated to phosphatidylinositol (3,4,5)-trisphosphate (PIP_3). PIP_3 can be dephosphorylated by phosphatase and tensin homolog (PTEN) to PIP_2. PIP_3 on the other hand can bind to pleckstrin homology (PH) domain of Akt, which is then phosphorylated on Thr308 through phosphoinositide-dependent protein kinase-1 (PDK1) and on Ser473 through phosphoinositide-dependent protein kinase-2 (PDK2). Phosphorylated Akt can decrease the phosphorylation of BAD (Bcl-2-associated death promoter), FKHR (forkhead transcription factor), GSK3β (Glycogen synthase kinase 3) and increases the phosphorylation state of mTOR (mammalian target of rapamycin), MDM2, and NF-κB. Through these mechanisms, Akt is involved in several cellular signaling processes. Image taken from Vivanco[108].

An important factor for the regulation of Akt is PTEN. If this negative regulator is missing, Akt activity is enhanced, which is characteristic for many tumor types. PTEN is a dual specificity phosphatase that exhibits activity against lipid and protein substrates [104, 108]. It consists of a catalytic Cys124 that forms a disulfide bond with Cys71 upon oxidation during oxidative stress[109]. The oxidation of Cys124 can be prevented by Prdx1 (Figure 3-30). During basal H_2O_2 levels, Prdx1 binds in a 1:1 (mol/mol) ratio to PTEN. Before oxidation of PTEN, Prdx1 will get oxidized by H_2O_2 to form dimers. Upon oxidative stress, Prdx1 will get overoxidized to sulfinic acids that can no longer be reduced. Therefore, the negative regulation property of PTEN is not protected and will be inactivated through oxidation. Akt signaling will be induced, which can lead to malignant transformations[51, 104].

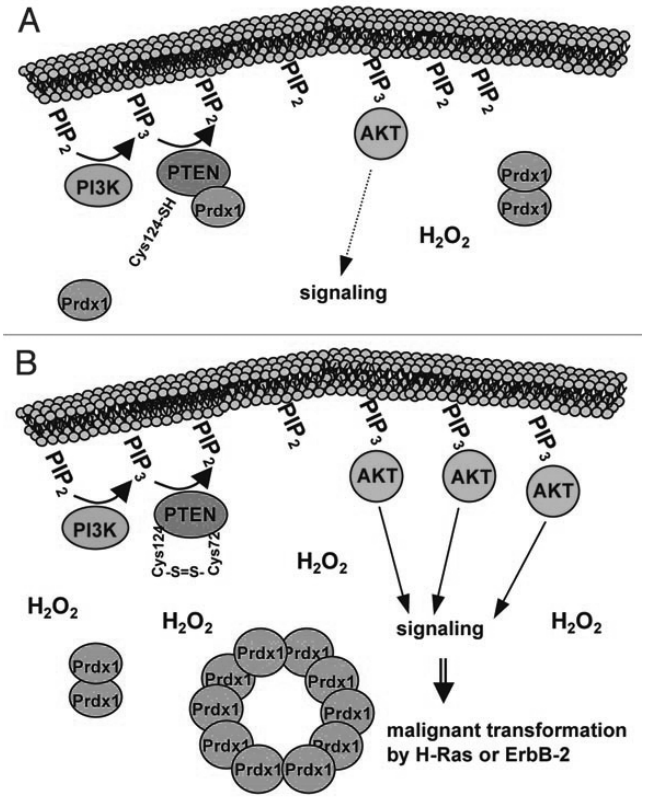

Figure 3-30 Involvement of Prdx1 in Akt signaling: PIP_2 is phosphorylated by PI3K to form PIP_3. PIP_3 can be dephosphorylated by PTEN to PIP_2. A: During basal levels of H_2O_2 Prdx1 is bound to PTEN in a 1:1 ratio to protect PTEN from oxidation of the catalytic Cys124. B: During oxidative stress, Prdx1 itself will get overoxidized to decamers that no longer exhibit protective effects for PTEN. Hence, Akt signaling is increased, which leads to malignant transformations. Image taken from Neumann[51].

The influence of Dex on Akt phosphorylation is not as easy to describe. The effect of Dex is dependent on the cell type, dose and the duration of the treatment. Akt phosphorylation is increased upon Dex treatment in epithelial ovarian cancer, breast cancer and cortical neurons. A decrease in Akt phosphorylation was shown for lymphoid cells, skin cells, chrondrocytes, pancreatic β-cells and muscle cells[3, 9, 31, 52, 106, 110].

It was also described, that GC treatment exhibits a cardioprotective effect. GC stimulates the PI3K signaling pathway through Akt phosphorylation in a GR dependent manner leading to eNOS (endothelial nitric oxide synthase) activation, which increases the NO production resulting in vasodilation[9, 82]. However, the opposed effect was described by Duckles et al. there an AktP decrease resulted in a decreased NO production and therefore a vasoconstriction[110]. Duckles pointed out, that this effect is cell-type-, dose- and treatment-duration-dependent[110]. For this reason, it is not easy to foresee the effect Dex will exert on Akt in A549 cells. An assay to investigate the signaling of Akt was developed to clarify the effect of Dex on Akt phosphorylation.

A549 cells were incubated for 15 min with different compounds as mentioned below prior to 15 min H_2O_2 treatment. The amount of phosphorylated Akt was measured

afterwards via Western blotting. IGF1 (insulin-like growth factor 1) is known to elevate the levels of AktP significantly[52] and was therefore used as a positive control. Ascorbic acid (VitC) as an antioxidant was used for all experiments. One control was not incubated with H_2O_2 (neg) to display the endogenous levels of AktP in the absence of oxidative stress. The other control was incubated solely with H_2O_2 (neg H_2O_2). Quantitative evaluation was performed using AIDA imaging software to normalize AktP levels with Akt as an internal standard. The calculation of n-different experiments was related to the amount of AktP of the negative control (neg) and then correlated to the negative control H_2O_2. The mean +/- SD calculation was performed using Prism (GraphPad Inc.).

Three different assays to investigate the signaling of Akt were performed. The difference between the first and the second is the amount of HC used. The first one (Figure 3-31) was incubated with 1 µM HC and the second one (Figure 3-32) with 25 µM HC. For both of them, cells were harvested by trypsination without phosphatase inhibitors. The third approach (Figure 3-33) was performed with 25 µM HC in Akt buffer including phosphatase inhibitors and cell scraping. Exact instructions can be found in section 2.7.

A representative Western blot for approach number 1 is shown in Figure 3-31 A. The negative control (neg) displays the endogenous levels of AktP present in the cells. When incubated with H_2O_2, the level of AktP is increased significantly. IGF1 shows a higher phosphorylation of Akt than the pure incubation with H_2O_2. VitC has an increased level of AktP compared to neg, but is lower than neg H_2O_2. HC displays a higher level of AktP than neg H_2O_2, and Dex shows a similar to lower level of Akt phosphorylation. The evaluation of 11 experiments is depicted in Figure 3-31 B. The positive control IGF1 showed an increase in phosphorylated Akt whereas the control ascorbic acid did not have a great or any impact on Akt phosphorylation. The standard deviations obtained are high and for Dex and HC, no significant difference compared to neg H_2O_2 can be detected.

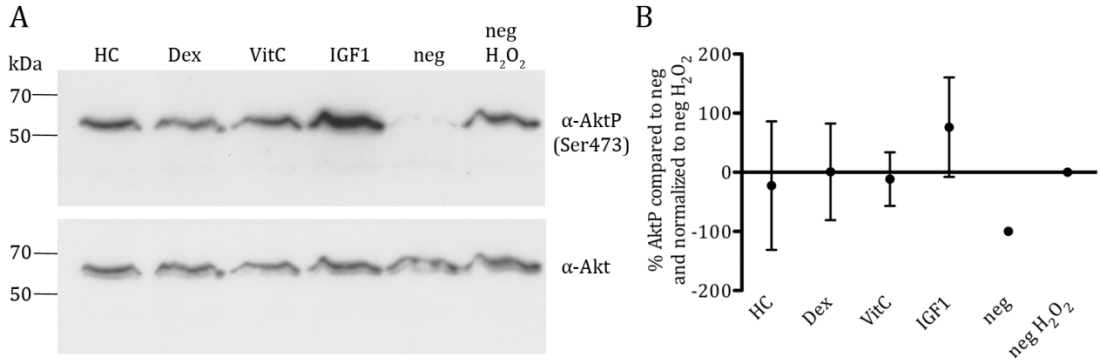

Figure 3-31 Akt assay with 1 µM HC: A549 cells were incubated with 1 µM HC, 1 µM Dex, 100 µM ascorbic acid (VitC), 2.3 nM IGF1 or vehicle (ethanol) for 15 min at 37°C, 8.5 % CO_2. Afterwards cells were exposed to 200 µM H_2O_2 for 15 min at 37°C and 8.5 % CO_2. Cells were harvested by trypsination and the protein concentration was determined with Bradford assay and subjected to SDS-PAGE and Western blotting; A: A representative Western blot with 25 µg protein against α-AktP (above) and α-Akt (below) is shown. B: Western blots were subjected to AIDA imaging software and normalized against levels of Akt. Calculations of 11 different experiments were related to amount of AktP of the negative control (neg) and then correlated with negative control H_2O_2. Mean +/- SD was obtained from Prism software (GraphPad Inc.).

A representative western blot for approach number 2 is shown in Figure 3-32 A. HC and Dex both display similar levels of AktP compared to the neg H_2O_2 control. The evaluation of 14 experiments is depicted in Figure 3-32 B. The positive control IGF1 and ascorbic acid do not have a great or any impact on Akt phosphorylation. The standard deviations obtained are high and for Dex and HC, no significant difference compared to neg H_2O_2 can be detected. Comparing approach 1 and 2 it becomes obvious that AktP levels of approach 1 are lower than AktP levels of approach 2. The reason for these diverse observations is the improvement of AktP antibodies performed by Cell Signaling (NEB, Frankfurt; Germany).

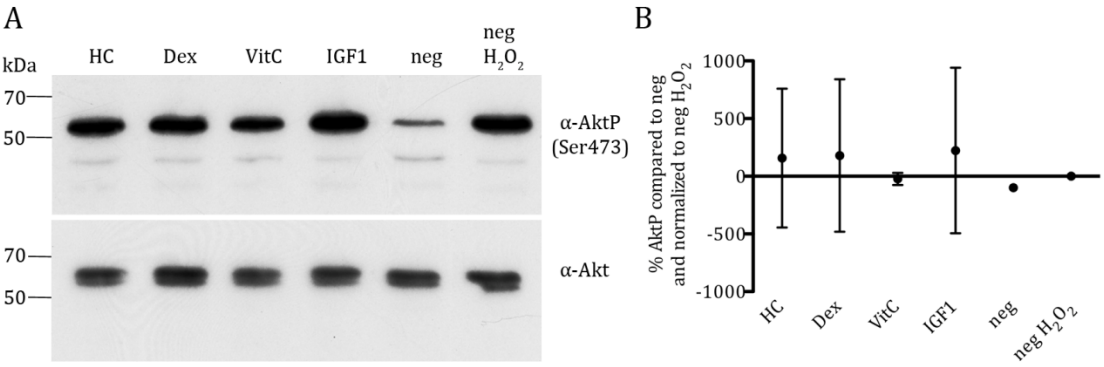

Figure 3-32 Akt assay without use of phosphatase inhibitor: A549 cells were incubated with 25 µM HC, 1 µM Dex, 100 µM ascorbic acid (VitC), 2.3 nM IGF1 or vehicle (ethanol) for 15 min at 37°C, 8.5 % CO_2. Afterwards, cells were exposed to 200 µM H_2O_2 for 15 min at 37°C and 8.5 % CO_2. Cells were harvested by trypsination and protein concentration was determined with Bradford assay followed by SDS-PAGE and Western blotting. A: A representative Western blot with 12.5 µg protein against α-AktP (above) and α-Akt (below) is shown. B: Western blots were subjected to AIDA imaging software and normalized against Akt levels. Calculations of 14 different experiments were related to amount of AktP of the negative control (neg) and then correlated with negative control H_2O_2. Mean +/- SD was obtained from Prism software (GraphPad Inc.).

A representative Western blot for approach number 3 is shown in Figure 3-33 A. HC and Dex do not exhibit a great impact on Akt phosphorylation. The Akt phosphorylation in

presence of HC is slightly lower than the one of Dex. The evaluation of 4 experiments is depicted in Figure 3-33 B. As a result, the positive control IGF1 and ascorbic acid do not have a great or any impact on Akt phosphorylation. The standard deviations obtained are high and for Dex and HC, no significant difference compared to neg H_2O_2 can be detected.

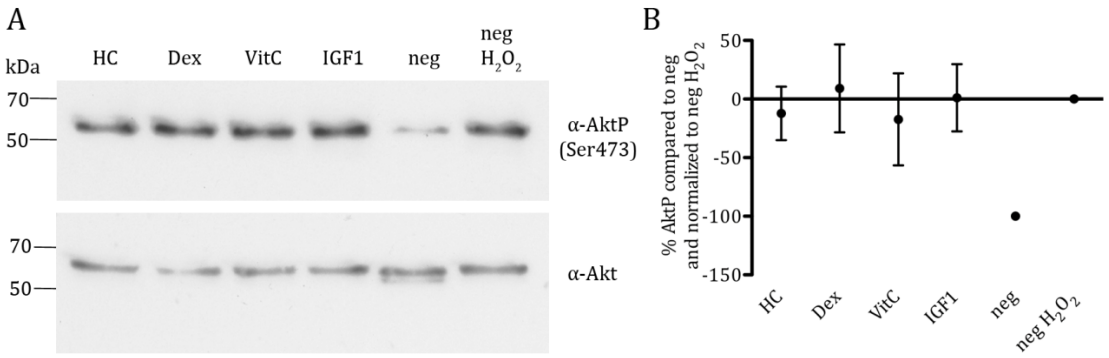

Figure 3-33 Akt assay with use of phosphatase inhibitor: A549 cells were incubated with 25 µM HC, 1 µM Dex, 100 µM ascorbic acid (VitC), 2.3 nM IGF1 or vehicle (ethanol) for 15 min at 37°C, 8.5 % CO_2. Afterwards, cells were exposed to 200 µM H_2O_2 for 15 min at 37°C and 8.5 % CO_2. Cells were harvested by application of Akt buffer for 10 min on ice and protein concentration was determined with Bradford assay followed by SDS-PAGE and Western blotting. A: A representative Western blot with 1 µg (AktP) or 5 µg (Akt) protein against α-AktP (above) and α-Akt (below) is shown. B: Western blots were subjected to AIDA imaging software and normalized against Akt levels. Calculations of 4 different experiments were related to amount of AktP of the negative control (neg) and then correlated with negative control H_2O_2. Mean +/- SD was obtained from Prism software (GraphPad Inc.).

The process is probably too complex, to control every side-reaction. The experiment was performed about 40 times with ambivalent results. Therefore, the cells were always transferred to the reaction well plates at a special time and in an appointed concentration. Solutions and buffers were always prepared freshly prior to experiment. After induction of phosphatase inhibitors to the experiment settings, the experiment was performed at 4°C. The work was done efficiently and fast to eliminate unspecific, slow occurring effects. However, even the positive control (IGF1) showed an ambivalent manner, suggesting a non-reproducible system in this experimental setup. A reason for this could also be that the phosphorylation of Akt was about 12 fold higher than for the approach without phosphatase inhibitor and 25 µM HC. It could point to a phosphorylation state that cannot be elevated by addition of IGF1 as seen in Figure 3-33.

4. Discussion

The aim of this thesis was to identify new possible drug targets for the glucocorticoids dexamethasone and hydrocortisone using the target-fishing approach. For this, chemically derivatized GCs were immobilized on a solid phase to perform chemical proteomics with cell lysates. Furthermore, the bioactivity of these modified GC compounds was tested *in vivo* with a nuclear translocation assay of the glucocorticoid receptor (GR). In fishing experiments, possible target proteins were separated by SDS-PAGE and promising bands were analyzed by mass spectrometry. However, the excision of bands from a SDS-PAGE to identify possible target proteins is biased and can only detect high abundant proteins. In order to overcome this obstacle, stable isotope labeling of amino acids in cell culture (SILAC) was applied. Two different experiments were carried out: The classical triple experiment and the soluble competition assay. Mass spectrometry of the classical SILAC approach identified 648 and the soluble competition 139 potential target proteins. The evaluation of drug-target candidates resulted in 33 proteins for the classical and 26 for the soluble competition approach. Both approaches proved to be suitable for the identification of glucocorticoid target proteins as known and probable interaction partners like heat shock proteins and tropomyosins could be identified. One protein that was already identified in prior experiments was also obtained with the classical SILAC approach. Therefore, this protein, Peroxiredoxin 1 (Prdx1), was investigated further. Prdx1 is an important protein in the cellular decomposition of hydrogen peroxides. It reduces hydrogen peroxides upon forming an intermolecular disulfide bond leading to a homodimer. Five homodimers of Prdx1 can form a decamer leading to a functional switching from peroxidase to chaperone activity. An influence of GCs on Prdx1 was tested using a Prdx1 activity assay that assessed the reductive character of Prdx1 on peroxides. In this setup, dexamethasone did not show any effect on Prdx1 peroxidase function. In addition, the oligomerization state and the chaperone activity of Prdx1 were compared in the presence and absence of dexamethasone. Here, dexamethasone was detected to influence the oligomerization pattern of Prdx1, indicating a role of Dex on Prdx1 chaperone activity.

4.1. Bioactivity of glucocorticoid derivatives

The genomic activity of used GCs was assessed by the ability of these modified GCs to translocate the GR into the nucleus. A lack of a translocation activity of glucocorticoid derivatives does not eliminate the possibility of a nongenomic mode of action that was not tested in this experiment. Furthermore, the compounds used for target-fishing experiments are immobilized to an amino functionalized surface, resulting in an amide bond. In the bioactivity assay, GCs were used still carrying the carboxylic acid function. An amide bond might influence the bioactivity, however, this was not examined in the present thesis.

17β-amides were used for purification of rat liver GR as described by Lustenberger et al.[111]. However, in the bioactivity assay presented here, the substances were inactive in the nuclear translocation activity of the GR. This seems contradictory, but in this thesis the substances were synthesized with an additional linker that could disrupt glucocorticoid GR function. However, GC-3-CMO derivatives did not show an impaired function of their biological activity when the linker was present. Manz et al. described the 17β-amides as competent glucocorticoid receptor binding compounds, which inhibit the glucocorticoid receptor activity[112]. An interaction of GC-17β-amides to the GR could not been shown neither by Manz nor by this thesis. In addition, the same report showed only a slightly diminished activity of GC-21-CMOs. These findings could not be confirmed. The biological activity assay revealed that the GC-21-CMOs are highly impaired in nuclear translocation activity of the GR. It is likely that the synthesized CMO linker could diminish the biological activity through interaction with the GR or the translocation machinery.

GC-3-CMO derivatives were already described, but they did not show whether the compounds exhibited any hormonal activity[113, 114]. In this thesis, the biological activity of GC-3-CMOs could be shown and hence, displays the first report about their biological activity.

4.2. Evaluation of SILAC experiments

Stable isotope labeling of amino acids in cell culture (SILAC) was performed to overcome biased 1D-SDS-PAGE selection techniques and further distinguish between unspecific and specific binding. The first GC experiment performed was the classical triple experiment. The choice of an optimal negative control is important and difficult. In this experiment, it was not possible to normalize ratios minimizing possible mixing

errors in the SILAC experiment. Mass spectrometry identified 648 proteins that were precipitated with dexamethasone. After applying different methods for the evaluation of these proteins, 33 possible drug-target candidates remained. Heat shock proteins are components of the multimeric glucocorticoid receptor complex and were among the evaluated proteins. Nucleoporin 62 and importin β are involved in the nuclear translocation of the glucocorticoid receptor and were also identified.

Using the soluble competition assay, there is no need of a chemically similar negative control, because the same beads are used with or without an excess of soluble drug. However, in this thesis the results could not be normalized as well due to the small amount of identified proteins. Mass spectrometry identified 139 proteins and after evaluation, 26 possible drug candidates remained.

4.2.1. Comparison classical vs. soluble competition SILAC experiment

Comparing the two SILAC approaches is difficult due to different bead immobilization techniques and amount of identified proteins. The classical experiment compared GC-immobilized beads to a negative control (acetic acid) whereas the soluble competition compared additionally GC-coupled beads with each other in presence or absence of soluble GC. For the classical triple experiment, the immobilization of GC derivatives with DMSO probably destroyed the hydroxyl function of the glucocorticoid scaffold[57], essential for GR binding[35]. Whether GR binding is necessary for the identification of GC nongenomic drug target interaction partners is unclear. Nevertheless, the classical triple experiment identified important GR multimeric complex partners like heat shock proteins or importin β and nucleoporin 62 that are involved in translocation of the GR into the nucleus (Table 3-2). This indicates in principle the functionality of the experimental setup used in this work. In addition peroxiredoxin 1, which was recognized in two earlier target-fishing 1D SDS-PAGE experiments (section 3.2.5), was identified as a possible interaction partner for glucocorticoids.

In the soluble competition assay, the immobilization was performed with Dioxan as a solvent and the hydroxyl function of the glucocorticoid scaffold remained active. In addition to soluble competition, a negative control with acetic acid like in the classical approach was used. The advantage of soluble competition can then be compared with the negative control. Unfortunately, the soluble competition SILAC experiment was neither able to identify any GR associated proteins nor peroxiredoxin 1. Low protein recovery might be the reason, so many previously identified proteins were missing.

However, Prdx1 was identified comparing heavy (Dex) to light (acetic acid as negative control), but not for the soluble competition assay. To validate this finding, soluble competition experiments were carried out in a cell-free system to validate the results from the SILAC experiment. Here, the *in vitro* soluble competition detected a direct interaction of recombinantly purified Prdx1 and Dex that can be disrupted in the presence of soluble dexamethasone (section 3.4.3).

Even though a distinct identification of interaction partners was obtained in the two SILAC approaches, both results require further validation by scientific experiments. The soluble competition was only partly successful due to the low amount of identified proteins, but the technique is excellent to clarify drug protein interactions and helps to narrow the amount of possible drug target candidates. The soluble competition experiments performed in collaboration with Pramod Sawant (group of Prof. Maier, Eberhard-Karls Universität Tübingen) were successful and could identify interesting proteins for atorvastatin and englerin A[46].

4.2.2. Discussion of identified proteins

As a number of proteins were identified in SILAC experiments, only the most promising candidates will be discussed here.

4.2.2.1. Influence of dexamethasone on actin filaments and tropomyosins

The soluble competition SILAC experiment with dexamethasone isolated different tropomyosin (Tm) isoforms belonging to the genes TPM1, TPM3 and TPM4. According to Mulcahy-Trinkle et al.[71] Tms are most likely contaminants in pull-down assays. However, Dex was described to have a partially protecting effect against actin filament disruption of cytochalasin D. Furthermore, a thickening effect of actin bundles after Dex treatment for 15 hours was shown[115]. Other steroids like testosterone, β-estradiol or progesterone did not show a protection against cytochalasin-induced actin filament disruption in the tested concentrations. After examination of actin stabilizing proteins, an increase of 550 % ± 50 % in the protein level of caldesmon was detected after Dex treatment in A549 cells[115]. Caldesmon is ubiquitously expressed and regulates interactions between actin, Tm and myosin in a Ca^{2+}/calmodulin-dependent manner. GC treated cells exhibit stress fibers that require merging and bundling of short actin filaments[116]. The ability of Tm to inhibit serious actin disruption by gelsolin and to reorganize as well as to lengthen already severed actin is elevated by caldesmon[115, 116]. In trabecular meshwork cells, Dex treatment can lead to an elevated level of intraocular

pressure in steroid responder tissues. This might be due to the formation of crosslinked actin networks[117], which is induced by caldesmon and arranged by Tm[116]. Besides the transcriptional interaction between GCs and caldesmon, there might also be a direct interaction between Tm and Dex.

Tm is crucial for the regulation of muscle contraction. It consists of a coiled-coil dimer and is situated in an end-to-end manner inside the actin groove[118]. In humans, four Tm genes are described: TPM1, TPM2, TPM3 and TPM4. A minimum of 22 different Tm isoforms can be expressed by alternative splicing[119]. Tm isoforms are distributed differently in each tissue and have distinct mode of actions. In skeletal muscle they bind to myosin binding sites in actin filaments. Upon influx of Ca^{2+} ions into the cytoplasm, Tm will enable binding of myosin to actin filaments leading to muscle contraction[119].

Tm and Dex are both involved in the regulation/reorganization of actin filaments. It is therefore possible that they exhibit a synergistic effect. Through caldesmon, dexamethasone could potentate the ability of Tm to stabilize the actin filament without an increase in the protein level. An interaction between Tm and Dex as seen in the SILAC experiment is therefore likely, but remains to be further elucidated.

4.2.2.2.Peroxisomal proteins and testosterone

In the classical SILAC experiment, four peroxisomal proteins were identified by testosterone. Peroxisomes are small single-membrane-bound organelles that are necessary for β-oxidation of long and very-long chain fatty acids, peroxide detoxification and synthesis of ether lipids, plasmalogens and cholesterol[120-122].

One of the proteins identified is alkyldihydroxyacteonephosphate synthase, which is located at the inner peroxisomal membrane and involved in glycerolipid metabolism and ether lipid synthesis[64].

Peroxisomal trans-2-enoyl-CoA dehydrogenase displays another protein identified with testosterone in the SILAC experiment, which is located inside the peroxisome and is required for lipid metabolism and fatty acid biosynthesis[64].

The other two proteins are Pex1 and Pex6. They exhibit AAA ATPase (ATPases associated with diverse cellular activities) activity and are involved in peroxisomal biogenesis. Pex1 and Pex6 are required for the export of mono-ubiquitinated Pex5 from peroxisomes (Figure 4-1). Pex5 is the import receptor for peroxisomal matrix proteins that exhibits a peroxisomal targeting sequence 1 (PTS1). After forming an 800 kDa docking complex with an oligomeric Pex14, Pex5 cargo is released into the peroxisome.

A 500 kDa translocation complex consisting of the RING (really interesting new gene) proteins ubiquitinates Pex5 at Cys11. Pex1 and Pex6, which require Pex26 for location to peroxisomes, recycle mono-ubiquitinated Pex5 in an ATP-dependent manner. For a review see Fujiki et. al.[120].

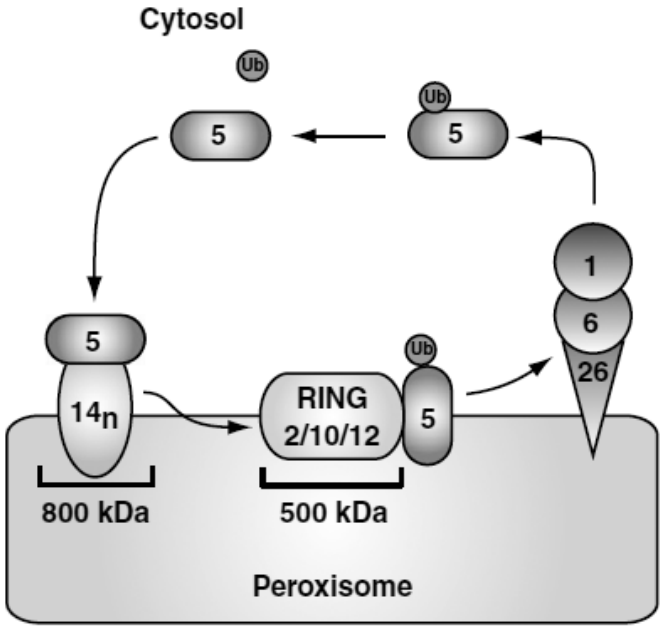

Figure 4-1 Recycling of Pex5 during matrix import: Pex5 is the import receptor for peroxisomal matrix proteins that exhibits a peroxisomal targeting sequence 1 (PTS1). After forming an 800 kDa docking complex with an oligomeric Pex14, Pex5 cargo is released into the peroxisome. A 500 kDa translocation complex consisting of the RING (really interesting new gene) proteins ubiquitinates Pex5 at Cys11. Pex1 and Pex6, which require Pex26 for location to peroxisomes, recycle mono-ubiquitinated Pex5 in an ATP-dependent manner. Image taken from Fujiki[120].

The function of peroxisomes is essential during development and the importance of the relationship between peroxisomes and testosterone becomes apparent in the male testis. Peroxisomal single-enzyme deficiency like X-linked adrenoleukodystrophy (X-ALD) leads to an impairment of the testicular function and therefore to infertility[122]. In other peroxisomal disorders such as Zellweger syndrome, little is known about the testicular function due to the early death of patients[123]. Peroxisomes display a distinct enzyme composition depending on the stage of spermatogenesis. Spermatogenesis starts at the basal lamina of the semniferous tubules with spermatogonia that display immature germ cells. The development from spermatogonia to spermatozoon takes place from the basal lamina to the semniferous tubule lumen (Figure 4-2 A and B)[124]. The concentration of testosterone and its function in spermatogenesis is not yet understood[125].

Peroxisomes exist during early spermiogenesis, which is the late stage of spermatogenesis, as single organelles. Throughout maturation of spermatids, peroxisomes cluster

into large and less numerous peroxisomes below mature spermatid nuclei from spermatid cytoplasm[122].

Testosterone is produced inside Leydig cells. In addition, catalase shows its highest expression in the testis, suggesting a role of peroxisomes in steroidogenesis. A high level of peroxides is known to inhibit steroidogenesis and catalase is able to prevent the inhibition by detoxifying peroxides[122].

The importance of Pex1 and Pex6 during the modification of peroxisomal occurrence and their relationship to testosterone and other metabolites needs more research to draw a significant conclusion.

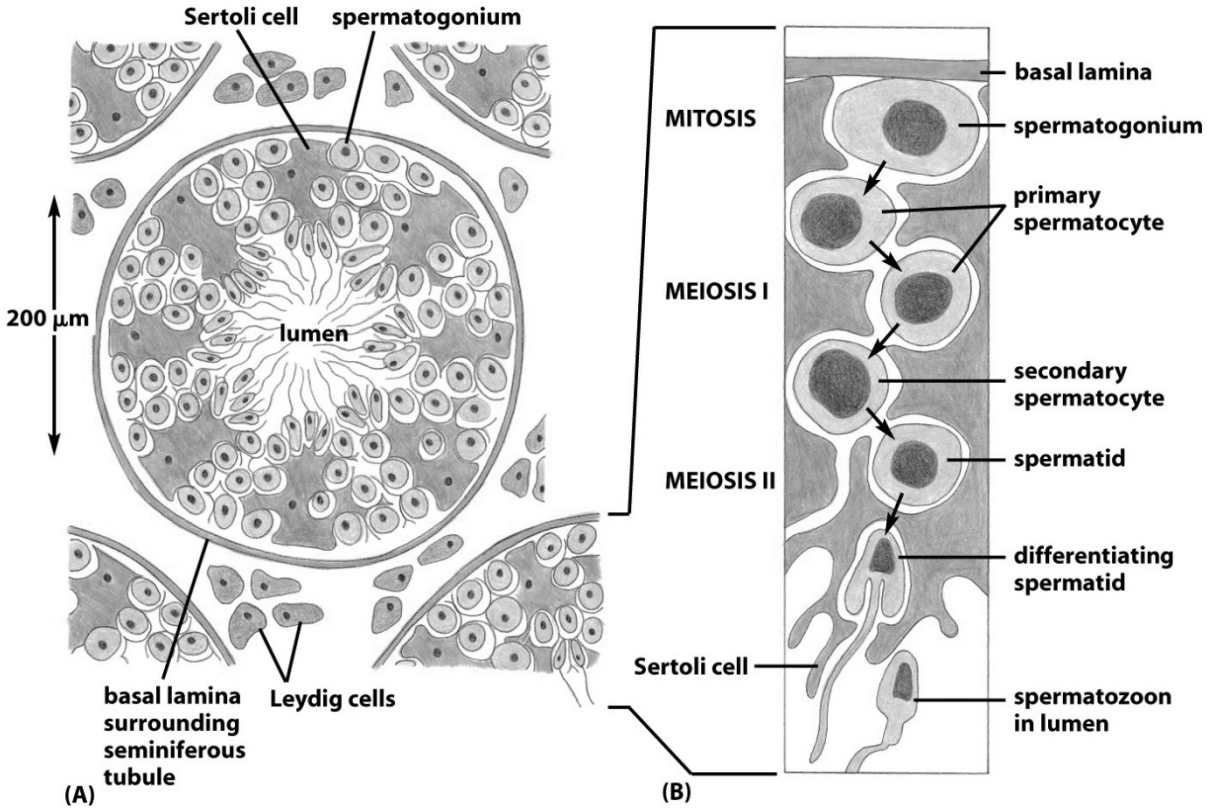

Figure 4-2 Cross section of a somniferous tubule in mammalian testis: A: location of specific cell types inside mammalian testis. B: Spermatogenesis stages and location inside mammalian testis. Image taken from Alberts[124].

4.2.2.3.Steroid receptors and dexamethasone

The soluble competition experiment with dexamethasone identified progesterone receptor membrane component 2 (PGRMC2). PGRMC1 has been identified as well, but was left out during the evaluation process. Little is known on PGRMC2 so far. PGRMC1 has 56 % sequence similarity to PGRMC2[126], they probably diverged from the same gene[127]. PGRMC1 and PGRMC2 differ in their transmembrane domain and the N-terminal amino acids suggesting distinct mode of actions[128].

Keator et al. investigated the expression level of PGRMC2 in the endometrium of macaques. They found that PGRMC2 expression was elevated after estradiol and progesterone treatment during mid-secretory phase of the menstrual cell cycle whereas the progesterone receptor and PGRMC1 were down regulated. Thus, it was shown that PGRMC1 and PGRMC2 have a distinct mode of action in the endometrium of macaques[127].

Further research is required to validate the results and to clarify the molecular function of PGRMC1 and PGRMC2 in relation to dexamethasone binding. As dexamethasone and progesterone exhibit similar structures, it is likely, that dexamethasone cross-reacts with PGRMC2.

As described in section 2.3.5, the precipitation of the GR with GC-coupled beads was not successful. The GR is a very sensitive protein. The instability index was calculated to be 51.7, classifying the GR as an unstable protein[129]. It is possible that the GR partly unfolds during the pull-down assay leading to a conformation that cannot bind to GC-immobilized beads. The use of recombinantly purified protein might facilitate the detection of the GC-GR interaction. As the GR can then be applied in a much higher concentration, it is more likely that at least part of the native protein might bind to GC-coupled beads.

4.3. Influence of dexamethasone on peroxiredoxin 1

Peroxiredoxin 1 exhibits a dual function inside the cell. During normal cellular conditions without oxidative stress Prdx1 acts as a dimeric peroxidase decompensating hydrogen peroxide. In higher concentrations of hydrogen peroxide, Prdx1 will be further oxidized leading to the formation of decamers consisting of five dimers[94-96]. This thesis studied the influence of dexamethasone on Prdx1. A direct binding assay with recombinantly purified Prdx1 revealed a direct interaction of Prdx1 and dexamethasone-immobilized beads. This interaction does not occur, when an excess of soluble dexamethasone is present. The Prdx1 activity assay with recombinantly purified proteins showed that Dex had no effect on Prdx1 peroxidase activity. The impact of Dex on Prdx1's chaperone activity was examined by the state of oligomerization and showed an increase of monomers and trimers compared to no dexamethasone treatment. An influence of Dex on Akt signaling through Prdx1 and PTEN could not be shown.

4.3.1. Influence of dexamethasone on peroxiredoxin 1 oligomerization

The oligomeric state of Prdx1 determines the executed protein function. A single post-translational modification may influence the oligomerization. Monoglutathionylation at Cys83 of Prdx1 for example leads to conversion of the enzyme from a decameric to a dimeric state[99, 130]. A phosphorylation at Thr90 inhibits the peroxidase activity and promotes oligomerization of Prdx1 and therefore chaperone function[102]. Besides post-translational modifications of 2-Cys Prdxs, the formation of decamers is also dependent on Prdx1 and H_2O_2 concentration.

In humans, for decameric Prdx1, Cys83 is involved in the formation of a disulfide bond between the five dimer-dimer interfaces[105]. Other reports have described a hydrophobic interaction between the five dimers[94, 96]. Therefore, it is not quite understood whether a disulfide bond or hydrophobic interactions are important for decamer formation.

The incubation of Dex with recombinantly purified Prdx1 prior to H_2O_2 treatment resulted in an increase in monomers and trimers whereas dimers and tetramers seemed to be decreased. A reduction in dimer formation would mean that less decamers could be formed. This would result in a protein function switch to a peroxidase rather than a molecular chaperone indicating that dexamethasone is able to influence Prdx1 function.

In the oligomerization assay used in this thesis, the formation of disulfide bonds between dimer-dimer interfaces to build up the decamers was assumed. For the gel electrophoresis, SDS was used that could have destroyed the hydrophobic interactions of Prdx1 dimers to form a decamer[94]. Non-reducing gel electrophoretic analysis of the oligomerization state (described in section 3.4.5) is not the optimal technique to gain insight into the influence of Dex on Prdx1 oligomerization. More efficient techniques could be tested like size exclusion chromatography, sedimentation velocity, sedimentation equilibrium as well as light scattering[95].

The analysis of the oligomerization state of Prdx1 is only an indirect examination of its molecular chaperone function. Additionally, measuring the protection from thermally induced aggregation of a substrate protein in presence or absence of GCs could detect a direct effect on the molecular chaperone activity. This technique can be performed using citrate synthase as a substrate. The thermally induced aggregation is measured by light scattering[105, 130]. This experiment can be further expanded by measuring the ability of Prdx1 to refold thermally aggregated citrate synthase in presence or absence of GCs similar to what was described for Hsp60[131, 132].

4.3.2. Influence of dexamethasone on the assay to investigate signaling of Akt

Dexamethasone influences the PI3K signaling cascade negatively through a decrease in Akt phosphorylation[52]. Akt is a serine/threonine kinase and exhibits important functions in cellular signaling, particularly in survival, proliferation and growth[108]. In this thesis, it was suggested that this decrease was due to an interaction between Prdx1 and Dex. Prdx1 protects PTEN from oxidation through hydrogen peroxide. Therefore, PTEN can dephosphorylate PIP_3 leading to a down-regulating of Akt (see section 3.4.6 and Figure 4-3)[51].

Ascorbic acid as an antioxidant and a putative inhibitor of Akt phosphorylation was used as a control. Ascorbic acid exhibits besides antioxidant also prooxidant properties and cannot be used as a negative regulator of Akt phosphorylation[133]. In this assay no change in Akt phosphorylation after ascorbic acid treatment was detected.

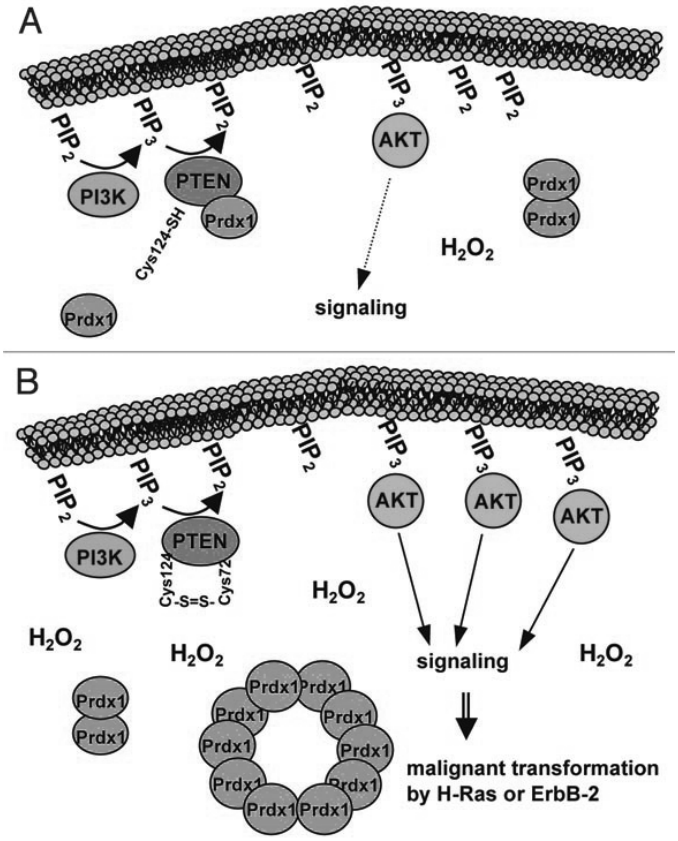

Figure 4-3 Involvement of Prdx1 in Akt signaling: PIP_2 is phosphorylated by PI3K to form PIP_3. PIP_3 can be dephosphorylated by PTEN to PIP_2. A: During basal levels of H_2O_2 Prdx1 is bound to PTEN in a 1:1 ratio to protect PTEN from oxidation of the catalytic Cys124. B: During oxidative stress, Prdx1 itself will get overoxidized forming decamers that no longer exhibit protective effects for PTEN. Hence, Akt signaling is increased that leads to malignant transformations. Image taken from Neumann[51].

The incubation of dexamethasone or hydrocortisone prior to H_2O_2 exposure did not influence the phosphorylation state of Akt (Figure 3-31 - Figure 3-33). The obtained results displayed a high standard deviation. The experimental setup used in this thesis

was probably not appropriate for detection of an interaction between Dex and Prdx1. Due to the described changes in Akt phosphorylation of dexamethasone by Avram et al., the Akt phosphorylation system is probably too complicated to study it with the used technique.

In order to overcome problems with the detection of Akt phosphorylation and to reduce complexity, the effect of Dex on PTEN through Prdx1 should be measured more directly. Kwon et al. described a possible assay[109]. They incubated PTEN with hydrogen peroxide and alkylated all free sulfhydryl groups. Afterwards, they reduced possible disulfide bonds resulting again in free sulfhydryl groups. Those free groups can be precipitated with biotinylated maleinimide. The amount of oxidated PTEN that lost its phosphatase activity can be detected with this experimental setup[109].

Walker et al. described the measurement of PTEN phosphatase activity. The assay uses radiolabeled PIP_3 as a substrate and detects the amount of free $[^{33}P]P_i$ that evolves from dephosphorylation of PIP_3 by PTEN[134]. Other phosphatase measurement techniques are available commercially.

4.4. Concluding remarks

Glucocorticoids are widely used in the treatment of inflammatory diseases, but exert severe side effects. The exact targets for the entire GC mode of actions are not yet known. In order to discover possible drug-target candidates, a target-fishing approach was applied. Peroxiredoxin 1 was identified as a putative target protein of dexamethasone and further investigated. Prdx1 exerts a dual function as a peroxidase and as a molecular chaperone depending on the oligomerization state of the protein. An influence of Dex on Prdx1's peroxidase activity could not be shown. However, an effect in the oligomerization state could be detected. The technique applied for the detection of the molecular chaperone function was not ideal. An improved technique should be used for the detection of the chaperone function in presence of GCs, like the effect of GCs on Prdx1 protection of thermally induced aggregation of citrate synthase[105, 130]. The impact of GCs and Prdx1 on PTEN and therefore on Akt phosphorylation should be addressed using a direct assay for PTEN[109].

Prdx1 displays an interesting target for GCs, whereas the direct effect of GCs on Prdx1 is not yet evident. A possible interaction of GCs on various Prdx1 functions needs to be addressed such as the impact of GCs on post-translational modifications of Prdx1 like glutathionylation, phosphorylation or oxidation.

5. Summary

Glucocorticoids are widely used in the treatment of rheumatic diseases, but the exact molecular targets especially for fast occurring effects are not yet understood. The identification of direct nongenomic drug-protein interaction partners was the objective of this thesis. For the used target-fishing approach it was necessary to immobilize the glucocorticoids onto a matrix. The required chemical modifications were tested for its biological activity. GC-3-CMO derivatives were the most active compounds and applied for further experiments. Using the target-fishing approach with GC-3-CMO immobilized beads a high number of possible target candidates were observed. A refinement of the elution techniques led to the elution of fewer nonspecific proteins. In addition, a membrane isolation in combination with the target-fishing approach resulted in the identification of proteins such as the adenosine nucleotide transporter.

The excision of bands from a SDS-PAGE is biased and can only detect high abundant proteins. To overcome this biased approach, stable isotope labeling of amino acids in cell culture (SILAC) was applied. SILAC metabolically labels the whole proteome of proliferating cells with heavy, medium or light amino acid isotopes. The chemical proteomics approach is applied for the different labeled cell lysates leading to three distinct experiments that will be mixed in the end and quantified. SILAC was performed for glucocorticoids and sex hormones to compare possible target candidates and eliminate unspecific interaction partners. The approach was able to identify 648 proteins for glucocorticoids and 480 proteins for sex hormones. After applying several evaluation techniques 33 target proteins for dexamethasone, 14 target proteins for progesterone and 27 target proteins for testosterone remained. Among the identified interaction partners for dexamethasone were several multimeric glucocorticoid receptor complex-containing proteins like heat shock proteins (Hsp90, Hsp70, Hsp40). Another protein that was identified in two previous target-fishing experiments, peroxiredoxin 1, was detected. An additional SILAC with an excess of soluble dexamethasone (=soluble competition) that competes with dexamethasone-immobilized beads was performed resulting in the identification of several tropomyosins.

Peroxiredoxin 1 (Prdx1) as possible direct interaction partner for dexamethasone was investigated in more detail. A direct binding of recombinant Prdx1 to glucocorticoid-immobilized beads was confirmed. This interaction does not occur, when an excess of

soluble dexamethasone competes with the dexamethasone-immobilized beads indicating a direct Prdx1-GC complex formation.

The influence of dexamethasone (Avram et al.) and Prdx1 (Neumann et al.) on Akt phosphorylation has already been described. Prdx1 protects phosphatase and tensin homolog (PTEN) from oxidation under normal cellular conditions regulating PI3K signaling leading to a decrease in Akt phosphorylation. The same relation was observed for dexamethasone. The exact molecular target for this dexamethasone-induced down-regulation of Akt phosphorylation is unknown. The experimental design used in this thesis for the detection of a possible interaction between dexamethasone and Prdx1 could not show any difference between glucocorticoid and vehicle treatment on Akt phosphorylation.

Prdx1 exhibits a dual function as a peroxidase under normal cellular conditions and as an oligomeric molecular chaperone during oxidative stress. The impacts of glucocorticoids on these two functions were characterized. A Prdx1 activity assay with recombinantly purified proteins was performed, which showed that dexamethasone does not influence Prdx1 peroxidase activity. The effect of dexamethasone on the chaperone function of Prdx1 was tested with an oligomerization assay. It could be shown that dexamethasone increases the formation of monomers and trimers and is likely to decrease dimers and tetramers. All these results indicate Prdx1 as a drug target for dexamethasone, however the exact molecular interaction and its implication on GC-induced cellular function remains to be further elucidated.

6. Zusammenfassung

Glukokortikoide werden häufig in der Behandlung der rheumatoiden Arthritis verwendet. Die molekularen Angriffspunkte der Glukokortikoide insbesondere für schnell einsetzende Effekte, die innerhalb von Sekunden bis Minuten eintreten, sind allerdings noch nicht bekannt. Die Identifizierung von direkten nicht genomischen Glukokortikoid-Interaktionspartnern war das Ziel dieser Dissertation. Die verwendete Technik war das Target-Fishing. Hierfür müssen Glukokortikoide an eine Matrix immobilisiert werden. Die nötige chemische Modifikation kann die biologische Aktivität der Glukokortikoide beeinflussen. Aus diesem Grund wurden die Glukokortikod-Derivate auf ihre biologische Aktivität getestet. Glukokortikoide, die an Position 3 eine Modifikation trugen, waren die biologisch aktivsten Derivate und aus diesem Grund wurden sie für weitere Experimente verwendet. Das Target-Fishing dieser führte zu einer Vielzahl an möglichen Zielproteinen. Deshalb wurden die Elutionstechniken angepasst, so dass weniger nicht spezifische Proteine eluiert wurden. Eine Membranisolierung reicherte spezifisch Membranproteine an und konnte zur Identifizierung des *adenosine nukleotide translocators* (ANT) verwendet werden.

Das Ausschneiden von Banden aus einer SDS-PAGE geschieht nach Augenmaß und ist auf häufig vorkommende Proteine beschränkt. Um diese Einschränkung zu umgehen, wurde das *stable isotope labeling of amino acids in cell culture* (SILAC) durchgeführt. SILAC markiert metabolisch das gesamte Proteom proliferierender Zellen mit schweren, mittleren oder leichten Aminosäurenisotopen. Das Target-Fishing wurde für die unterschiedlich markierten Zelllysate angewendet. Dies führte zu drei unterschiedlichen Experimenten, die am Ende gemischt und quantifiziert wurden. SILAC wurde für Glukokortikoide und Sexualhormone verwendet damit mögliche Zielproteine verglichen und unspezifische Interaktionspartner eliminiert werden konnten. Es wurden für Glukokortikoide 648 Proteine und für Sexualhormone 480 Proteine identifiziert. Nach Anwendung diverser Evaluierungstechniken blieben 33 mögliche Interaktionspartner für Dexamethason, 14 für Progesteron und 27 für Testosteron übrig. Unter den identifizierten Interaktionspartnern waren verschiedene Proteine wie *Heat shock* Proteine, die mit dem Glukokortikoid Rezeptor Komplex assoziiert sind. Ein anderes Protein, das in zwei vorherigen Target-Fishing Experimenten identifiziert wurde, Peroxiredoxin 1, konnte erneut detektiert werden. Ein zusätzliches SILAC Experiment bei dem ein Überschuss an Dexamethason mit dem an der Matrix immobilisierten

Dexamethason konkurriert wurde durchgeführt und verschiedene Tropomyosine konnten ermittelt werden.

Peroxiredoxin 1 (Prdx1) als möglicher Interaktionspartner für Dexamethason wurde genauer untersucht. Eine direkte Bindung von rekombinanten Prdx1 an Glukokortikoid-immobilisierten Matrices konnte gezeigt werden. Diese Interaktion findet nicht statt, wenn ein Überschuss an Dexamethason mit dem an der Matrix immobilisierten Dexamethason konkurriert. Dies lässt auf eine direkte Interaktion zwischen Dexamethason und Prdx1 schließen.

Der Einfluss von Dexamethason (Avram et al.) und Prdx1 (Neumann et al.) auf die Akt Phosphorylierung wurde bereits beschrieben. Prdx1 schützt PTEN (*phosphatase and tensin homolog*) unter normalen zellulären Konditionen vor oxidativem Stress, das zu einer Abnahme der Akt Phosphorylierung führt. Eine Senkung der Akt Phosphorylierung wurde auch für Dexamethason beschrieben, allerdings ist das molekulare Ziel dieser Wirkung unbekannt. Der hier verwendete experimentelle Aufbau zur Untersuchung eines möglichen Zusammenhangs zwischen Dexamethason und Prdx1 konnte keinen Unterschied zwischen Dexamethason und Kontrollbehandlung in der Akt Phosphorylierung feststellen.

Prdx1 besitzt eine duale Funktion. Unter normalen zellulären Stoffwechseleigenschaften wirkt Prdx1 als eine Peroxidase, während oxidativen Stresses wirkt Prdx1 als ein oligomeres Chaperon. Der Einfluss von Dexamethason auf diese beiden Funktionen wurde untersucht. Eine Prdx1 Aktivitätstest mit rekombinant gereinigten Proteinen wurde durchgeführt. Dieser zeigte, dass Dexamethason keinen Einfluss auf die Peroxidasen Aktivität von Prdx1 ausübt. Der Effekt von Dexamethason auf die Chaperon Funktion wurde mit einem Oligomerisationstest geprüft. Es konnte gezeigt werden, dass Dexamethason die Formierung von Monomeren und Trimeren erhöht und es scheint, dass Dexamethason die Bildung von Dimeren und Tetrameren senkt. Diese Ergebnisse deuten daraufhin, dass Prdx1 ein möglicher Interaktionspartner für Dexamethason ist. Allerdings ist die exakte molekulare Wirkweise noch ungeklärt und muss weiterhin untersucht werden.

7. References

1. Eberhardt, W. & Kilz, T. [On genomic and nongenomic effects. Molecular basis of glucocorticoid action]. Pharmazie in unserer Zeit 32, 288-294 (2003).
2. Newton, R. & Holden, N.S. Separating transrepression and transactivation: a distressing divorce for the glucocorticoid receptor? Mol Pharmacol 72, 799-809 (2007).
3. Hafezi-Moghadam, A., Simoncini, T., Yang, Z., Limbourg, F.P., Plumier, J.C., Rebsamen, M.C., Hsieh, C.M., Chui, D.S., Thomas, K.L., Prorock, A.J., Laubach, V.E., Moskowitz, M.A., French, B.A., Ley, K. & Liao, J.K. Acute cardiovascular protective effects of corticosteroids are mediated by non-transcriptional activation of endothelial nitric oxide synthase. Nat Med 8, 473-479 (2002).
4. Groeneweg, F.L., Karst, H., de Kloet, E.R. & Joels, M. Rapid non-genomic effects of corticosteroids and their role in the central stress response. The Journal of endocrinology 209, 153-167 (2011).
5. Buttgereit, F. Mechanisms and clinical relevance of nongenomic glucocorticoid actions. Z Rheumatol 59 Suppl 2, II/119-123 (2000).
6. Dziurla, R. & Buttgereit, F. [Glucocorticoids in rheumatology]. Z Rheumatol 67, 583-591; quiz 592 (2008).
7. Du, J., Cheng, B., Zhu, X. & Ling, C. Ginsenoside Rg1, a novel glucocorticoid receptor agonist of plant origin, maintains glucocorticoid efficacy with reduced side effects. J Immunol 187, 942-950 (2011).
8. Schoneveld, O.J., Gaemers, I.C. & Lamers, W.H. Mechanisms of glucocorticoid signalling. Biochim Biophys Acta 1680, 114-128 (2004).
9. Rhen, T. & Cidlowski, J.A. Antiinflammatory action of glucocorticoids--new mechanisms for old drugs. The New England journal of medicine 353, 1711-1723 (2005).
10. Schoneveld, J.L., Fritsch-Stork, R.D. & Bijlsma, J.W. Nongenomic glucocorticoid signaling: new targets for immunosuppressive therapy? Arthritis Rheum 63, 3665-3667 (2011).
11. Buttgereit, F. & Scheffold, A. Rapid glucocorticoid effects on immune cells. Steroids 67, 529-534 (2002).
12. Boldizsar, F., Talaber, G., Szabo, M., Bartis, D., Palinkas, L., Nemeth, P. & Berki, T. Emerging pathways of non-genomic glucocorticoid (GC) signalling in T cells. Immunobiology 215, 521-526 (2010).
13. Losel, R. & Wehling, M. Nongenomic actions of steroid hormones. Nat Rev Mol Cell Biol 4, 46-56 (2003).
14. Nicolaides, N.C., Galata, Z., Kino, T., Chrousos, G.P. & Charmandari, E. The human glucocorticoid receptor: molecular basis of biologic function. Steroids 75, 1-12 (2010).
15. Schmidt, B.M., Gerdes, D., Feuring, M., Falkenstein, E., Christ, M. & Wehling, M. Rapid, nongenomic steroid actions: A new age? Frontiers in neuroendocrinology 21, 57-94 (2000).
16. Stahn, C. & Buttgereit, F. Genomic and nongenomic effects of glucocorticoids. Nature clinical practice. Rheumatology 4, 525-533 (2008).
17. Labeur, M. & Holsboer, F. Molecular mechanisms of glucocorticoid receptor signaling. Medicina (B Aires) 70, 457-462 (2010).

18. Alangari, A.A. Genomic and non-genomic actions of glucocorticoids in asthma. Annals of thoracic medicine 5, 133-139 (2010).
19. Buttgereit, F., Straub, R.H., Wehling, M. & Burmester, G.R. Glucocorticoids in the treatment of rheumatic diseases: an update on the mechanisms of action. Arthritis Rheum 50, 3408-3417 (2004).
20. Vandevyver, S., Dejager, L. & Libert, C. On the trail of the glucocorticoid receptor: into the nucleus and back. Traffic 13, 364-374 (2011).
21. Smith, D.F. & Toft, D.O. Minireview: the intersection of steroid receptors with molecular chaperones: observations and questions. Mol Endocrinol 22, 2229-2240 (2008).
22. Echeverria, P.C., Mazaira, G., Erlejman, A., Gomez-Sanchez, C., Piwien Pilipuk, G. & Galigniana, M.D. Nuclear import of the glucocorticoid receptor-hsp90 complex through the nuclear pore complex is mediated by its interaction with Nup62 and importin beta. Mol Cell Biol 29, 4788-4797 (2009).
23. Gehring, U. [Glucocorticoid receptors: basis for the diverse clinical actions of glucocorticoids]. Med Klin (Munich) 99, 228-235 (2004).
24. Smoak, K.A. & Cidlowski, J.A. Mechanisms of glucocorticoid receptor signaling during inflammation. Mechanisms of ageing and development 125, 697-706 (2004).
25. Barnes, P.J. & Adcock, I. Anti-inflammatory actions of steroids: molecular mechanisms. Trends in pharmacological sciences 14, 436-441 (1993).
26. Neumann, M. & Naumann, M. Beyond IkappaBs: alternative regulation of NF-kappaB activity. FASEB J 21, 2642-2654 (2007).
27. Majdalawieh, A. & Ro, H.S. Regulation of IkappaBalpha function and NF-kappaB signaling: AEBP1 is a novel proinflammatory mediator in macrophages. Mediators of inflammation 2010, 823821 (2010).
28. Auphan, N., DiDonato, J.A., Rosette, C., Helmberg, A. & Karin, M. Immunosuppression by glucocorticoids: inhibition of NF-kappa B activity through induction of I kappa B synthesis. Science 270, 286-290 (1995).
29. Scheinman, R.I., Cogswell, P.C., Lofquist, A.K. & Baldwin, A.S., Jr. Role of transcriptional activation of I kappa B alpha in mediation of immunosuppression by glucocorticoids. Science 270, 283-286 (1995).
30. Selye, H. Correlations between the chemical structure and the pharmacological actions of steroids. Endocrinology 30, 437-453 (1942).
31. Lowenberg, M., Stahn, C., Hommes, D.W. & Buttgereit, F. Novel insights into mechanisms of glucocorticoid action and the development of new glucocorticoid receptor ligands. Steroids 73, 1025-1029 (2008).
32. Strehl, C., Gaber, T., Lowenberg, M., Hommes, D.W., Verhaar, A.P., Schellmann, S., Hahne, M., Fangradt, M., Wagegg, M., Hoff, P., Scheffold, A., Spies, C.M., Burmester, G.R. & Buttgereit, F. Origin and functional activity of the membrane-bound glucocorticoid receptor. Arthritis Rheum 63, 3779-3788 (2011).
33. Lowenberg, M., Tuynman, J., Bilderbeek, J., Gaber, T., Buttgereit, F., van Deventer, S., Peppelenbosch, M. & Hommes, D. Rapid immunosuppressive effects of glucocorticoids mediated through Lck and Fyn. Blood 106, 1703-1710 (2005).
34. Zhou, J., Liu, D.F., Liu, C., Kang, Z.M., Shen, X.H., Chen, Y.Z., Xu, T. & Jiang, C.L. Glucocorticoids inhibit degranulation of mast cells in allergic asthma via nongenomic mechanism. Allergy 63, 1177-1185 (2008).
35. Steinhilber, D.S.-Z., Manfred; Roth, Hermann J. Medizinische Chemie: Targets und Arzneistoffe, Edn. 1st. (Deutscher Apotheker Verlag, 2005).

36. De Bosscher, K., Van Craenenbroeck, K., Meijer, O.C. & Haegeman, G. Selective transrepression versus transactivation mechanisms by glucocorticoid receptor modulators in stress and immune systems. European journal of pharmacology 583, 290-302 (2008).
37. Conway-Campbell, B.L., Pooley, J.R., Hager, G.L. & Lightman, S.L. Molecular dynamics of ultradian glucocorticoid receptor action. Mol Cell Endocrinol 348, 383-393 (2012).
38. Biddie, S.C., Conway-Campbell, B.L. & Lightman, S.L. Dynamic regulation of glucocorticoid signalling in health and disease. Rheumatology (Oxford) 51, 403-412 (2012).
39. Lomenick, B., Olsen, R.W. & Huang, J. Identification of direct protein targets of small molecules. ACS chemical biology 6, 34-46 (2011).
40. Harding, M.W., Galat, A., Uehling, D.E. & Schreiber, S.L. A receptor for the immunosuppressant FK506 is a cis-trans peptidyl-prolyl isomerase. Nature 341, 758-760 (1989).
41. Fischer, J.J., Michaelis, S., Schrey, A.K., Graebner, O.G., Glinski, M., Dreger, M., Kroll, F. & Koester, H. Capture compound mass spectrometry sheds light on the molecular mechanisms of liver toxicity of two Parkinson drugs. Toxicological sciences : an official journal of the Society of Toxicology 113, 243-253 (2010).
42. Rix, U. & Superti-Furga, G. Target profiling of small molecules by chemical proteomics. Nature chemical biology 5, 616-624 (2009).
43. Geurink, P.P., Prely, L.M., van der Marel, G.A., Bischoff, R. & Overkleeft, H.S. Photoaffinity labeling in activity-based protein profiling. Topics in current chemistry 324, 85-113 (2012).
44. Golkowski, M. Chemical proteomics strategies for elucidation of cellular steroid hormone targets. (2012).
45. Golkowski, M., Pergola, C., Werz, O. & Ziegler, T. Strategy for catch and release of azide-tagged biomolecules utilizing a photolabile strained alkyne construct. Organic & biomolecular chemistry 10, 4496-4499 (2012).
46. Sawant, P. Photoaffinity Based Immobilization and Target Fishing of Atorvastatin Lactone and Synthesis of the C1-C13 Fragment of Biselyngbyaside. (2012).
47. Kanoh, N., Honda, K., Simizu, S., Muroi, M. & Osada, H. Photo-cross-linked small-molecule affinity matrix for facilitating forward and reverse chemical genetics. Angew Chem Int Ed Engl 44, 3559-3562 (2005).
48. Lomenick, B., Hao, R., Jonai, N., Chin, R.M., Aghajan, M., Warburton, S., Wang, J., Wu, R.P., Gomez, F., Loo, J.A., Wohlschlegel, J.A., Vondriska, T.M., Pelletier, J., Herschman, H.R., Clardy, J., Clarke, C.F. & Huang, J. Target identification using drug affinity responsive target stability (DARTS). Proc Natl Acad Sci U S A 106, 21984-21989 (2009).
49. Bantscheff, M., Eberhard, D., Abraham, Y., Bastuck, S., Boesche, M., Hobson, S., Mathieson, T., Perrin, J., Raida, M., Rau, C., Reader, V., Sweetman, G., Bauer, A., Bouwmeester, T., Hopf, C., Kruse, U., Neubauer, G., Ramsden, N., Rick, J., Kuster, B. & Drewes, G. Quantitative chemical proteomics reveals mechanisms of action of clinical ABL kinase inhibitors. Nat Biotechnol 25, 1035-1044 (2007).
50. Zieske, L.R. A perspective on the use of iTRAQ reagent technology for protein complex and profiling studies. Journal of experimental botany 57, 1501-1508 (2006).
51. Neumann, C.A., Cao, J. & Manevich, Y. Peroxiredoxin 1 and its role in cell signaling. Cell Cycle 8, 4072-4078 (2009).

52. Avram, D., Ranta, F., Hennige, A.M., Berchtold, S., Hopp, S., Haring, H.U., Lang, F. & Ullrich, S. IGF-1 protects against dexamethasone-induced cell death in insulin secreting INS-1 cells independent of AKT/PKB phosphorylation. Cell Physiol Biochem 21, 455-462 (2008).
53. Reddy, T.E., Pauli, F., Sprouse, R.O., Neff, N.F., Newberry, K.M., Garabedian, M.J. & Myers, R.M. Genomic determination of the glucocorticoid response reveals unexpected mechanisms of gene regulation. Genome research 19, 2163-2171 (2009).
54. Muntau, A.C., Roscher, A.A., Kunau, W.H. & Dodt, G. Interaction of PEX3 and PEX19 visualized by fluorescence resonance energy transfer (FRET). Adv Exp Med Biol 544, 221-224 (2003).
55. Ong, S.E., Blagoev, B., Kratchmarova, I., Kristensen, D.B., Steen, H., Pandey, A. & Mann, M. Stable isotope labeling by amino acids in cell culture, SILAC, as a simple and accurate approach to expression proteomics. Mol Cell Proteomics 1, 376-386 (2002).
56. Ong, S.E. & Mann, M. A practical recipe for stable isotope labeling by amino acids in cell culture (SILAC). Nat Protoc 1, 2650-2660 (2006).
57. Pfitzner, K.E.a.M., J. G. A New and Selective Oxidation of Alcohols. Journal of American Chemical Society 85, 3027-3028 (1963).
58. Carey, K.L., Richards, S.A., Lounsbury, K.M. & Macara, I.G. Evidence using a green fluorescent protein-glucocorticoid receptor chimera that the Ran/TC4 GTPase mediates an essential function independent of nuclear protein import. J Cell Biol 133, 985-996 (1996).
59. Modarress, K.J., Cavanaugh, A.H., Chakraborti, P.K. & Simons, S.S., Jr. Metal oxyanion stabilization of the rat glucocorticoid receptor is independent of thiols. J Biol Chem 269, 25621-25628 (1994).
60. Cox, J. & Mann, M. MaxQuant enables high peptide identification rates, individualized p.p.b.-range mass accuracies and proteome-wide protein quantification. Nat Biotechnol 26, 1367-1372 (2008).
61. Ong, S.E., Schenone, M., Margolin, A.A., Li, X., Do, K., Doud, M.K., Mani, D.R., Kuai, L., Wang, X., Wood, J.L., Tolliday, N.J., Koehler, A.N., Marcaurelle, L.A., Golub, T.R., Gould, R.J., Schreiber, S.L. & Carr, S.A. Identifying the proteins to which small-molecule probes and drugs bind in cells. Proc Natl Acad Sci U S A 106, 4617-4622 (2009).
62. Kim, J.A., Park, S., Kim, K., Rhee, S.G. & Kang, S.W. Activity assay of mammalian 2-cys peroxiredoxins using yeast thioredoxin reductase system. Anal Biochem 338, 216-223 (2005).
63. Bao, R., Zhang, Y., Lou, X., Zhou, C.Z. & Chen, Y. Structural and kinetic analysis of Saccharomyces cerevisiae thioredoxin Trx1: implications for the catalytic mechanism of GSSG reduced by the thioredoxin system. Biochim Biophys Acta 1794, 1218-1223 (2009).
64. Consortium, T.U. Reorganizing the protein space at the Universal Protein Resource (UniProt). Nucleic Acids Res 40, D71-D75 (2012).
65. Gasteiger, E., Gattiker, A., Hoogland, C., Ivanyi, I., Appel, R.D. & Bairoch, A. ExPASy: The proteomics server for in-depth protein knowledge and analysis. Nucleic Acids Res 31, 3784-3788 (2003).
66. Bradford, M.M. A rapid and sensitive method for the quantitation of microgram quantities of protein utilizing the principle of protein-dye binding. Anal Biochem 72, 248-254 (1976).

67. Laemmli, U.K. Cleavage of structural proteins during the assembly of the head of bacteriophage T4. Nature 227, 680-685 (1970).
68. Behnke, F. Target-fishing of drugs relevant to inflammation and biochemical molecular pharmacological characterisation of the drug-target interaction. (2011).
69. Weißer, M. Synthese von Liganden zum Target-Fishing. (2012).
70. Arvier, M., Lagoutte, L., Johnson, G., Dumas, J.F., Sion, B., Grizard, G., Malthiery, Y., Simard, G. & Ritz, P. Adenine nucleotide translocator promotes oxidative phosphorylation and mild uncoupling in mitochondria after dexamethasone treatment. Am J Physiol Endocrinol Metab 293, E1320-1324 (2007).
71. Trinkle-Mulcahy, L., Boulon, S., Lam, Y.W., Urcia, R., Boisvert, F.M., Vandermoere, F., Morrice, N.A., Swift, S., Rothbauer, U., Leonhardt, H. & Lamond, A. Identifying specific protein interaction partners using quantitative mass spectrometry and bead proteomes. J Cell Biol 183, 223-239 (2008).
72. Boulon, S., Ahmad, Y., Trinkle-Mulcahy, L., Verheggen, C., Cobley, A., Gregor, P., Bertrand, E., Whitehorn, M. & Lamond, A.I. Establishment of a protein frequency library and its application in the reliable identification of specific protein interaction partners. Mol Cell Proteomics 9, 861-879 (2010).
73. Jensen, L.J., Kuhn, M., Stark, M., Chaffron, S., Creevey, C., Muller, J., Doerks, T., Julien, P., Roth, A., Simonovic, M., Bork, P. & von Mering, C. STRING 8--a global view on proteins and their functional interactions in 630 organisms. Nucleic Acids Res 37, D412-416 (2009).
74. von Mering, C., Jensen, L.J., Snel, B., Hooper, S.D., Krupp, M., Foglierini, M., Jouffre, N., Huynen, M.A. & Bork, P. STRING: known and predicted protein-protein associations, integrated and transferred across organisms. Nucleic Acids Res 33, D433-437 (2005).
75. Pereira, S.R., Vasconcelos, V.M. & Antunes, A. The phosphoprotein phosphatase family of Ser/Thr phosphatases as principal targets of naturally occurring toxins. Crit Rev Toxicol 41, 83-110 (2010).
76. Shi, Y. Serine/threonine phosphatases: mechanism through structure. Cell 139, 468-484 (2009).
77. Silverstein, A.M., Galigniana, M.D., Chen, M.S., Owens-Grillo, J.K., Chinkers, M. & Pratt, W.B. Protein phosphatase 5 is a major component of glucocorticoid receptor.hsp90 complexes with properties of an FK506-binding immunophilin. J Biol Chem 272, 16224-16230 (1997).
78. Van Hoof, C. & Goris, J. Phosphatases in apoptosis: to be or not to be, PP2A is in the heart of the question. Biochim Biophys Acta 1640, 97-104 (2003).
79. Ranta, F., Avram, D., Berchtold, S., Dufer, M., Drews, G., Lang, F. & Ullrich, S. Dexamethasone induces cell death in insulin-secreting cells, an effect reversed by exendin-4. Diabetes 55, 1380-1390 (2006).
80. Tumlin, J.A., Lea, J.P., Swanson, C.E., Smith, C.L., Edge, S.S. & Someren, J.S. Aldosterone and dexamethasone stimulate calcineurin activity through a transcription-independent mechanism involving steroid receptor-associated heat shock proteins. J Clin Invest 99, 1217-1223 (1997).
81. Pereira, S.R., Vasconcelos, V.M. & Antunes, A. Computational study of the covalent bonding of microcystins to cysteine residues - a reaction involved in the inhibition of the PPP family of protein phosphatases. FEBS J (2012).
82. Beck, I.M., Vanden Berghe, W., Vermeulen, L., Yamamoto, K.R., Haegeman, G. & De Bosscher, K. Crosstalk in inflammation: the interplay of glucocorticoid receptor-

based mechanisms and kinases and phosphatases. Endocrine reviews 30, 830-882 (2009).
83. Nouh, M.A., Wu, X.X., Okazoe, H., Tsunemori, H., Haba, R., Abou-Zeid, A.M., Saleem, M.D., Inui, M., Sugimoto, M., Aoki, J. & Kakehi, Y. Expression of autotaxin and acylglycerol kinase in prostate cancer: association with cancer development and progression. Cancer science 100, 1631-1638 (2009).
84. Sharifi, N. & Auchus, R.J. Steroid biosynthesis and prostate cancer. Steroids 77, 719-726 (2012).
85. Foster, K.G. & Fingar, D.C. Mammalian target of rapamycin (mTOR): conducting the cellular signaling symphony. J Biol Chem 285, 14071-14077.
86. Wang, X. & Proud, C.G. mTORC1 signaling: what we still don't know. J Mol Cell Biol 3, 206-220 (2011).
87. Weichhart, T. Mammalian target of rapamycin: a signaling kinase for every aspect of cellular life. Methods Mol Biol 821, 1-14 (2012).
88. Moe, B.G., Vereide, A.B., Orbo, A. & Sager, G. High concentrations of progesterone and mifepristone mutually reinforce cell cycle retardation and induction of apoptosis. Anticancer Res 29, 1053-1058 (2009).
89. Tang, L., Zhang, Y., Pan, H., Luo, Q., Zhu, X.M., Dong, M.Y., Leung, P.C., Sheng, J.Z. & Huang, H.F. Involvement of cyclin B1 in progesterone-mediated cell growth inhibition, G2/M cell cycle arrest, and apoptosis in human endometrial cell. Reprod Biol Endocrinol 7, 144 (2009).
90. Cohen, P.T. Novel protein serine/threonine phosphatases: variety is the spice of life. Trends Biochem Sci 22, 245-251 (1997).
91. Rhee, S.G. & Woo, H.A. Multiple functions of peroxiredoxins: peroxidases, sensors and regulators of the intracellular messenger H(2)O(2), and protein chaperones. Antioxidants & redox signaling 15, 781-794 (2011).
92. Knoops, B., Loumaye, E. & Van Der Eecken, V. Evolution of the peroxiredoxins. Sub-cellular biochemistry 44, 27-40 (2007).
93. Rhee, S.G., Woo, H.A., Kil, I.S. & Bae, S.H. Peroxiredoxin functions as a peroxidase and a regulator and sensor of local peroxides. J Biol Chem 287, 4403-4410 (2012).
94. Jang, H.H., Lee, K.O., Chi, Y.H., Jung, B.G., Park, S.K., Park, J.H., Lee, J.R., Lee, S.S., Moon, J.C., Yun, J.W., Choi, Y.O., Kim, W.Y., Kang, J.S., Cheong, G.W., Yun, D.J., Rhee, S.G., Cho, M.J. & Lee, S.Y. Two enzymes in one; two yeast peroxiredoxins display oxidative stress-dependent switching from a peroxidase to a molecular chaperone function. Cell 117, 625-635 (2004).
95. Wood, Z.A., Poole, L.B., Hantgan, R.R. & Karplus, P.A. Dimers to doughnuts: redox-sensitive oligomerization of 2-cysteine peroxiredoxins. Biochemistry 41, 5493-5504 (2002).
96. Barranco-Medina, S., Lazaro, J.J. & Dietz, K.J. The oligomeric conformation of peroxiredoxins links redox state to function. FEBS Lett 583, 1809-1816 (2009).
97. Aran, M., Ferrero, D.S., Pagano, E. & Wolosiuk, R.A. Typical 2-Cys peroxiredoxins--modulation by covalent transformations and noncovalent interactions. FEBS J 276, 2478-2493 (2009).
98. Aran, M., Ferrero, D., Wolosiuk, A., Mora-Garcia, S. & Wolosiuk, R.A. ATP and Mg2+ promote the reversible oligomerization and aggregation of chloroplast 2-Cys peroxiredoxin. J Biol Chem 286, 23441-23451 (2011).
99. Jeong, W., Han Bae, S., Toledano, M.B. & Goo Rhee, S. Role of sulfiredoxin as a regulator of peroxiredoxin function and regulation of its expression. Free radical biology & medicine (2012).

100. Wood, Z.A., Poole, L.B. & Karplus, P.A. Peroxiredoxin evolution and the regulation of hydrogen peroxide signaling. Science 300, 650-653 (2003).
101. Hall, A., Karplus, P.A. & Poole, L.B. Typical 2-Cys peroxiredoxins--structures, mechanisms and functions. FEBS J 276, 2469-2477 (2009).
102. Woo, H.A., Yim, S.H., Shin, D.H., Kang, D., Yu, D.Y. & Rhee, S.G. Inactivation of peroxiredoxin I by phosphorylation allows localized H(2)O(2) accumulation for cell signaling. Cell 140, 517-528 (2010).
103. Wood, Z.A., Schroder, E., Robin Harris, J. & Poole, L.B. Structure, mechanism and regulation of peroxiredoxins. Trends Biochem Sci 28, 32-40 (2003).
104. Cao, J., Schulte, J., Knight, A., Leslie, N.R., Zagozdzon, A., Bronson, R., Manevich, Y., Beeson, C. & Neumann, C.A. Prdx1 inhibits tumorigenesis via regulating PTEN/AKT activity. The EMBO journal 28, 1505-1517 (2009).
105. Lee, W., Choi, K.S., Riddell, J., Ip, C., Ghosh, D., Park, J.H. & Park, Y.M. Human peroxiredoxin 1 and 2 are not duplicate proteins: the unique presence of CYS83 in Prx1 underscores the structural and functional differences between Prx1 and Prx2. J Biol Chem 282, 22011-22022 (2007).
106. Kfir-Erenfeld, S., Sionov, R.V., Spokoini, R., Cohen, O. & Yefenof, E. Protein kinase networks regulating glucocorticoid-induced apoptosis of hematopoietic cancer cells: fundamental aspects and practical considerations. Leukemia & lymphoma 51, 1968-2005 (2010).
107. Schroder, E., Littlechild, J.A., Lebedev, A.A., Errington, N., Vagin, A.A. & Isupov, M.N. Crystal structure of decameric 2-Cys peroxiredoxin from human erythrocytes at 1.7 A resolution. Structure 8, 605-615 (2000).
108. Vivanco, I. & Sawyers, C.L. The phosphatidylinositol 3-Kinase AKT pathway in human cancer. Nature reviews. Cancer 2, 489-501 (2002).
109. Kwon, J., Lee, S.R., Yang, K.S., Ahn, Y., Kim, Y.J., Stadtman, E.R. & Rhee, S.G. Reversible oxidation and inactivation of the tumor suppressor PTEN in cells stimulated with peptide growth factors. Proc Natl Acad Sci U S A 101, 16419-16424 (2004).
110. Duckles, S.P. & Miller, V.M. Hormonal modulation of endothelial NO production. Pflugers Archiv : European journal of physiology 459, 841-851 (2010).
111. Lustenberger, P., Formstecher, P. & Dautrevaux, M. Purification of rat liver glucocorticoid receptor by affinity chromatography: design of a suitable adsorbent. J Steroid Biochem 14, 697-703 (1981).
112. Manz, B., Grill, H.J. & Pollow, K. Steroid side-chain modification and receptor affinity: binding of synthetic derivatives of corticoids to human spleen tumor and rat liver glucocorticoid receptors. J Steroid Biochem 17, 335-342 (1982).
113. Hammer, S., Spika, I., Sippl, W., Jessen, G., Kleuser, B., Holtje, H.D. & Schafer-Korting, M. Glucocorticoid receptor interactions with glucocorticoids: evaluation by molecular modeling and functional analysis of glucocorticoid receptor mutants. Steroids 68, 329-339 (2003).
114. Dressendorfer, R.A., Kirschbaum, C., Rohde, W., Stahl, F. & Strasburger, C.J. Synthesis of a cortisol-biotin conjugate and evaluation as a tracer in an immunoassay for salivary cortisol measurement. J Steroid Biochem Mol Biol 43, 683-692 (1992).
115. Castellino, F., Heuser, J., Marchetti, S., Bruno, B. & Luini, A. Glucocorticoid stabilization of actin filaments: a possible mechanism for inhibition of corticotropin release. Proc Natl Acad Sci U S A 89, 3775-3779 (1992).

116. Castellino, F., Ono, S., Matsumura, F. & Luini, A. Essential role of caldesmon in the actin filament reorganization induced by glucocorticoids. J Cell Biol 131, 1223-1230 (1995).
117. Clark, A.F., Brotchie, D., Read, A.T., Hellberg, P., English-Wright, S., Pang, I.H., Ethier, C.R. & Grierson, I. Dexamethasone alters F-actin architecture and promotes cross-linked actin network formation in human trabecular meshwork tissue. Cell Motil Cytoskeleton 60, 83-95 (2005).
118. Lin, J.J., Eppinga, R.D., Warren, K.S. & McCrae, K.R. Human tropomyosin isoforms in the regulation of cytoskeleton functions. Adv Exp Med Biol 644, 201-222 (2008).
119. Wang, C.L. & Coluccio, L.M. New insights into the regulation of the actin cytoskeleton by tropomyosin. Int Rev Cell Mol Biol 281, 91-128 (2010).
120. Fujiki, Y., Nashiro, C., Miyata, N., Tamura, S. & Okumoto, K. New insights into dynamic and functional assembly of the AAA peroxins, Pex1p and Pex6p, and their membrane receptor Pex26p in shuttling of PTS1-receptor Pex5p during peroxisome biogenesis. Biochim Biophys Acta 1823, 145-149 (2012).
121. Luers, G.H., Thiele, S., Schad, A., Volkl, A., Yokota, S. & Seitz, J. Peroxisomes are present in murine spermatogonia and disappear during the course of spermatogenesis. Histochem Cell Biol 125, 693-703 (2006).
122. Nenicu, A., Luers, G.H., Kovacs, W., David, M., Zimmer, A., Bergmann, M. & Baumgart-Vogt, E. Peroxisomes in human and mouse testis: differential expression of peroxisomal proteins in germ cells and distinct somatic cell types of the testis. Biol Reprod 77, 1060-1072 (2007).
123. Baes, M. & Van Veldhoven, P.P. Generalised and conditional inactivation of Pex genes in mice. Biochim Biophys Acta 1763, 1785-1793 (2006).
124. Bruce Alberts, A.J., Julian Lewis, Martin Raff, Keith Roberts, Peter Walter Molecular Biology of the Cell, Edn. 5th (Garland Science, 2008).
125. Nieschlag, E.B., H.; Nieschlag, S. Andrologie: Grundlagen und Klinik der reproduktiven Gesundheit des Mannes, Edn. 3. Edition. (Springer, Heidelberg, Germany; 2009).
126. Huang, X.M., M A time-efficient, linear-space local similarity algorithm. Adv. Appl. Math. 12, 337-357 (1991).
127. Keator, C.S., Mah, K. & Slayden, O.D. Alterations in progesterone receptor membrane component 2 (PGRMC2) in the endometrium of macaques afflicted with advanced endometriosis. Mol Hum Reprod (2012).
128. Cahill, M.A. Progesterone receptor membrane component 1: an integrative review. J Steroid Biochem Mol Biol 105, 16-36 (2007).
129. Wilkins, M.R., Gasteiger, E., Bairoch, A., Sanchez, J.C., Williams, K.L., Appel, R.D. & Hochstrasser, D.F. Protein identification and analysis tools in the ExPASy server. Methods Mol Biol 112, 531-552 (1999).
130. Park, J.W., Piszczek, G., Rhee, S.G. & Chock, P.B. Glutathionylation of peroxiredoxin I induces decamer to dimers dissociation with concomitant loss of chaperone activity. Biochemistry 50, 3204-3210 (2011).
131. Nagumo, Y., Kakeya, H., Shoji, M., Hayashi, Y., Dohmae, N. & Osada, H. Epolactaene binds human Hsp60 Cys442 resulting in the inhibition of chaperone activity. Biochem J 387, 835-840 (2005).
132. Nielsen, K.L. & Cowan, N.J. A single ring is sufficient for productive chaperonin-mediated folding in vivo. Molecular cell 2, 93-99 (1998).

133. Ivashchenko, O., Van Veldhoven, P.P., Brees, C., Ho, Y.S., Terlecky, S.R. & Fransen, M. Intraperoxisomal redox balance in mammalian cells: oxidative stress and interorganellar cross-talk. Mol Biol Cell 22, 1440-1451 (2011).
134. Walker, S.M., Downes, C.P. & Leslie, N.R. TPIP: a novel phosphoinositide 3-phosphatase. Biochem J 360, 277-283 (2001)

8. Appendix

8.1. Denotation of compounds

HC-3-CMO = 1-{[(11β)-20-Oxo-11,17,21-trihydroxypregn-4-en-3-ylidene]aminooxy}-2-oxo-6,9,12-trioxa-3-azatetradecanoic acid

Dex-3-CMO = 1-{[(11β,16α)-9-Fluoro-20-oxo-11,17,21-trihydroxy-16-methylpregna-1,4-dien-3-ylidene]aminooxy}-2-oxo-6,9,12-trioxa-3-azatetradecanoic acid

N-Met Dex-3-CMO = 1-{[(11β,16α)-9-Fluoro-20-oxo-11,17,21-trihydroxy-16-methylpregna-1,4-dien-3-ylidene]aminooxy}-2-oxo-6,9,12-trioxa-3-aza-3-methyltetradecanoic acid

HC-17β-amide = 1-[(11β,17α)-3-Oxo-11,17-dihydroxyandrost-4-en-17-carboxamido]-2-oxo-6,9,12-trioxa-3-azatetradecanoic acid

Dex-17β-amide = 1-[(11β,16α,17α)-9-Fluoro-3-oxo-11,17-dihydroxy-16-methylandrosta-1,4-dien-17-carboxamido]-2-oxo-6,9,12-trioxa-3-azatetradecanoic acid

HC-21-CMO = 1-{[(11β)-3,20-Dioxo-11,17-dihydroxypregn-4-en-21-ylidene]oxyamino}-2-oxo-6,9,12-trioxa-3-azatetradecanoic acid

Dex-21-CMO = 1-{[(11β,16α)-9-Fluoro-3,20-dioxo-11,17-dihydroxy-16-methylpregna-1,4-dien-21-ylidene]oxyamino}-2-oxo-6,9,12-trioxa-3-azatetradecanoic acid

8.2. SILAC appendix

Figure 8-1 shows the histograms of $\log_2$ frequency distributions plotted against the number of proteins identified in the appropriate SILAC experiment. The meaning of each of the histograms is explained in section 3.3.

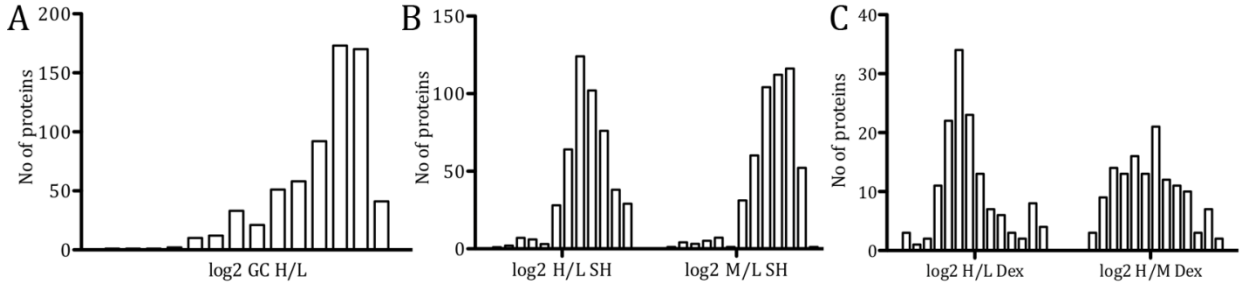

Figure 8-1 Histogram of $\log_2$ frequency distribution was plotted against the number of proteins of SILAC experiments: A Glucocorticoid H/L, B: Sex hormones H/L and M/L, C: Dexamethasone soluble competition H/L and H/M. For description see section 3.3.2.

In Figure 8-2 the log_2 enrichment of GC M/L was plotted against the number of proteins. It was used for evaluation of the scatter plot intersections explained in section 3.3.2.

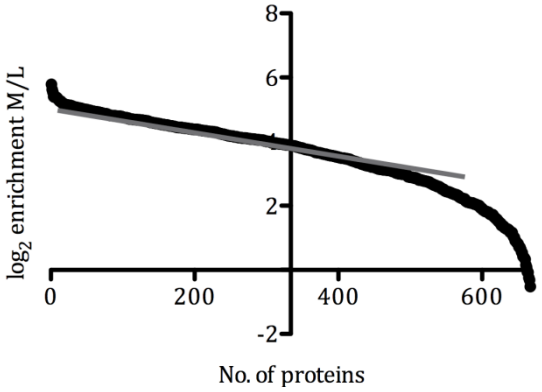

Figure 8-2 SILAC evaluation GC: The log_2 enrichment of M/L was plotted against number of proteins. A line was drawn through the linear part of the graph and intersects at protein 70.

8.3. Abbreviations and short summary of identified proteins

The SILAC results are discussed in section 3.3. Through the described evaluation, specific proteins were identified. In this section, the abbreviations of the mentioned genes in Figure 3-10, Figure 3-12 and Figure 3-15 will be explained. For each of the mentioned genes, a short description of the protein function will be given. These data was obtained from STRING database[73].

8.3.1. Glucocorticoid – dexamethasone

ABHD14B abhydrolase domain containing 14B; Has hydrolase activity towards p-nitrophenyl butyrate (*in vitro*). May activate transcription.

ALDH18A1 aldehyde dehydrogenase 18 family, member A1

BAG2 BCL2-associated athanogene 2; Inhibits the chaperone activity of HSP70/HSC70 by promoting substrate release

CAPZB capping protein (actin filament) muscle Z-line, beta; F-actin-capping proteins bind in a Ca^{2+}-independent manner to the fast growing ends of actin filaments (barbed end) thereby blocking the exchange of subunits at these ends. Unlike other capping proteins (such as gelsolin and severin), these proteins do not sever actin filaments.

CCT4 chaperonin containing TCP1, subunit 4 (delta); Molecular chaperone; assist the folding of proteins upon ATP hydrolysis. Known to play a role, *in vitro*, in the folding of actin and tubulin

CCT8 chaperonin containing TCP1, subunit 8 (theta); Molecular chaperone; assist the folding of proteins upon ATP hydrolysis. Known to play a role, *in vitro*, in the folding of actin and tubulin

CPSF3 cleavage and polyadenylation specific factor 3, 73kDa; Component of the cleavage and polyadenylation specificity factor (CPSF) complex that play a key role in pre-mRNA 3'-end formation, recognizing the AAUAAA signal sequence and interacting with poly(A) polymerase and other factors to bring about cleavage and poly(A) addition. Has endonuclease activity, and functions as mRNA 3'-end-processing endonuclease. Also involved in the histone 3'-end pre-mRNA processing. U7 snRNP- dependent protein.

CTBP1 C-terminal binding protein 1; Involved in controlling the equilibrium between tubular and stacked structures in the Golgi complex. Functions in brown adipose tissue (BAT) differentiation. Corepressor targeting diverse transcription regulators such as GLIS2. Has dehydrogenase activity

DNAJA1 DnaJ (Hsp40) homolog, subfamily A, member 1; Co-chaperone of Hsc70. Seems to play a role in protein import into mitochondria

DNAJA2 DnaJ (Hsp40) homolog, subfamily A, member 2; Co-chaperone of Hsc70

DNAJC10 DnaJ (Hsp40) homolog, subfamily C, member 10; This endoplasmic reticulum co-chaperone may play a role in protein folding and translocation across the endoplasmic reticulum membrane. May act as a co-chaperone for HSPA5.

DTYMK deoxythymidylate kinase (thymidylate kinase); Catalyzes the conversion of dTMP to dTDP.

EXOC3 exocyst complex component 3; Component of the exocyst complex involved in the docking of exocystic vesicles with fusion sites on the plasma membrane.

HADHA hydroxyacyl-Coenzyme A dehydrogenase/3-ketoacyl-Coenzyme A thiolase/ enoyl-Coenzyme A hydratase (trifunctional protein), alpha subunit; Bifunctional subunit

HSP90AA1 heat shock protein 90kDa alpha (cytosolic), class A member 1; Molecular chaperone. Has ATPase activity (By similarity)

HSPA1A heat shock 70kDa protein 1A

KPNB1 karyopherin (importin) beta 1; Functions in nuclear protein import, either in association with an adapter protein, like an importin-alpha subunit, which binds to nuclear localization signals (NLS) in cargo substrates, or by acting as autonomous nuclear transport receptor. Acting autonomously, serves itself as NLS receptor. Docking of the importin/substrate complex to the nuclear pore complex (NPC) is mediated by KPNB1 through binding to nucleoporin FxFG repeats and the complex is subsequently translocated through the pore by an energy requiring, Ran-dependent mechanism.

MTHFD1 methylenetetrahydrofolate dehydrogenase (NADP+ dependent) 1, methenyltetrahydrofolate cyclohydrolase, formyltetrahydrofolate synthetase

NDUFS2 NADH dehydrogenase (ubiquinone) Fe-S protein 2, 49kDa (NADH-coenzyme Q reductase); Core subunit of the mitochondrial membrane respiratory chain NADH dehydrogenase (Complex I) that is believed to belong to the minimal assembly required for catalysis. Complex I functions in the transfer of electrons from NADH to the respiratory chain. The immediate electron acceptor for the enzyme is believed to be ubiquinone (By similarity).

NUP62 nucleoporin 62kDa; Essential component of the nuclear pore complex. The N-terminal is probably involved in nucleocytoplasmic transport. The C-terminal is probably involved in protein-protein interaction via coiled-coil formation and may function in anchorage of p62 to the pore complex.

PDCD2L programmed cell death 2-like

PDCD6 programmed cell death 6; Mediates dioxin toxicity and is involved in regulation of cell growth and differentiation. Represses the transcription activity of AHR by competing with this transcription factor for heterodimer formation with the ARNT and subsequently binding to

the xenobiotic response element (XRE) sequence present in the promoter regulatory region of variety of genes. Represses CYP1A1 by binding the XRE sequence and recruiting ANKRA2, HDAC4 and/or HDAC5. Autoregulates its expression by associating with its own XRE site

POLR2E polymerase (RNA) II (DNA directed) polypeptide E, 25kDa; DNA-dependent RNA polymerase catalyzes the transcription of DNA into RNA using the four ribonucleoside triphosphates as substrates. Common component of RNA polymerases I, II and III, which synthesize ribosomal RNA precursors, mRNA precursors and many functional non-coding RNAs, and small RNAs, such as 5S rRNA and tRNAs, respectively. Pol II is the central component of the basal RNA polymerase II transcription machinery. Pols are composed of mobile elements that move relative to each other.

PPP2CA protein phosphatase 2 (formerly 2A), catalytic subunit, alpha isoform; PP2A can modulate the activity of phosphorylase B kinase casein kinase 2, mitogen-stimulated S6 kinase, and MAP-2 kinase. Can dephosphorylate SV40 large T antigen and p53. Dephosphorylates SV40 large T antigen, preferentially on serine residues 120, 123, 677, and perhaps 679. The C subunit was most active, followed by the AC form, which was more active than the ABC form, and activity of all three forms was strongly stimulated by manganese, and to a lesser extent by magnesium.

PRDX1 peroxiredoxin 1; Involved in redox regulation of the cell. Reduces peroxides with reducing equivalents provided through the thioredoxin system but not from glutaredoxin. May play an important role in eliminating peroxides generated during metabolism. Might participate in the signaling cascades of growth factors and tumor necrosis factor-alpha by regulating the intracellular concentrations of H_20_2. Reduces an intramolecular disulfide bond in GDPD5 that gates the ability to GDPD5 to drive postmitotic motor neuron differentiation (By similarity).

PRMT1 protein arginine methyltransferase 1; Methylates (mono and asymmetric dimethylation) the guanidino nitrogens of arginyl residues present in a glycine and arginine-rich domain (may methylate HNRNPA1 and histones).

RUVBL1 RuvB-like 1 (E. coli); Possesses single-stranded DNA-stimulated ATPase and ATP-dependent DNA helicase (3' to 5') activity. Component of the NuA4 histone acetyltransferase complex, which is involved in transcriptional activation of select genes principally by acetylation of nucleosomal histones H4 and H2A. This modification may both alter nucleosome - DNA interactions and promote interaction of the modified histones with other proteins, which positively regulate transcription.

SF3A3 splicing factor 3a, subunit 3, 60kDa; Subunit of the splicing factor SF3A required for 'A' complex assembly formed by the stable binding of U2 snRNP to the branchpoint sequence (BPS) in pre-mRNA. Sequence independent binding of SF3A/SF3B complex upstream of the branch site is essential, it may anchor U2 snRNP to the pre-mRNA.

TTC9C tetratricopeptide repeat domain 9C

UPP1 uridine phosphorylase 1; Catalyzes the reversible phosphorylytic cleavage of uridine and deoxyuridine to uracil and ribose- or deoxyribose-1- phosphate. The produced molecules are then utilized as carbon and energy sources or in the rescue of pyrimidine bases for nucleotide synthesis

YWHAE tyrosine 3-monooxygenase/tryptophan 5-monooxygenase activation protein, epsilon polypeptide; Adapter protein implicated in the regulation of a large spectrum of both general and specialized signaling pathway. Binds to a large number of partners, usually by recognition of a phosphoserine or phosphothreonine motif. Binding generally results in the modulation of the activity of the binding partner.

YWHAZ tyrosine 3-monooxygenase/tryptophan 5-monooxygenase activation protein, zeta polypeptide; Adapter protein implicated in the regulation of a large spectrum of both general and specialized signaling pathway. Binds to a large number of partners, usually by recognition of a phosphoserine or phosphothreonine motif. Binding generally results in the modulation of the activity of the binding partner.

8.3.2. Sex hormones – testosterone

ACADS acyl-Coenzyme A dehydrogenase, C-2 to C-3 short chain

ACADVL acyl-Coenzyme A dehydrogenase, very long chain; Active toward esters of long-chain and very long chain fatty acids such as palmitoyl-CoA, mysritoyl-CoA and stearoyl-CoA. Can accomodate substrate acyl chain lengths as long as 24 carbons, but shows little activity for substrates of less than 12 carbons.

ACOT9 acyl-CoA thioesterase 9; Acyl-CoA thioesterases are a group of enzymes that catalyze the hydrolysis of acyl-CoAs to the free fatty acid and coenzyme A (CoASH), providing the potential to regulate intracellular levels of acyl-CoAs, free fatty acids and CoASH. Active on long chain acyl-CoAs.

AGK acylglycerol kinase; Lipid kinase that can phosphorylate both monoacylglycerol and diacylglycerol to form lysophosphatidic acid (LPA) and phosphatidic acid (PA), respectively. Does not phosphorylate sphingosine. Overexpression increases the formation and secretion of LPA, resulting in transactivation of EGFR and activation of the downstream MAPK signaling pathway, leading to increased cell growth.

AGPS alkylglycerone phosphate synthase

ARL1 ADP-ribosylation factor-like 1; GTP-binding protein that has very low efficiency as allosteric activator of the cholera toxin catalytic subunit, an ADP-ribosyltransferase. Can activate phospholipase D with very low efficiency. Important for normal function of the Golgi apparatus.

ATP2A2 ATPase, Ca^{2+} transporting, cardiac muscle, slow twitch 2; This magnesium-dependent enzyme catalyzes the hydrolysis of ATP coupled with the translocation of calcium from the cytosol to the sarcoplasmic reticulum lumen. Isoform SERCA2A is involved in the regulation of the contraction/relaxation cycle.

COX4I1 cytochrome c oxidase subunit IV isoform 1; This protein is one of the nuclear-coded polypeptide chains of cytochrome c oxidase, the terminal oxidase in mitochondrial electron transport.

DDOST dolichyl-diphosphooligosaccharide-protein glycosyltransferase; Essential subunit of N-oligosaccharyl transferase enzyme, which catalyzes the transfer of a high mannose oligosaccharide to an asparagine residue within an Asn-X-Ser/Thr consensus motif in nascent polypeptide chains.

ERLIN2 ER lipid raft associated 2; Component of the ERLIN1/ERLIN2 complex which mediates the endoplasmic reticulum-associated degradation (ERAD) of inositol 1,4,5-trisphosphate receptors (IP3Rs). Also involved in ITPR1 degradation by the ERAD pathway.

GBA glucosidase, beta; acid (includes glucosylceramidase)

GBAS glioblastoma amplified sequence

HMOX1 heme oxygenase (decycling) 1; Heme oxygenase cleaves the heme ring at the alpha methene bridge to form biliverdin. Biliverdin is subsequently converted to bilirubin by biliverdin reductase. Under physiological conditions, the activity of heme oxygenase is highest in the spleen, where senescent erythrocytes are sequestrated and destroyed.

HPGD hydroxyprostaglandin dehydrogenase 15-(NAD); Prostaglandin inactivation. Contributes to the regulation of events that are under the control of prostaglandin levels. Catalyzes the NAD-dependent dehydrogenation of lipoxin A4 to form 15-oxo-lipoxin A4. Inhibits in vivo proliferation of colon cancer cells.

IMMT inner membrane protein, mitochondrial (mitofilin)

INCA1 inhibitor of CDK, cyclin A1 interacting protein 1

ITPA inosine triphosphatase (nucleoside triphosphate pyrophosphatase); Hydrolyzes ITP and dITP to their respective monophosphate derivatives. Xanthosine 5'-triphosphate (XTP) is also a potential substrate. May be the major enzyme responsible for regulating ITP concentration in cells.

LGALS3BP lectin, galactoside-binding, soluble, 3 binding protein; Promotes integrin-mediated cell adhesion. May stimulate host defense against viruses and tumor cells.

LGALS7 lectin, galactoside-binding, soluble, 7; Could be involved in cell-cell and/or cell-matrix interactions necessary for normal growth control. Pro-apoptotic protein that functions intracellularly upstream of JNK activation and cytochrome c release.

LYPLA2 lysophospholipase II; May hydrolyze fatty acids from S-acylated cysteine residues in proteins such as trimeric G alpha proteins or HRAS. Has lysophospholipase activity (By similarity).

NAMPT nicotinamide phosphoribosyltransferase; Catalyzes the condensation of nicotinamide with 5-phosphoribosyl-1-pyrophosphate to yield nicotinamide mononucleotide, an intermediate in the biosynthesis of NAD. It is the rate-limiting component in the mammalian NAD biosynthesis pathway (By similarity).

PECR peroxisomal trans-2-enoyl-CoA reductase; Participates in chain elongation of fatty acids. Has no 2,4-dienoyl-CoA reductase activity.

PEX1 peroxisomal biogenesis factor 1; Required for stability of PEX5 and protein import into the peroxisome matrix. Anchored by PEX26 to peroxisome membranes, possibly to form heteromeric AAA ATPase complexes required for the import of proteins into peroxisomes.

PEX6 peroxisomal biogenesis factor 6; Involved in peroxisome biosynthesis. Required for stability of the PTS1 receptor. Anchored by PEX26 to peroxisome membranes, possibly to form heteromeric AAA ATPase complexes required for the import of proteins into peroxisomes.

RPN1 ribophorin I; Essential subunit of N-oligosaccharyl transferase enzyme, which catalyzes the transfer of a high mannose oligosaccharide from a lipid-linked oligosaccharide donor to an asparagine residue within an Asn-X-Ser/Thr consensus motif in nascent polypeptide chains.

SCD stearoyl-CoA desaturase (delta-9-desaturase); Terminal component of the liver microsomal stearyl-CoA desaturase system, that utilizes O_2 and electrons from reduced cytochrome b5 to catalyze the insertion of a double bond into a spectrum of fatty acyl-CoA substrates including palmitoyl-CoA and stearoyl-CoA.

TOMM40 translocase of outer mitochondrial membrane 40 homolog (yeast); Channel-forming protein essential for import of protein precursors into mitochondria (By similarity).

8.3.3. Sex hormones – progesterone

CHP Calcium-binding protein p22 (Calcium-binding protein CHP)(Calcineurin homologous protein)(Calcineurin B homolog); Required for constitutive membrane traffic. Inhibits GTPase-stimulated Na^+/H^+ exchange. Also inhibits calcineurin phosphatase activity.

DARS aspartyl-tRNA synthetase; Catalyzes the specific attachment of an amino acid to its cognate tRNA in a 2 step reaction: the amino acid (AA) is first activated by ATP to form AA-AMP and then transferred to the acceptor end of the tRNA.

DNAJA2 DnaJ (Hsp40) homolog, subfamily A, member 2; Co-chaperone of Hsc70

FECH ferrochelatase (protoporphyria); Catalyzes the ferrous insertion into protoporphyrin IX (By similarity).

GALK1 galactokinase 1; Major enzyme for galactose metabolism.

HADHA hydroxyacyl-Coenzyme A dehydrogenase/3-ketoacyl-Coenzyme A thiolase/ enoyl-Coenzyme A hydratase (trifunctional protein), alpha subunit; Bifunctional subunit

HSDL2 hydroxysteroid dehydrogenase like 2; Has apparently no steroid dehydrogenase activity.

KARS lysyl-tRNA synthetase; Catalyzes the specific attachment of an amino acid to its cognate tRNA in a 2 step reaction: the amino acid (AA) is first activated by ATP to form AA-AMP and then transferred to the acceptor end of the tRNA. When secreted, acts as a signaling molecule that induces immune response through the activation of monocyte/macrophages. Catalyzes the synthesis of diadenosine oligophosphate (Ap4A), a signaling molecule involved in the activation of MITF transcriptional activity.

MLST8 mTOR associated protein, LST8 homolog (S. cerevisiae); Subunit of both mTORC1 and mTORC2, which regulate cell growth and survival in response to nutrient and hormonal signals. mTORC1 is activated in response to growth factors or amino-acids. Amino-acid-signaling to mTORC1 is mediated by Rag GTPases, which cause amino-acid-induced relocalization of mTOR within the endomembrane system. Growth factor-stimulated mTORC1 activation involves AKT1-mediated phosphorylation of TSC1-TSC2, which leads to the activation of the RHEB GTPase that potently activates the protein kinase activity of mTORC.

PPP6C protein phosphatase 6, catalytic subunit; Catalytic subunit of protein phospatase 6 (PP6). PP6 is a component of a signaling pathway regulating cell cycle progression in response to IL-2 receptor stimulation. N-terminal domain restricts G1 to S phase progression in cancer cells, in part through control of cyclin D1. Downregulates MAP3K7 kinase activation of the IL-1 signaling pathway by dephosphorylation of MAP3K7.

PTGES2 prostaglandin E synthase 2; Isomerase that catalyzes the conversion of unstable intermediate of prostaglandin E2 H2 (PGH2) into the more stable prostaglandin E2 (PGE2) form. May also have transactivation activity toward IFN-gamma (IFNG), possibly via an interaction with CEBPB; however, the relevance of transcription activation activity remains unclear.

STRAP serine/threonine kinase receptor associated protein; The SMN complex plays an essential role in spliceosomal snRNP assembly in the cytoplasm and is required for pre-mRNA splicing in the nucleus. STRAP may play a role in the cellular distribution of the SMN complex.

VAT1 vesicle amine transport protein 1 homolog

YWHAG tyrosine 3-monooxygenase/tryptophan 5-monooxygenase activation protein, gamma polypeptide; Adapter protein implicated in the regulation of a large spectrum of both general and specialized signaling pathway. Binds to a large number of partners, usually by recognition of a phosphoserine or phosphothreonine motif. Binding generally results in the modulation of the activity of the binding partner.

8.3.4. Dexamethasone

ACADVL acyl-Coenzyme A dehydrogenase, very long chain; Active toward esters of long-chain and very long chain fatty acids such as palmitoyl-CoA, mysritoyl-CoA and stearoyl-CoA. Can accommodate substrate acyl chain lengths as long as 24 carbons, but shows little activity for substrates of less than 12 carbons.

C8orf55 UPF0670 protein C8orf55 Precursor (Mesenchymal stem cell protein DSCD75).

CFL1 cofilin 1 (non-muscle); Controls reversibly actin polymerization and depolymerization in a pH-sensitive manner. It has the ability to bind G- and F-actin in a 1:1 ratio of cofilin to actin. It is the major component of intranuclear and cytoplasmic actin rods.

CHCHD3 coiled-coil-helix-coiled-coil-helix domain containing 3

CHCHD6 coiled-coil-helix-coiled-coil-helix domain containing 6

CHP Calcium-binding protein p22 (Calcium-binding protein CHP)(Calcineurin homologous protein)(Calcineurin B homolog); Required for constitutive membrane traffic. Inhibits GTPase-stimulated Na(+)/H(+) exchange. Also inhibits calcineurin phosphatase activity.

CLTA clathrin, light chain (Lca); Clathrin is the major protein of the polyhedral coat of coated pits and vesicles.

IMMT inner membrane protein, mitochondrial (mitofilin)

MYH9 myosin, heavy chain 9, non-muscle; Cellular myosin that appears to play a role in cytokinesis, cell shape, and specialized functions such as secretion and capping.

MYL12B myosin, light chain 12B, regulatory; Myosin regulatory subunit that plays an important role in regulation of both smooth muscle and nonmuscle cell contractile activity via its phosphorylation. Phosphorylation triggers actin polymerization in vascular smooth muscle. Implicated in cytokinesis, receptor capping, and cell locomotion (By similarity).

NIPSNAP1 nipsnap homolog 1 (C. elegans)

PGRMC2 progesterone receptor membrane component 2; Receptor for steroids (Potential)

PHB prohibitin; Prohibitin inhibits DNA synthesis. It has a role in regulating proliferation. As yet it is unclear if the protein or the mRNA exhibits this effect. May play a role in regulating mitochondrial respiration activity and in aging.

PHB2 prohibitin 2; Acts as a mediator of transcriptional repression by nuclear hormone receptors via recruitment of histone deacetylases (By similarity). Functions as an estrogen receptor (ER)-selective coregulator that potentiates the inhibitory activities of antiestrogens and represses the activity of estrogens. Competes with NCOA1 for modulation of ER transcriptional activity. Probably involved in regulating mitochondrial respiration activity and in aging.

RPS18 ribosomal protein S18; Located at the top of the head of the 40S subunit, it contacts several helices of the 18S rRNA (By similarity).

SFXN1 sideroflexin 1; Might be involved in the transport of a component required for iron utilization into or out of the mitochondria.

TMOD3 tropomodulin 3 (ubiquitous); Blocks the elongation and depolymerization of the actin filaments at the pointed end. The Tmod/TM complex contributes to the formation of the short actin protofilament, which in turn defines the geometry of the membrane skeleton (By similarity)

TPM1 tropomyosin 1 (alpha); Binds to actin filaments in muscle and non-muscle cells. Plays a central role, in association with the troponin complex, in the calcium dependent regulation of vertebrate striated muscle contraction. Smooth muscle contraction is regulated by interaction with caldesmon. In non-muscle cells is implicated in stabilizing cytoskeleton actin filaments.

TPM3 tropomyosin 3; Binds to actin filaments in muscle and non-muscle cells. Plays a central role, in association with the troponin complex, in the calcium dependent regulation of vertebrate striated muscle contraction. Smooth muscle contraction is regulated by interaction with caldesmon. In non-muscle cells is implicated in stabilizing cytoskeleton actin filaments.

TPM4 tropomyosin 4; Binds to actin filaments in muscle and non-muscle cells. Plays a central role, in association with the troponin complex, in the calcium dependent regulation of vertebrate striated muscle contraction. Smooth muscle contraction is regulated by interaction with caldesmon. In non-muscle cells is implicated in stabilizing cytoskeleton actin filaments. Binds calcium

VDAC1 voltage-dependent anion channel 1 pseudogene 1; Forms a channel through the mitochondrial outer membrane and also the plasma membrane. The channel at the outer mitochondrial membrane allows diffusion of small hydrophilic molecules; in the plasma membrane it is involved in cell volume regulation and apoptosis. It adopts an open conformation at low or zero membrane potential and a closed conformation at potentials above 30-40 mV. The open state has a weak anion selectivity whereas the closed state is cation-selective.

VDAC2 voltage-dependent anion channel 2; Forms a channel through the mitochondrial outer membrane that allows diffusion of small hydrophilic molecules. The channel adopts an open conformation at low or zero membrane potential and a closed conformation at potentials above 30-40 mV. The open state has a weak anion selectivity whereas the closed state is cation-selective.

VDAC3 voltage-dependent anion channel 3; Forms a channel through the mitochondrial outer membrane that allows diffusion of small hydrophilic molecules (By similarity).

VIM vimentin; Vimentins are class-III intermediate filaments found in various non-epithelial cells, especially mesenchymal cells.

YWHAZ tyrosine 3-monooxygenase/tryptophan 5-monooxygenase activation protein, zeta polypeptide; Adapter protein implicated in the regulation of a large spectrum of both general and specialized signaling pathway. Binds to a large number of partners, usually by recognition of a phosphoserine or phosphothreonine motif. Binding generally results in the modulation of the activity of the binding partner.

8.4. SILAC tables

Table 8-1 Protein hit list of classical SILAC evaluation GC – dexamethasone: The protein list is arranged by highest ratios for GC H/L. The other ratios in this table represent results from the different SILAC experiments performed in this thesis. H represents the intensity of identified heavy peptides of the corresponding protein. M and L behave accordingly.

Protein Names	Gene Names	Ratio M/L Dex	Ratio H/L Dex	No H/L	Ratio H/M Dex	No H/M	Ratio M/L GCs	No HC	Ratio H/L GCs	No Dex	No	Ratio H/M GCs	Ratio M/L SH	No Prog	Ratio H/L SH	No Testo	Ratio H/M norm SH	No SH H/M norm
40S ribosomal protein S14	RPS14	0,24	0,17	70	0,71	45	55,3	1	78,6	1		1,28	4,58	310	2,14	293	0,93	247
Elongation factor 1-alpha 1	EEF1A1	0,14	0,04	123	0,79	40	19,7	227	51,6	2		2,45	3,68	345	1,39	373	0,7	361
40S ribosomal protein S13	RPS13	6,26	0,22	59	0,03	113	46,7	3	50,3	3		1,07	29,2	19	13,5	57	1,15	147
60S ribosomal protein L35	RPL35	7,32	0,17	68	0,02	124	30,6	61	49,8	4		1		528		528		528
Elongation factor Tu, mitochondrial	TUFM			331		336	17,3	267	48,3	5		2,46	9,72	193	3,64	201	0,77	317
Nuclear pore glycoprotein p62	NUP62			167		173	32,4	45	47,5	6	1	1,18		537		537		537
Thymidylate kinase	DTYMK			421		424	13,1	365	45,3	7	2	1,92	10,3	178	0,47	455	0,11	484
14-3-3 protein epsilon	YWHAE			228		234	25,3	130	44,4	8	3	1,84	21,5	64	6,39	127	0,66	376
cDNA FLJ58953, highly similar to 40S ribosomal protein S20	RPS20	0,03		205		211	27,6	97	44	9		1,46	6,03	271	2,29	281	0,84	280
Heat shock 40 kDa protein 4	DNAJA1			367		372	15,8	306	43,7	10	4	2,62	18,7	83	4,81	161	0,76	325
Splicing factor 3A subunit 3	SF3A3			178		184	30,7	60	42,9	11	5	0,97		540		540		540
Nucleoside diphosphate kinase	NME1-NME2			210		216	26,8	106	42,5	12		1,82	17,5	99	7,3	110	0,71	348
40S ribosomal protein SA	RPSA	0,09		160		166	33,5	36	42,2	13		1,3	22,4	56	4,69	166	0,64	385
Cleavage and polyadenylation specificity factor subunit 3	CPSF3			317		322	18,1	249	42	14	6	1,72		605		605		605
Delta-1-pyrroline-5-carboxylate synthetase	ALDH18A1			498		501	9,23	449	42	15	7	2,51		691		691		691
60S ribosomal protein L13a	RPL13A	3,47	0,06	113	0,05	108	38,2	14	42	16		1,15		522		522		522
Importin subunit beta-1	KPNB1			314		319	18,3	246	41,9	17	8	2,27	9,78	192	4,74	162	0,69	363
60S ribosomal protein L11	RPL11	0,22	0,24	56	0,1	94	41,9	6	41,8	18		1,31	22,8	53	10,2	76	0,97	227
Tetratricopeptide repeat protein 9C	TTC9C			337		342	17,2	273	41,7	19	9	2,2		617		617		617
Serine/threonine-protein phosphatase 2A catalytic subunit	PPP2CA			389		392	14,9	331	41,7	20	10	2,1		643		643		643
60S ribosomal protein L23a	RPL23A	5,17	0,15	77	0,03	116	36,8	16	41,4	21		1,15	3,88	337	1,98	310	0,99	215
60S ribosomal protein L12	RPL12	0,23	0,15	75	0,1	93	27,8	92	41	22		1,35	14,4	136	6,74	116	0,87	269
Protein arginine N-methyltransferase 1	PRMT1			360		365	16,2	299	40,7	23	11	2,35		627		627		627
60S acidic ribosomal protein P0	RPLP0	0,05	0,04	126	0,2	78	27,4	99	40,5	24		1,36	20,8	71	6,65	120	0,82	290
Programmed cell death protein 2-like	PDCD2L			287		292	20,3	210	40,4	25	12	1,18		585		585		585
40S ribosomal protein S15a	RPS15A	0,01	0,2	64	0,56	54	34,8	28	40,3	26		1,06	27,7	28	15,6	44	1,21	127
40S ribosomal protein S3	RPS3	0,65	0,11	89	0,15	83	26,1	111	39,9	27		1,43	24,7	40	9,47	81	0,81	294
BAG family molecular chaperone regulator 2	BAG2			250		255	22,5	166	39,9	28	13	1,56	18,5	87	7,22	111	0,89	263
RuvB-like 1				345		350	16,9	283	39,9	29	14	1,96	9,51	200	1,56	353	0,46	437
40S ribosomal protein S18	RPS18	0,45	0,41	40	0,92	37	31,9	50	39,8	30		1,14	36,2	5	14,2	53	0,94	244
40S ribosomal protein S7	RPS7	0	0	139		145	27,1	101	39,6	31		1,26	6,35	257	2,8	249	0,7	359
cDNA FLJ50617, highly similar to Tubulin beta-7 chain	TUBB			281		286	20,8	202	39,4	32		1,39	24,2	42	16,6	39	1,23	118
C-1-tetrahydrofolate synthase, cytoplasmic	MTHFD1			344		349	16,9	282	39,1	33	15	1,88	8,59	218	3,58	204	0,49	432
Heat shock protein HSP 90-beta	HSP90A	0,92	0,09	101	0,08	99	20,4	208	39,1	34	16	1,76	9,82	190	3,46	212	0,5	427

Protein Names	Gene Names	Ratio M/L Dex	Ratio H/L Dex	No H/L	Ratio H/M Dex	No H/M	Ratio M/L GCs	No HC	Ratio H/L GCs	No Dex	No	Ratio H/M GCs	Ratio M/L SH	No Prog	Ratio H/L SH	No Testo	Ratio H/M norm SH	No SH H/M norm
Exocyst complex component 3	EXOC3	357		368			16,5	296	39,1	35	17	2,7		624		624		624
40S ribosomal protein S25	RPS25	0,41	0,33	44	0,78	41	30,3	66	39	36		1,27	6,29	263	2,62	257	0,89	261
Capping protein (Actin filament) muscle Z-line, beta	CAPZB			409		412	13,7	352	38,9	37	18	2,5	11,7	161	5,08	153	0,77	315
Abhydrolase domain-containing protein 14B	ABHD14B			263		268	21,7	182	38,9	38	19	1,64		572		572		572
Glucose-6-phosphate 1-dehydrogenase	G6PD			299		304	19,8	224	38,8	39		1,78	10,4	177	2,44	272	0,46	438
cDNA FLJ56825, highly similar to WD repeat protein 57	SNRNP40			326		331	17,5	261	38,4	40		1,33		611		611		611
C-terminal-binding protein 1	CTBP1			556		559	6,99	514	38,3	41	20	1,7		731		731		731
Acyl-Coenzyme A dehydrogenase, very long chain variant	ACADVl	3,11	7,08	14	1,88	30	18	254	38,2	42		1,8	16,8	107	32,8	5	3,7	11
Uridine phosphorylase 1	UPP1			333		338	17,3	269	38	43	21	1,8		615		615		615
Heat shock protein HSP 90-alpha	HSP90AA1			408		411	13,8	351	37,8	44	22	2,22	5,81	280	2,3	279	0,63	386
NADH dehydrogenase [ubiquinone] iron-sulfur protein 2, mitochondrial	NDUFS2			501		504	9,15	452	37,6	45	23	1,8		694		694		694
Mitochondrial import inner membrane translocase subunit TIM50	TIMM50			153		159	35,1	25	37,6	46		1,14	19,4	77	19	35	1,51	63
Plectin-1	PLEC1	0,26	0,27	53	2	29	21,3	190	37,6	47		1,55	6,28	264	1,45	364	0,43	446
Poly(rC)-binding protein 1	PCBP1			285		290	20,5	207	37,4	48		1,84	11,8	159	3,92	188	0,67	375
T-complex protein 1 subunit theta	CCT8			514		517	8,64	468	37,2	49	24	1,95	8,14	223	1,26	388	0,83	287
40S ribosomal protein S19	RPS19			231		237	24,9	135	37,1	50		1,31	7,21	244	3,15	227	0,72	347
Cleavage and polyadenylation specificity factor subunit 5	NUDT21			177		183	30,8	59	37,1	51		1,14	23,9	44	11,4	65	1,12	160
Prohibitin	PHB	1,81	36,3	1	18,8	3	30,3	65	37	52		1,14	30,1	17	24,2	26	1,41	79
40S ribosomal protein S11	RPS11	3,66	0,06	112	0,02	123	32,4	44	37	53		1,19	4,52	316	2,67	256	1,11	166
40S ribosomal protein S16	RPS16	0,2	0,15	78	0,1	92	24	143	36,9	54		1,28	23,4	48	11	68	0,81	295
40S ribosomal protein S2	RPS2	1,74	0,1	97	0,07	104	32,8	42	36,9	55		1,07	18,3	91	6,23	131	0,87	270
26S proteasome non-ATPase regulatory subunit 8	PSMD8			527		530	8,1	482	36,9	56		2,24		713		713		713
DNA-directed RNA polymerases I, II, and III subunit RPABC1	POLR2E			456		459	11,3	403	36,8	57	25	1,72		669		669		669
Programmed cell death protein 6	PDCD6			282		287	20,8	203	36,8	58	26	1,76		583		583		583
Erlin-1	ERLIN1			171		177	31,6	52	36	59		0,9	18,4	90	23,5	28	2,03	35
T-complex protein 1 subunit delta	CCT4			504		507	8,91	455	36	60	27	2,09		695		695		695
DnaJ homolog subfamily A member 2	DNAJA2			376		381	15,4	315	35,8	61	28	2,37	30,7	16	7,42	108	0,62	391
DnaJ homolog subfamily C member 10	DNAJC10			270		275	21,3	189	35,7	62	29	1,4		577		577		577
Eukaryotic translation elongation factor 1 epsilon-1	EEF1E1			157		163	33,9	31	35,7	63		1,1		536		536		536
40S ribosomal protein S4	RPS4X	5,78	0,23	58	0,04	110	18,8	239	35,6	64		1,18	23,9	45	7,82	103	1,2	128
Heat shock 70 kDa protein 1	HSPA1A			297		302	19,9	221	35,5	65	30	1,56	10,1	182	4,93	157	1,06	186
ATP synthase subunit b, mitochondrial	ATP5F1			406		409	14	348	35,4	66		1,69	9,68	196	20,2	32	3,66	12
Peroxiredoxin-1	PRDX1	7,03	1,2	25	0,15	86	23,9	144	35,4	67	31	1,41	21,5	65	2,86	245	0,22	478
Trifunctional enzyme subunit alpha, mitochondrial	HADHA			341		346	17	278	35,3	68	32	1,58	28,5	23	4,87	158	0,42	451

Protein Names	Gene Names	Ratio M/L Dex	Ratio H/L Dex	No H/L	Ratio H/M Dex	No H/M	Ratio M/L GCs	No HC	Ratio H/L GCs	No Dex	No	Ratio H/M GCs	Ratio M/L SH	No Prog	Ratio H/L SH	No Testo	Ratio H/M norm SH	No SH H/M norm
40S ribosomal protein S3a	RPS3A	13	0,4	42	0,03	114	33,8	33	35,2	69		1,04	23,2	50	10,1	77	0,89	260
14-3-3 protein zeta/delta	YWHA	0,21	0,59	35	2,27	28	21,2	191	35,2	70	33	1,82	13,6	141	5,91	138	0,72	344

Table 8-2 Protein hit list of classical SILAC evaluation SH – testosterone: The protein list is arranged by highest ratios for SH H/M normalized. The other ratios in this table represent results from the different SILAC experiments performed in this thesis. H represents the intensity of identified heavy peptides of the corresponding protein. M and L behave accordingly.

Protein Names	Gene Names	Ratio M/L Dex	Ratio H/L Dex	No H/L	Ratio H/M Dex	No H/M	Ratio M/L GCs	No HC	Ratio H/L GCs	No Dex	Ratio M/L SH	No Prog	Ratio H/L SH	No Testo	No	Ratio H/M norm SH	No SH H/M norm
Acyl-protein thioesterase 2	LYPLA2			974		974		971		968	2,6	393	33,9	4	1	18,6	1
Acyl-CoA desaturase	SCD			1226		1226		1226		1225	1,61	444	8,44	93	2	9,73	2
Transitional endoplasmic reticulum ATPase	VCP			503		506	9,02	454	22	312	8,44	221	29,6	12		4,76	3
Acylglycerol kinase, mitochondrial	AGK			901		901		898		895	0,96	468	14,4	52	3	4,52	4
Transketolase	TKT			175		181	31	57	10,5	520	15,1	128	32	7		4,2	5
Voltage-dependent anion-selective channel protein 3	VDAC3	3,21	18,8	8	5,08	15		675		670	11,4	169	34,2	2		4,19	6
Protein NipSnap homolog 1	NIPSNAP1	10,8	14,4	10	1,28	35	23,2	155	9,74	531	20	74	41	1		4,15	7
Dolichyl-diphosphooligosaccharide--protein glycosyltransferase subunit 1	RPN1			615		618	4,34	580	29,9	153	3,07	371	10,4	73	4	4,06	8
Cytochrome c oxidase subunit 4 isoform 1, mitochondrial	COX4I1			757		757		753		749	11,4	167	27,4	16	5	3,98	9
Protein NipSnap homolog 2	GBAS	7,38	3,36	17	0,67	46	40,1	10	27,2	200	13,1	147	34	3	6	3,84	10
Acyl-Coenzyme A dehydrogenase, very long chain variant	ACADVL	3,11	7,08	14	1,88	30	18	254	38,2	42	16,8	107	32,8	5	7	3,7	11
Galectin-7	LGALS7	0,03		1157		1157		1157		1154	0,02	497	0,09	471	8	3,55	13
Peroxisome biogenesis factor 1	PEX1			1308		1308		1308		1307	6,16	268	24,1	27	9	3,35	14
Eukaryotic initiation factor 4A-III	EIF4A3			164		170	33	40	17,8	407	18,9	82	8,89	85		3,21	15
Peroxisomal biogenesis factor 6	PEX6			1223		1223		1223		1222	1,7	440	26,9	17	10	3,18	16
Mitochondrial import receptor subunit TOM40 homolog	TOMM40			634		637	3,55	605	9,45	537	12,3	152	28,4	14	11	2,91	17
Mitofilin	IMMT	0,59	15,6	9	9,71	10	19,1	234	32,6	109	9,83	189	25,1	23	12	2,9	18
Voltage-dependent anion-selective channel protein 2	VDAC2	12,8	19,1	7	1,32	34	29,2	76	6,75	586	19,1	80	31,2	8		2,72	20
Sarcoplasmic/endoplasmic reticulum calcium ATPase 2	ATP2A2			1118		1118		1117		1114	2,33	406	6,78	114	13	2,65	21
Erlin-2	ERLIN2			971		971		968		965	16,4	116	30,6	10	14	2,62	22
15-hydroxyprostaglandin dehydrogenase [NAD+]	HPGD			203		209	27,7	94	27,1	207	21,8	61	28,9	13	15	2,59	23
L-lactate dehydrogenase	LDHA	0,41	0,1	96	0,22	76	22,1	173	28,9	171	7,47	237	11,3	67		2,41	24
Acyl-coenzyme A thioesterase 9, mitochondrial	ACOT9			213		219	26	112	33,4	95	16,1	122	26,2	20	16	2,41	25
D-3-phosphoglycerate dehydrogenase	PHGDH			158		164	33,6	34	28,8	174	16,5	113	23	29		2,32	26
Glucosylceramidase	GBA			313		318	18,3	245	17,8	406	11,7	162	15,5	46	17	2,25	27
Visfatin	NAMPT			216		222	25,9	115	26,4	223	13,7	140	15,4	48	18	2,18	28
Alkyldihydroxyacetonephosphate synthase, peroxisomal	AGPS			338		343	17,1	274	20,3	348	17,9	94	20,8	30	19	2,15	30
ADP-ribosylation factor-like protein 1	ARL1			1161		1161		1161		1158	4,96	301	8,61	92	20	2,15	31
Voltage-dependent anion-selective channel protein 1	VDAC1	8	27,8	3	3,25	20	29,4	73	27,7	191	23,4	47	30,7	9		2,14	32
Heme oxygenase 1	HMOX1			565		568	6,67	525	11,4	507	3,74	343	5,05	155	21	2,1	33
Apoptosis-inducing factor 2	AIFM2			208		214	26,8	104	30,4	140	21,4	66	26,7	18		2,05	34
Erlin-1	ERLIN1			171		177	31,6	52	36	59	18,4	90	23,5	28		2,03	35
Dolichyl-diphosphooligosaccharide--protein glycosyltransferase 48 kDa subunit	DDOST			599		602	5,13	561	15,5	443	4,44	319	5,2	151	22	1,96	37

Protein Names	Gene Names	Ratio M/L Dex	Ratio H/L Dex	No H/L	Ratio H/M Dex	No H/M	Ratio M/L GCs	No HC	Ratio H/L GCs	No Dex	Ratio M/L SH	No Prog	Ratio H/L SH	No Testo	No	Ratio H/M norm SH	No SH H/M norm
Protein INCA1	INCA1			674		677	1,75	650	31,9	120	9,37	203	32,6	6	23	1,95	38
Far upstream element-binding protein 1	FUBP1			159		165	33,6	35	27,2	202	26	36	25,6	21		1,87	41
Galectin-3-binding protein	LGALS3BP			943		943		940		937	11,5	164	12	62	24	1,85	42
Inosine triphosphate pyrophosphatase	ITPA			898		898		895		892	17,2	103	11,8	63	25	1,79	43
Peroxisomal trans-2-enoyl-CoA reductase	PECR			424		427	12,7	368	16,3	427	21,6	63	30	11	26	1,74	45
Short-chain specific acyl-CoA dehydrogenase, mitochondrial	ACADS			981		981		978		975	10,3	179	7,87	102	27	1,74	46
Coiled-coil-helix-coiled-coil-helix domain-containing protein 3, mitochondrial	CHCHD3	2,49	30,6	2	12,5	8	25,5	124	29,9	152	28,2	24	24,7	25		1,73	48
Tubulin alpha-1C chain	TUBA1C	2,94	0,75	30	0,26	74	34,5	30	26,6	218	14,9	131	12,2	61		1,68	50
Tubulin alpha-4A chain	TUBA4A	3,22	0,77	28	0,29	72	37	15	24,9	253	17,3	100	14,8	49		1,66	51
XTP3-transactivated gene B protein	C2orf30			1384		1384		1384		1383	24,7	41	15,5	47		1,64	53

Table 8-3 Protein hit list of classical SILAC evaluation SH – progesterone: The protein list is arranged by lowest ratios for SH H/M. The other ratios in this table represent results from the different SILAC experiments performed in this thesis. H represents the intensity of identified heavy peptides of the corresponding protein. M and L behave accordingly.

Protein Names	Gene Names	Ratio M/L Dex	Ratio H/L Dex	No H/L	Ratio H/M Dex	No H/M Dex	Ratio M/L GCs	No HC	Ratio H/L GCs	No Dex	Ratio H/M GCs	Ratio M/L SH	No Prog	No	Ratio H/L SH	No Testo	Ratio H/M SH	Ratio H/M norm SH	No SH H/M norm
Synaptic vesicle membrane protein VAT-1 homolog	VAT1			1087		1087		1086		1083		26,1	33	1	2,26	283	0,1	0,17	481
Hydroxysteroid dehydrogenase-like protein 2	HSDL2			625		628	4,02	595	4,75	608	1,53	32,3	11	2		481	0,09	0,17	480
Prostaglandin E synthase 2	PTGES2			148		154	35,6	20	30,3	143	0,81	40,7	3	3	2,09	300	0,14	0,24	476
Ferrochelatase, mitochondrial	FECH			365		370	16	304	28,8	173	1,8	46,8	1	4	5,56	145	0,15	0,25	474
Lysyl-tRNA synthetase	KARS			186		192	29,2	74	34,8	78	1,09	34,8	9	5	3,49	211	0,12	0,25	473
Serine/threonine-protein phosphatase 6 catalytic subunit	PPP6C			286		291	20,4	209	31,9	119	1,23	42,1	2	6	5,74	142	0,17	0,29	470
Target of rapamycin complex subunit LST8	MLST8			254		259	22,3	170	19,5	371	0,88	36,5	4	7	7,7	107	0,21	0,35	462
Aspartyl-tRNA synthetase, cytoplasmic	DARS			141		147	42,3	4	25	248	0,69	28,1	26	8	0,61	442	0,21	0,41	456
Trifunctional enzyme subunit alpha, mitochondrial	HADHA			341		346	17	278	35,3	68	1,58	28,5	23	9	4,87	158	0,21	0,42	451
Trifunctional enzyme subunit beta, mitochondrial	HADHB	0,14	0,1	95	0,77	42	19,9	223	34,5	80	1,7	31,2	12		5,87	139	0,22	0,43	447
Galactokinase 1	GALK1			481		484	9,87	432	34,2	84	1,41	26	34	10	6,67	119	0,27	0,44	444
Serine-threonine kinase receptor-associated protein	STRAP			352		357	16,6	291	29,8	157	1,4	33,1	10	11	4,57	170	0,24	0,45	440
Calcium-binding protein p22	CHP	0,3	7,21	13	16,8	4	24,4	137	33,5	93	1,26	35,9	6	12	8,62	90	0,29	0,54	416
14-3-3 protein gamma	YWHAG			401		404	14,2	343	35	72	1,75	25,6	37	13	6,59	121	0,34	0,56	411
DnaJ homolog subfamily A member 2	DNAJA2			376		381	15,4	315	35,8	61	2,37	30,7	16	14	7,42	108	0,31	0,62	391

8.5. Plasmid

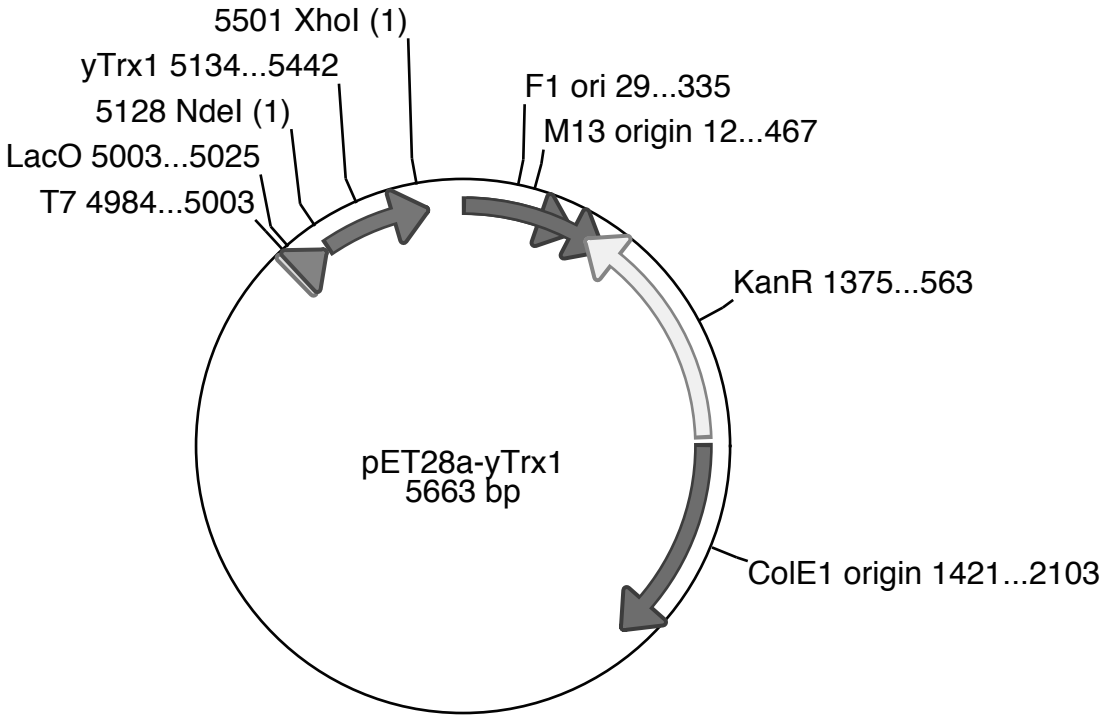

Figure 8-3 Plasmid yHisTrx1: yTrx1 in pET28a. The protein is expressed with an N-terminal His_6-tag.

Presentation of results

- Tübingen, Juni 2012: Internal seminar of the IFIB, oral presentation
    - "Discovering new targets for glucocorticoids"
- Tübingen, Juli 2011: poster presentation of PhD students
    - Etzel, Y.; Golkowski, M.; Ziegler, T.; Dodt, G.:
      "Discovering new drug targets for glucocorticoids"
- Blaubeuren, Juni 2010: 1st Young Scientist Symposium of the IFIB, oral presentation
    - "Discovering new targets for glucocorticoids"
- Amsterdam, August 2009: EMBO Meeting poster presentation
    - Etzel, Y.; Behnke F.; Golkowski, M.; Kutter, T.; Ziegler, T.; Werz, O.; Dodt,G.:
      "Discovering drug-target interactions: the target-fishing approach"
- Tübingen, Juli 2009: poster presentation of PhD students
    - Etzel, Y.; Behnke F.; Golkowski, M.; Ziegler, T.; Werz, O.; Dodt,G.:
      "Discovering drug-target interactions: the target-fishing approach"

Publication

- Golkowski, M.; Etzel, Y.; Werz, O.; Laufer, S.; Dodt, G.; Ziegler, T.:
  "Preparation and biological activity of glucocorticoid-ethylene glycol conjugates suitable for affinity purification" (in preparation)

Danksagung

Mein Dank gilt Gabi Dodt für die interessante Promotionsmöglichkeit, die weit genug gefasst war, um mir nicht die Freiheit bei der Ausgestaltung meiner Doktorarbeit zu nehmen, sowie die Unterstützung durch eine große Diskussionsbereitschaft und Anregungen.
Ganz besonders möchte ich mich bei Prof. Oliver Werz für seine Ideen, Ratschläge und das Schreiben diverser Gutachten bedanken. Dem ganzen Labor des Arbeitskreises Werz in Tübingen für die nette Aufnahme als Neuling und beim Einleben in Tübingen. Vor allem meinem engsten Kooperationspartner Felix Behnke möchte ich mich für die vielen guten und produktiven Gespräche, die Einführung in den Laboralltag sowie alle wichtigen Handgriffe rund um das Target-Fishing recht herzlich danken! Carlo Pergola für die Idee meines Assays und seinen Einsatz zum Aufbau eben dieses.
Bei Thilo Stehle möchte ich mich für die finanzielle Unterstützung sowie alle Geräte bedanken ohne die ich kein Protein hätte reinigen können!
Ein recht herzlicher Dank geht auch an Martin Golkowski ohne den ich keinen Köder für meine Angel gehabt hätte. Vielen Dank für die unzähligen Synthesearbeiten, die wissenschaftlichen Diskussionen, das offene Ohr am Telefon und letztendlich die leckeren Sektflaschen. Aus dem Promotionsverbund möchte ich mich auch noch für die gute Zusammenarbeit bei Marc Weißer (Wir haben Metamizol noch auf den letzten Metern meiner praktischen Arbeit bezwungen!), Thomas Kutter (Danke für deinen UV-Linker!) und Pramod Sawant bedanken. Ein herzlicher Dank gilt auch Prof. Laufer, Prof. Ziegler und Prof. Maier für die Gelegenheit eines produktiven Austauschs innerhalb und außerhalb des Promotionsverbundes.
Bei Prof. Schwarzer möchte ich mich für die guten Ratschläge zur Auswertung des SILAC Versuches bedanken. Es war eine harte Arbeit und der Durchbruch kam durch seine hilfreichen Anregungen und Gabi Dodts Ideen. Vielen Dank!
Meinem berühmt berüchtigtem Ladies Lab Riki, Vera, Denise und unserem Küken Dhaarsi möchte ich herzlichst danken. Vielen Dank für die unzähligen tollen wissenschaftlichen und privaten Gespräche! Danke für eine tolle Stimmung im Labor, vielen unvergesslichen Ereignissen, schlechten Witzen und guter Laune!
Bei Anna Katharina Speidel, Anita Ripplinger und Karin Steiger möchte ich mich für die Durchführung einiger wissenschaftlicher Experimente bedanken.
Vielen Dank an alle IFIB Mitarbeiter! Feuerzangenbowle, Grillabende, Midsommar und andere große und kleine Ereignisse (z.B. Sommerkurse für Studenten) werde ich so schnell nicht vergessen!
Dem KSO lab danke ich für die Benutzung des ELISA readers und Eva Alexander (die Pfalz war super!) für ihre Hilfsbereitschaft. Bei der Gruppe von Prof. Rapaport für die Benutzung der AIDA imaging Software!
Meinen Eltern möchte ich von Herzen danken, dass sie mich immer unterstützt und ermutigt haben. Nicht nur im Schreiburlaub haben Sie mir meine Sorgen genommen, sodass ich mich voll und ganz aufs Promovieren konzentrieren konnte.
Konrad möchte ich als meinem Fels in der Brandung besonders herzlich danken, dafür dass du den Glauben an mich nicht verloren hast und für deine unglaubliche Fürsorge und Geduld!